

Nuclear Forces on the lattice

Noriyoshi Ishii

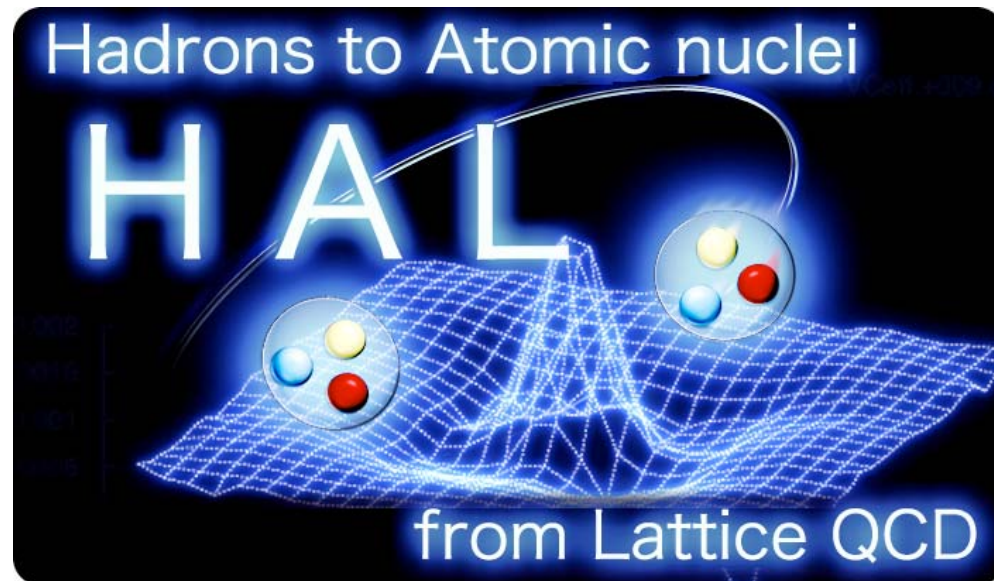
(Univ. of Tokyo)

for

PACS-CS Collaboration

and

HAL QCD Collaboration



S.Aoki (Univ. of Tsukuba),
T.Doi (Univ. of Tsukuba),
T.Hatsuda (Univ. of Tokyo),
Y.Ikeda (RIKEN),
T.Inoue (Nihon Univ.),
K.Murano (KEK),
H.Nemura (Tohoku Univ.)
K.Sasaki (Univ. of Tsukuba)

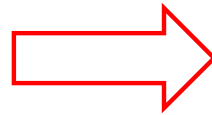
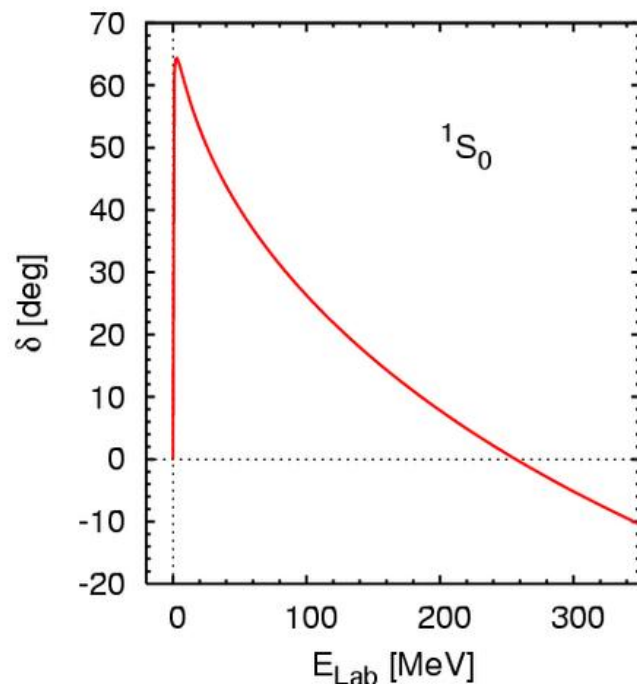
Background

(2)

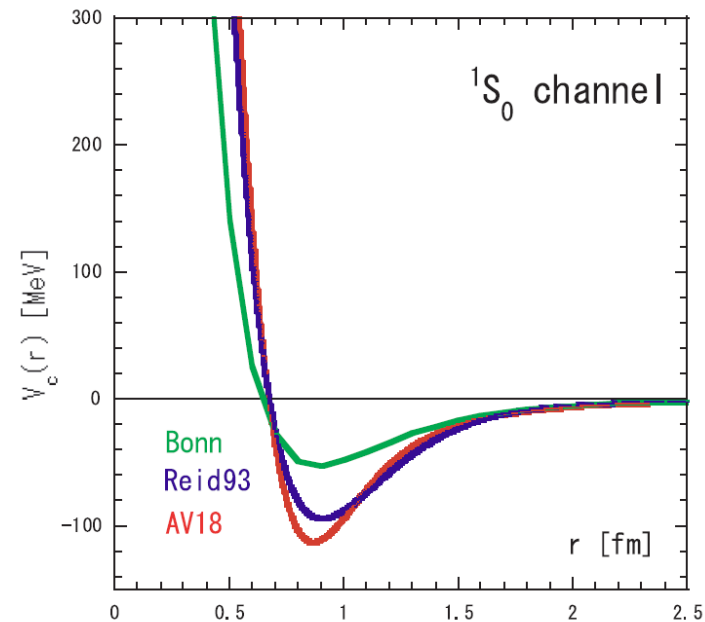
➤ Realistic nuclear force

Large number of NN scattering data is used to construct realistic nuclear force

NN scattering data
(~ 4000 data)



Realistic nuclear potential
(18 fit parameter $\rightarrow \chi^2/\text{dof} \sim 1$ [AV18])



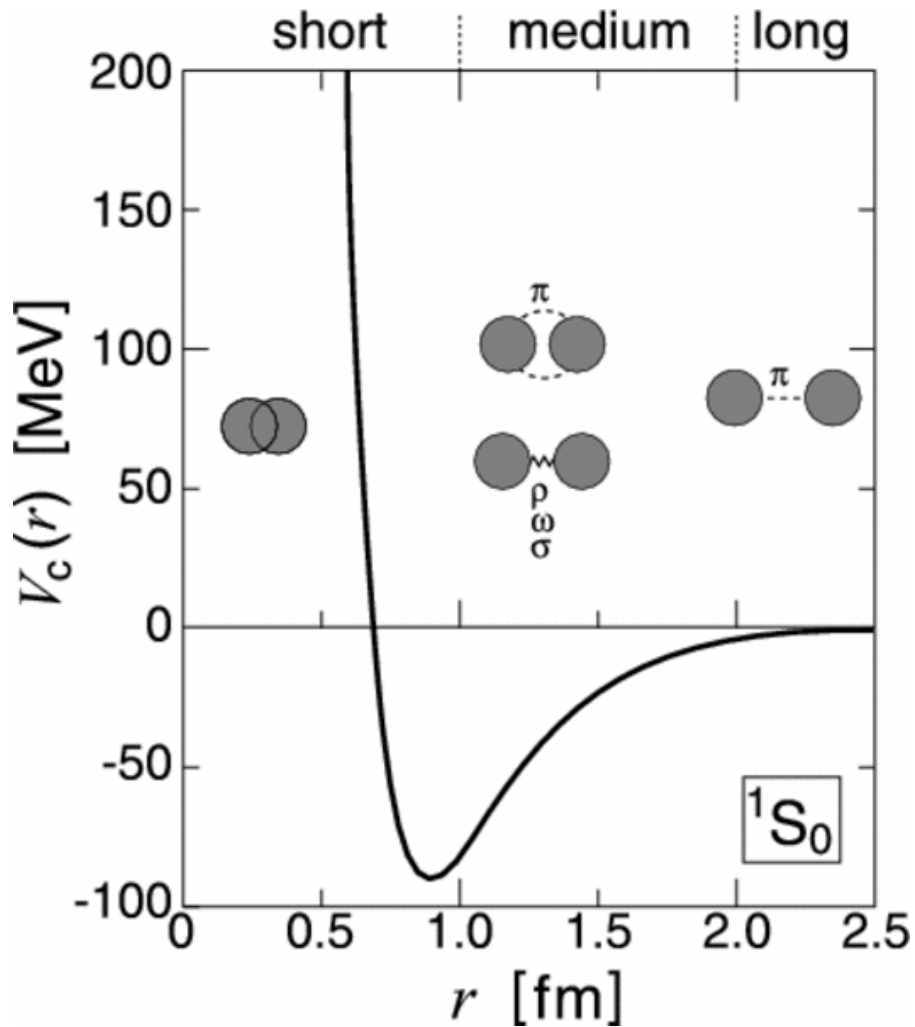
➤ Once it is constructed, it can be conveniently used to study

➤ nuclear structure and nuclear reaction

➤ equation of state of nuclear matter

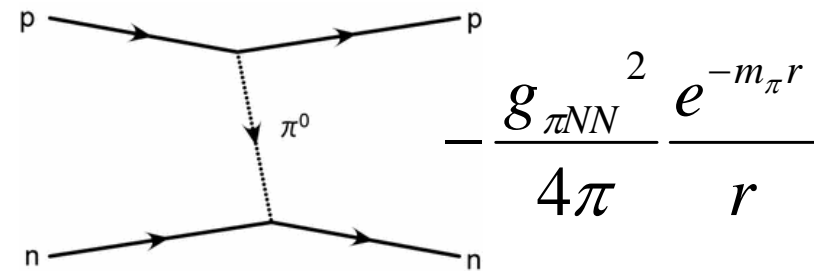
➔ supernova explosion, structure of neutron star

Nuclear Force



➤ **Long distance ($r > 2$ fm)**

OPEP [H.Yukawa(1935)]
(One Pion Exchange)



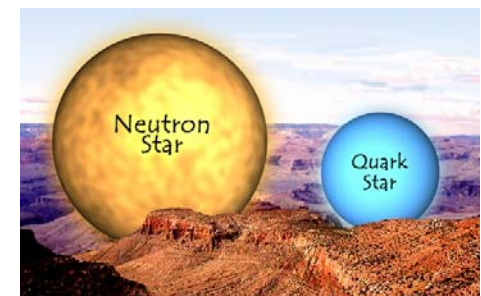
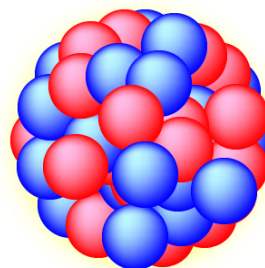
➤ **Medium distance ($1 \text{ fm} < r < 2 \text{ fm}$)**

multi-pion, ρ , ω , " σ ", ...

Attraction → essential for bound nuclei

➤ **Short distance ($r < 1$ fm)**

Repulsive core [R.Jastrow(1950)]



There are several methods:

➤ **Method which utilizes the static quarks**

D.G.Richards et al., PRD42, 3191 (1990).

A.Mihaly et la., PRD55, 3077 (1997).

C.Stewart et al., PRD57, 5581 (1998).

C.Michael et al., PRD60, 054012 (1999).

P.Pennanen et al, NPPS83, 200 (2000),

A.M.Green et al., PRD61, 014014 (2000).

H.R Fiebig, NPPS106, 344 (2002); 109A, 207 (2002).

T.T.Takahashi et al, ACP842,246(2006),

T.DoI et al., ACP842,246(2006)

W.Detmold et al.,PRD76,114503(2007)

➤ **Method which utilizes the Bethe-Salpeter wave function**

Ishii, Aoki, Hatsuda, PRL99,022011(2007).

Nemura, Ishii, Aoki, Hatsuda, PLB673,136(2009).

Aoki, Hatsuda, Ishii, CSD1,015009(2008).

Aoki, Hatsuda,Ishii, PTP123,89(2010).

➤ **Strong coupling limit**

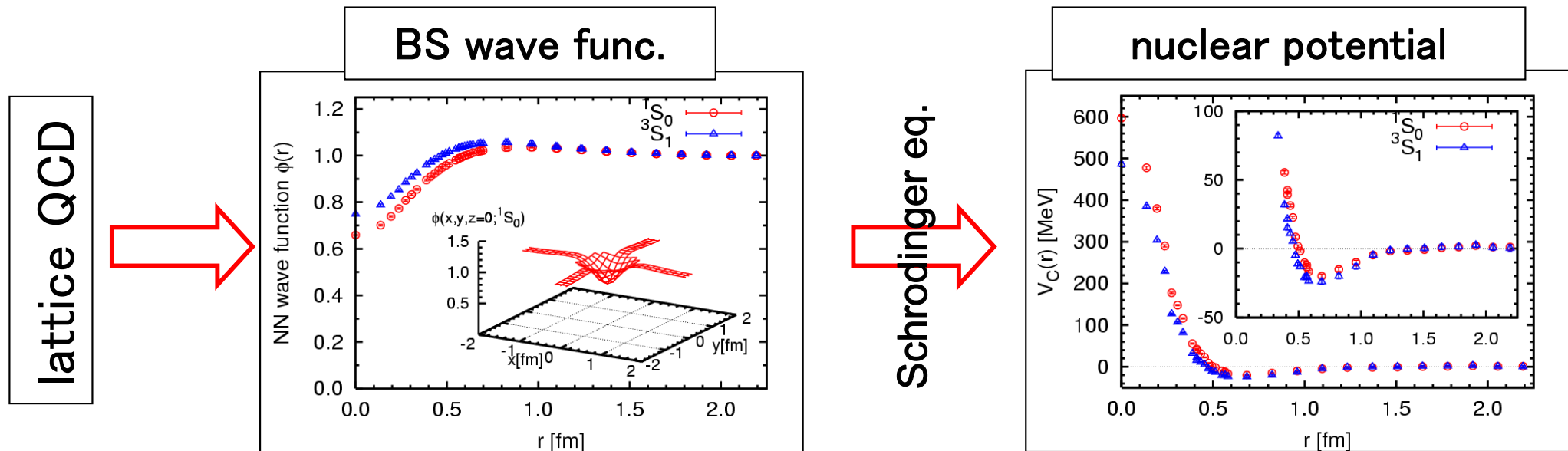
Ph. de Forcrand and M.Fromm, PRL104,112005(2010).

Nuclear force by lattice QCD

(5)

- Method which utilizes BS wave function

[Ishii,Aoki,Hatsuda,PRL99,022001(2007)]



➤ Advantages

- ◆ An extension to the Luscher's finite volume method for scattering phase shift.
- ◆ Asymptotic form of BS wave function ($r \rightarrow$ large)

$$\langle 0 | N(\vec{x})N(\vec{0}) | N(\vec{k})N(-\vec{k}), in \rangle \simeq Z_N e^{i\delta(k)} \frac{\sin(kr + \delta(k))}{kr} + \dots$$

is used to construct NN potentials, which can reproduce the NN scattering data.

- ◆ Scattering data is not needed in constructing hadron potentials.
 - ➔ It is usable to experimentally difficult objects such as hyperon potentials (YN and YY) and three nucleon potentials (NNN).

- General Strategy and Derivative expansion
- Central potential
- How good is the derivative expansion ?
- Tensor potential
- 2+1 flavor QCD results
- Hyperon potential
- Summary and Outlook

General Strategy

- **Bethe-Salpeter (BS) wave function (equal time)**

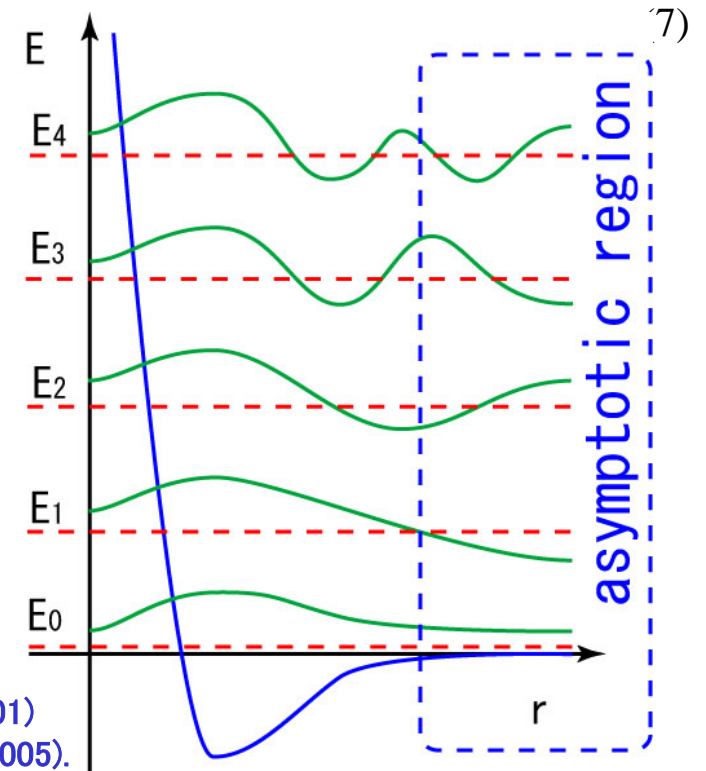
$$\psi(\vec{x} - \vec{y}) \equiv \langle 0 | N(\vec{x})N(\vec{y}) | N(\vec{k})N(-\vec{k}), in \rangle$$

- An amplitude to find (quite naïve picture)
3 quark at x and another 3 quark at y

- desirable asymptotic behavior as $r \rightarrow$ large.

$$\psi(\vec{r}) = Z_N e^{i\delta(k)} \frac{\sin(kr + \delta(k))}{kr} + \dots$$

C.-J.D.Lin et al., NPB619,467(2001)
CP-PACS Coll., PRD71,094504(2005).



- **Definition of nuclear potential (E-independent non-local)**

$$(E - H_0)\psi_E(\vec{x}) \equiv \int d^3 y U(\vec{x}, \vec{y})\psi_E(\vec{y})$$

$U(x,y)$ is defined by demanding

$\psi_E(\vec{x})$ (at multiple energies E_n) satisfy this equation simultaneously.

Comments:

- (1) Exact phase shifts at $E = E_n$
- (2) As number of BS wave functions increases, the potential becomes more and more faithful to (Luesher's) phase shifts.
- (3) $U(x,y)$ does NOT depend on energy E .
- (4) $U(x,y)$ is most generally a non-local object.

Aoki,Hatsuda,Ishii, PTP123,89(2010).

General Strategy: Derivative expansion

(8)

We construct $U(x,y)$ step by step.

- Derivative expansion of the non-local potential

$$S_{12} \equiv 3(\vec{\sigma}_1 \cdot \vec{r})(\vec{\sigma}_2 \cdot \vec{r})/r^2 - \vec{\sigma}_1 \cdot \vec{\sigma}_2$$

$$U(\vec{x}, \vec{y}) = V(\vec{x}, \vec{\nabla}) \delta(\vec{x} - \vec{y})$$

$$V(\vec{x}, \vec{\nabla}) = V_C(r) + V_T(r) \cdot S_{12} + V_{LS}(r) \cdot \vec{L} \cdot \vec{S} + \{V_D(r), \vec{\nabla}^2\} + \dots$$

- Leading Order:

Use BS wave function of the lowest-lying state to obtain $V_C(r), V_T(r)$

$$V(\vec{x}, \vec{\nabla}) = V_C(r) + V_T(r) \cdot S_{12} + \cancel{O(\vec{\nabla})}$$

Example (1S_0): Only $V_C(r)$ survives for 1S_0 channel:

$$(E - H_0) \psi_E(\vec{x}) = V_C(r) \psi_E(\vec{x}) \quad \Longrightarrow \quad V_C(r) = \frac{(E - H_0) \psi_E(\vec{x})}{\psi_E(\vec{x})}$$

- Next to Leading Order:

Include another BS wave function to obtain $V_C(r), V_T(r), V_{LS}(r)$

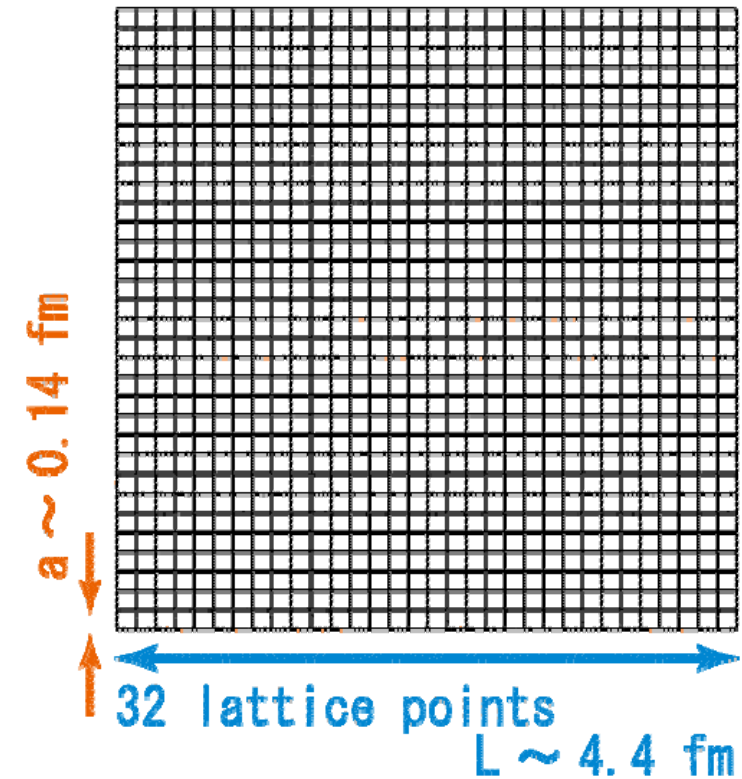
$$V(\vec{x}, \vec{\nabla}) = V_C(r) + V_T(r) \cdot S_{12} + V_{LS}(r) \cdot \vec{L} \cdot \vec{S} + \cancel{O(\vec{\nabla}^2)}$$

- Repeat this procedure to obtain higher derivative terms.

$$V(\vec{x}, \vec{\nabla}) = V_C(r) + V_T(r) \cdot S_{12} + V_{LS}(r) \cdot \vec{L} \cdot \vec{S} + \{V_D(r), \vec{\nabla}^2\} + \cancel{O(\vec{\nabla}^3)}$$

Numerical Setups

- Quenched QCD
plaquette gauge + Wilson quark action
 $m_{\pi} = 380 - 730 \text{ MeV}$
 $a = 0.137 \text{ fm}$, $L = 32a = 4.4 \text{ fm}$

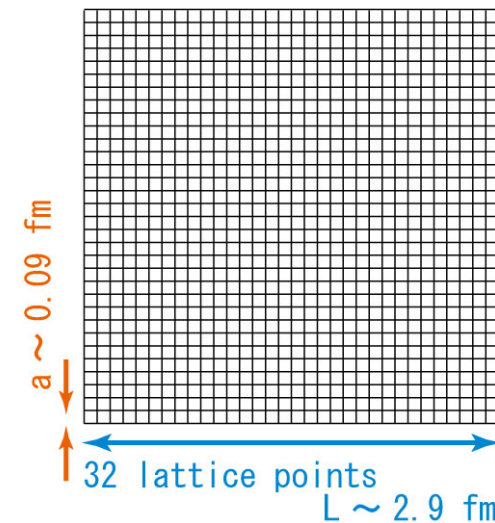


- 2+1 flavor QCD (by PACS-CS)
Iwasaki gauge + clover quark action
 $m_{\pi} = 411 - 700 \text{ MeV}$
 $a = 0.091 \text{ fm}$, $L = 32a = 2.9 \text{ fm}$

PACS-CS@Tsukuba



T2K@Tsukuba



BS wave function

(10)

BS wave function is obtained in the large t region of nucleon four point function.

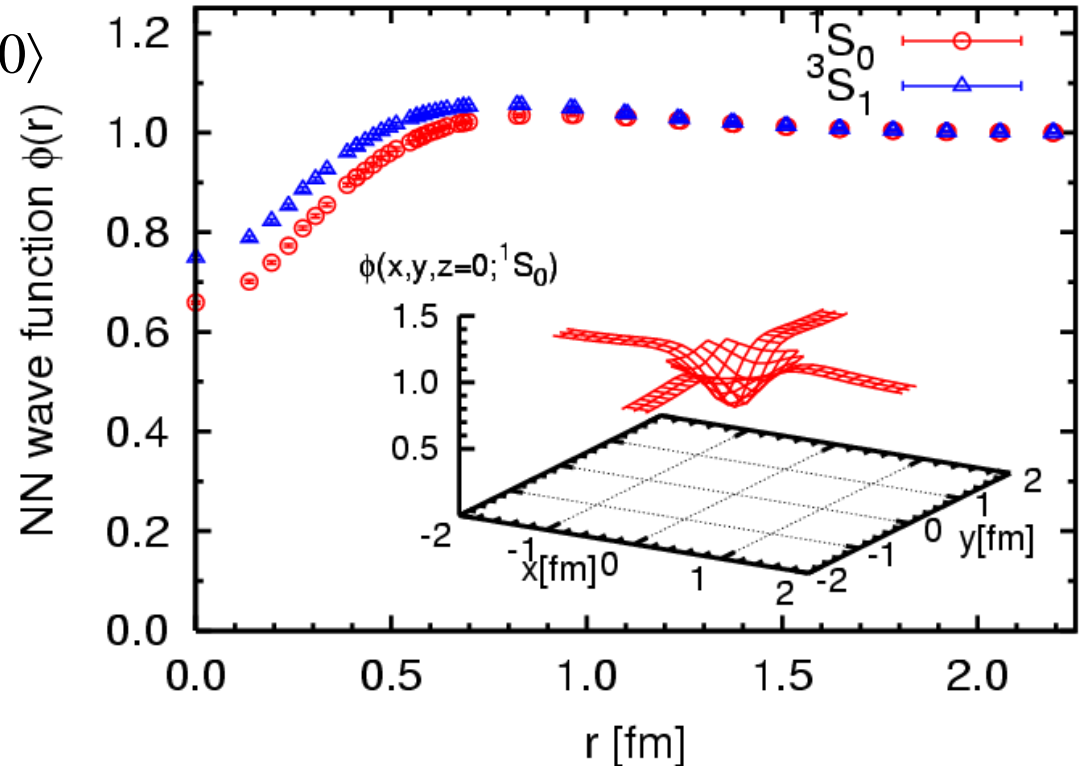
$$\psi(\vec{x} - \vec{y}) \equiv \langle 0 | N(\vec{x})N(\vec{y}) | NN \rangle$$

$$\begin{aligned} & \langle 0 | T[N(\vec{x}, t)N(\vec{y}, t)\bar{N}\bar{N}(t_0)] | 0 \rangle \\ &= \sum_n \langle 0 | N(\vec{x})N(\vec{y}) | n \rangle e^{-(t-t_0)E_n} \langle n | \bar{N}\bar{N} | 0 \rangle \\ &= \sum_n \psi_n(\vec{x} - \vec{y}) A_n e^{-(t-t_0)E_n} \end{aligned}$$

We adopted

$$p(x) = \epsilon_{abc} \left(u_a^T C \gamma_5 d_b \right) u_c(x)$$

$$n(x) = \epsilon_{abc} \left(u_a^T C \gamma_5 d_b \right) d_c(x)$$

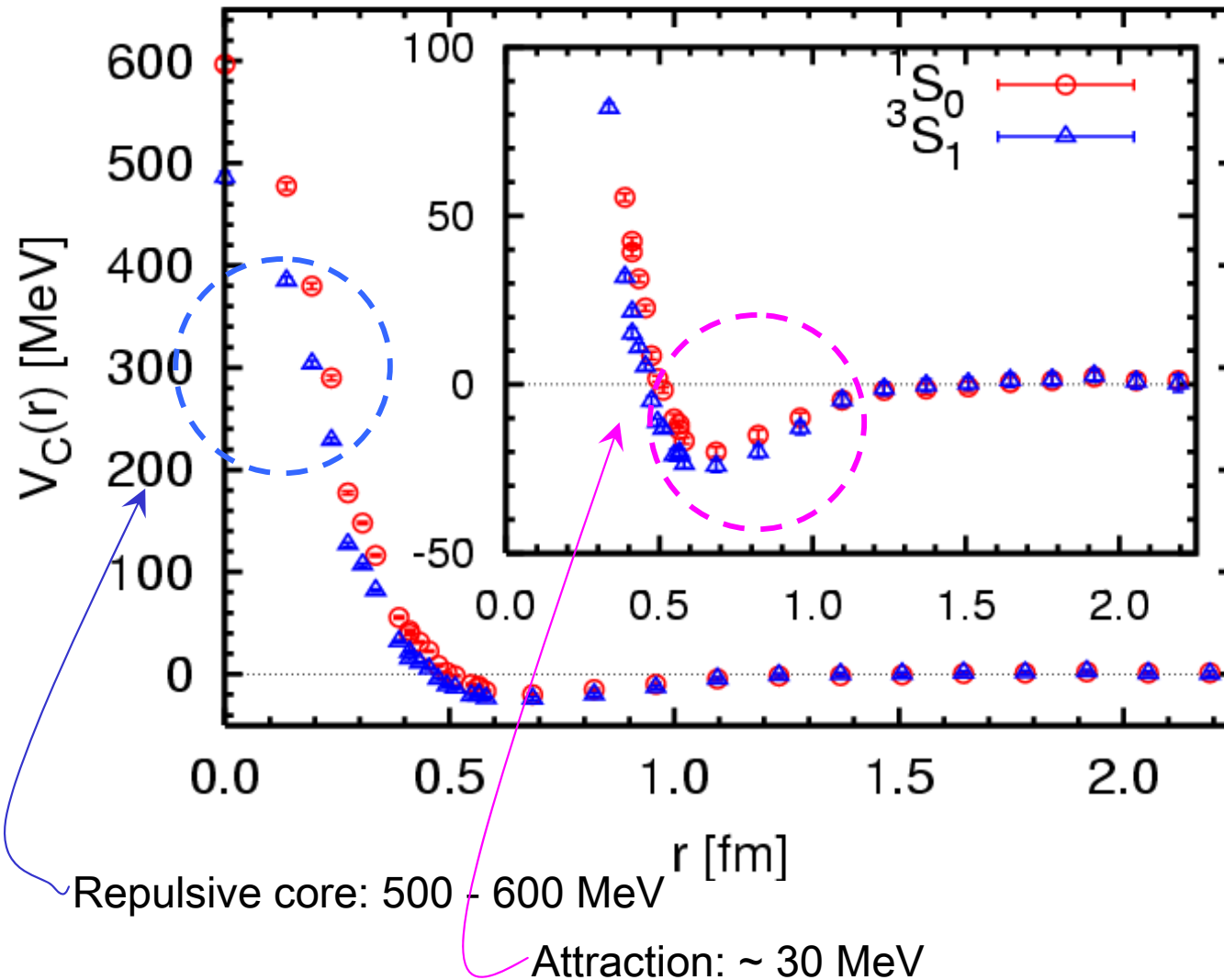


Comments

- ◆ As far as the proper asymptotic form is satisfied, any interpolating fields can be used.
- ◆ They lead to phase equivalent potentials.
 - ◆ Good choice \leftrightarrow potentials with small non-locality and small E dependence.
 - Bad choice \leftrightarrow highly non-local potential or highly E dependent potential.

Central potential (leading order) by quenched QCD

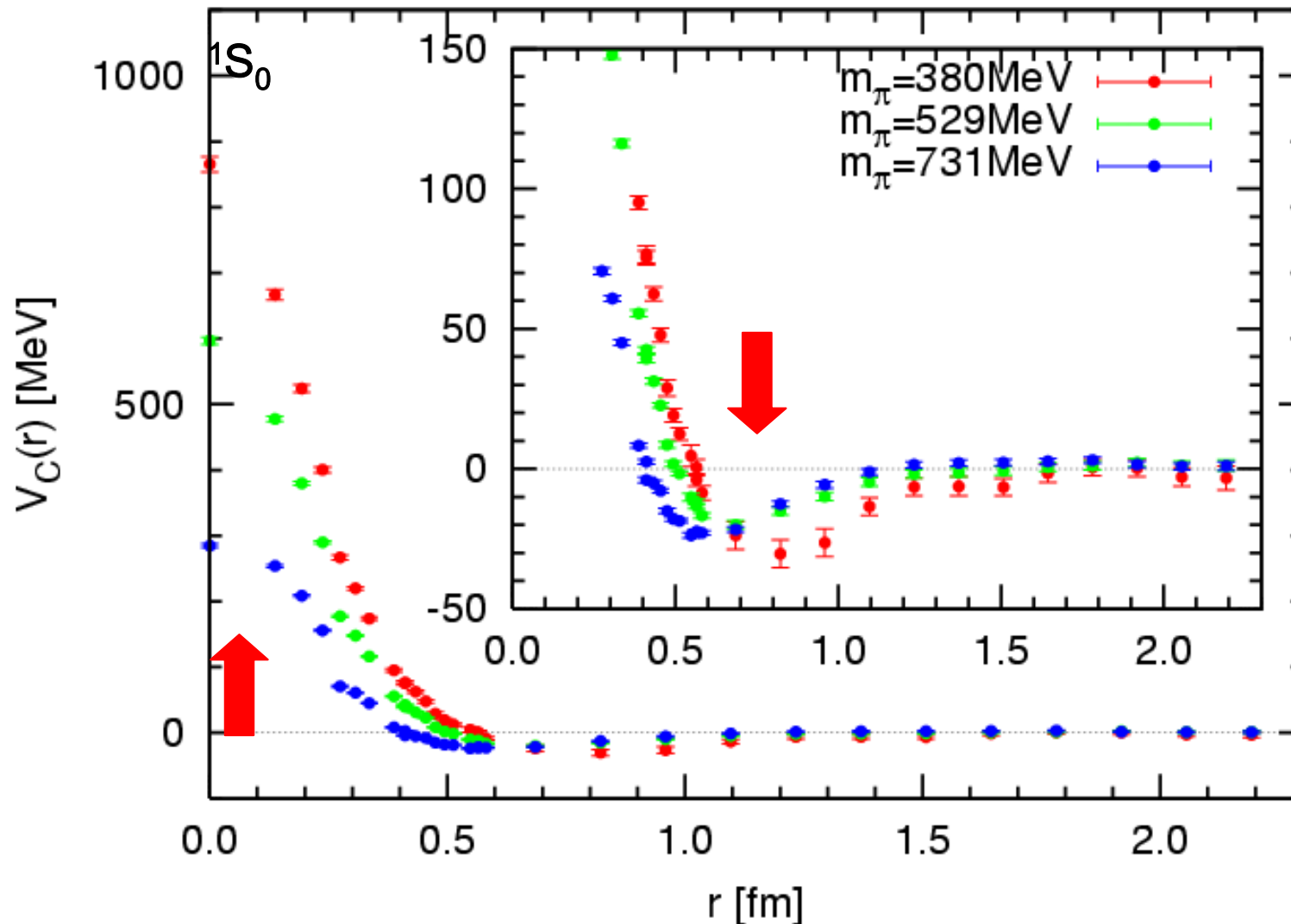
(11)



$$V_C(r) = \frac{(E - H_0)\psi_E(\vec{x})}{\psi_E(\vec{x})}$$

Qualitative features of the nuclear force are reproduced.

Quark mass dependence



In the light quark mass region,

- ✓ The repulsive core grows rapidly.
- ✓ Attraction gets stronger.

How good is the derivative expansion ?

(13)

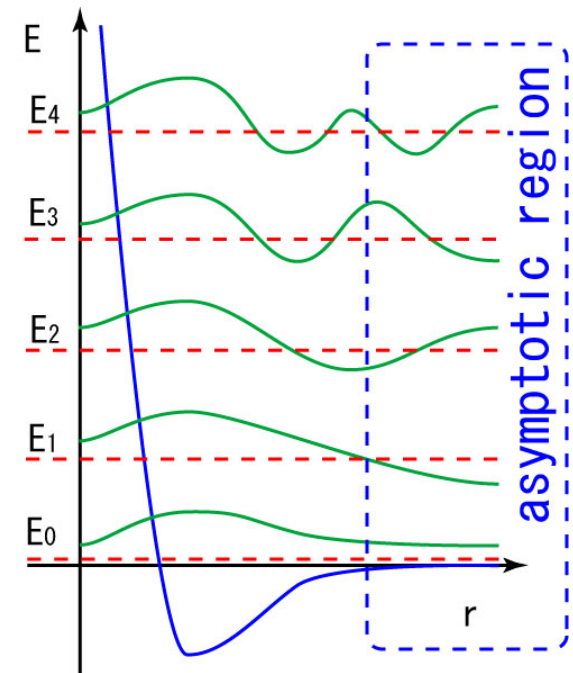
- **The non-local potential $U(\vec{x}, \vec{y})$** is faithful to scattering data in wide range of energy region (by construction)

- ◆ Def. by effective Schroedinger eq.

$$(E - H_0) \psi_E(\vec{x}) \equiv \int d^3 y U(\vec{x}, \vec{y}) \psi_E(\vec{y})$$

- ◆ Desirable asymptotic behavior at large separation

$$\psi(\vec{r}) = Z_N e^{i\delta(k)} \frac{\sin(kr + \delta(k))}{kr} + \dots$$



- **The local potential at $E \sim 0$**
(obtained at leading order derivative expansion)

$$U(\vec{x}, \vec{y}) = \left(V_C(r) + V_T(r) \cdot S_{12} + V_{LS}(r) \cdot \vec{L} \cdot \vec{S} + \{ V_D(r) \cdot \vec{\nabla}^2 \} + \dots \right) \delta(\vec{x} - \vec{y})$$

is faithful to scattering data only at $E \sim 0$ (scattering length).

However, it is not guaranteed to reproduce the scattering data at different energy.

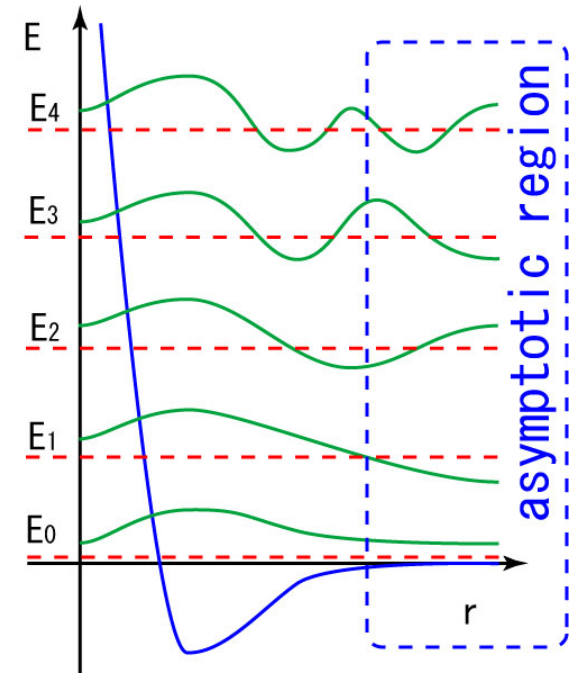
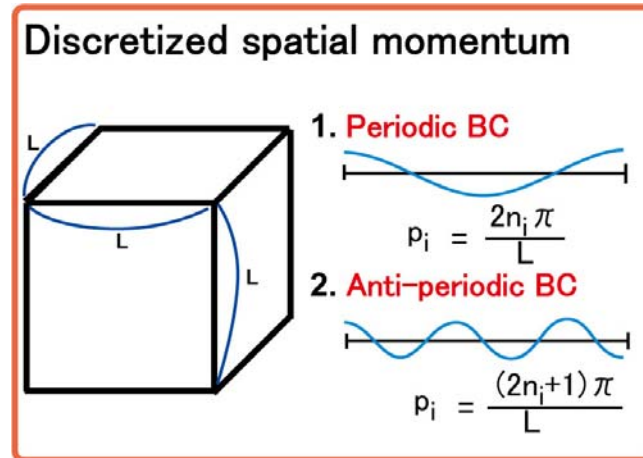
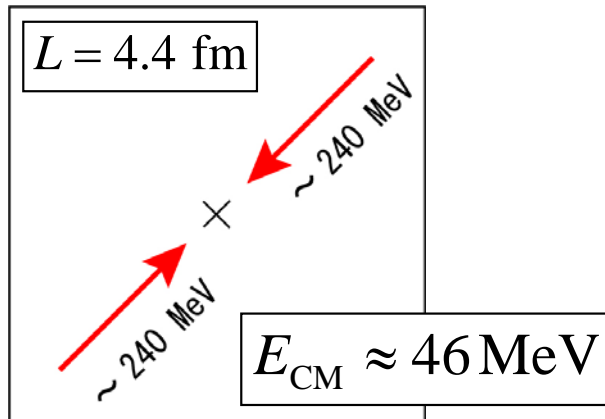


Convergence of the derivative expansion has to be examined in order to see its validity in the different energy region.

How good is derivative expansion ?

Strategy:

- generate two local potentials at different energies
Potential at $E \neq 0$ is constructed by anti-periodic BC



- Difference \leftrightarrow truncation error (of derivative expansion)
= size of higher order effect (= non-locality)
- $V_C(r)$ at $E \sim 0 \text{ MeV}$
- $V_C(r)$ at $E \sim 46 \text{ MeV}$

$$U(\vec{x}, \vec{y}) = \left(V_C(r) + V_T(r) \cdot S_{12} + V_{LS}(r) \cdot \vec{L} \cdot \vec{S} + \{V_D(r) \cdot \vec{\nabla}^2\} + \dots \right) \delta(\vec{x} - \vec{y})$$

How good is the derivative expansion ? (cont'd)

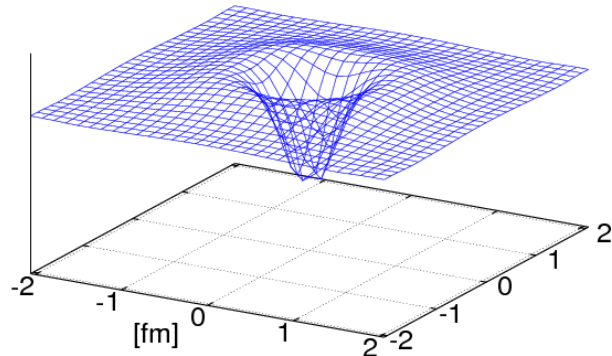
(15)

BS wave functions

[K.Murano@Lattice2009]

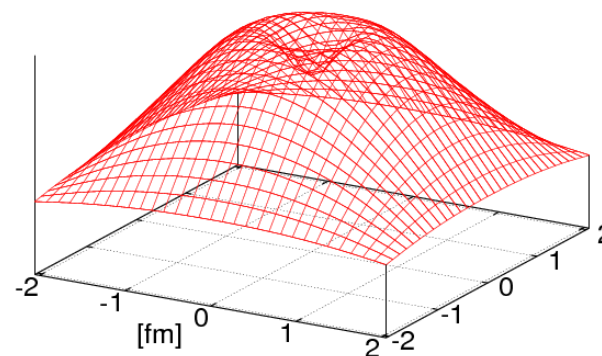
$E \sim 0$ MeV

PBC BS wave function



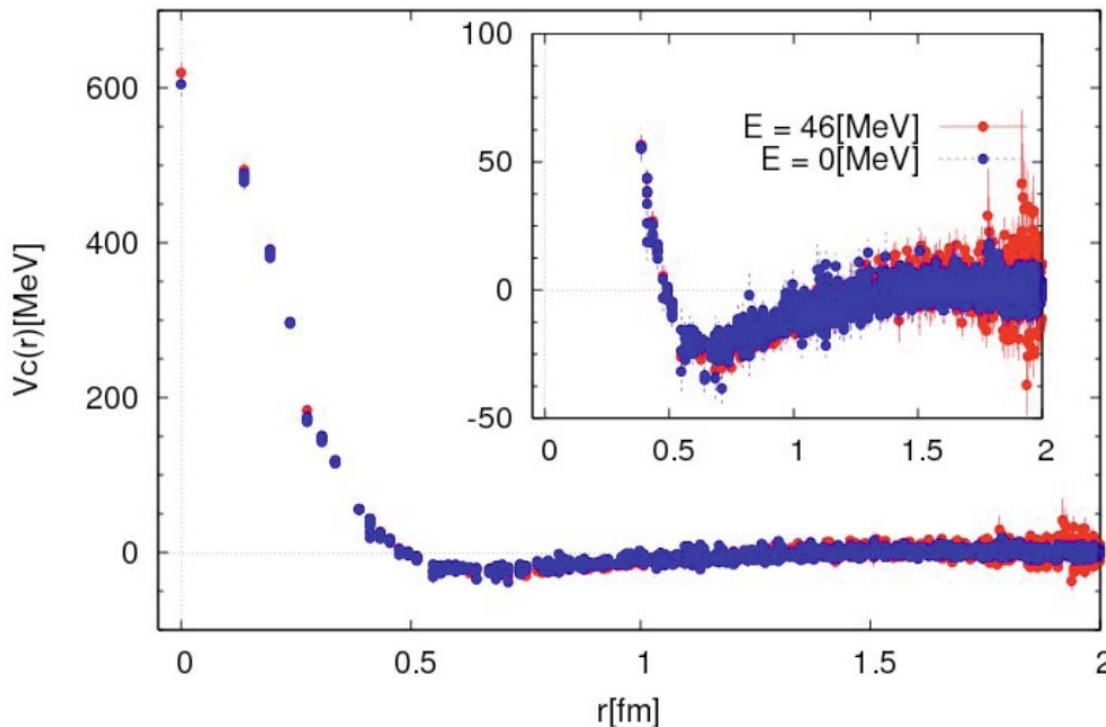
$E \sim 46$ MeV

APBC BS wave function



Potentials

$V_c(r; {}^1S_0)$: PBC v.s. APBC $t=10$



➤ Small discrepancy at short distance.
(really small)

◆ Derivative expansion works.

◆ Local potential is safely used
in the region $E_{CM} = 0 - 46$ MeV

➤ Non-locality may increase,
if we go close to the pion threshold.
($NN \rightarrow NN \pi$)

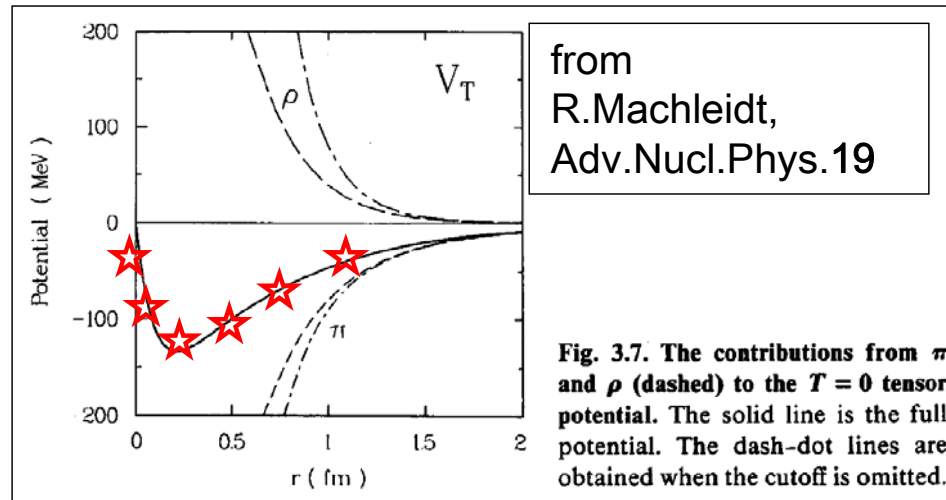
$E_{CM} \sim 530$ MeV. (in our setup)

Tensor Potential

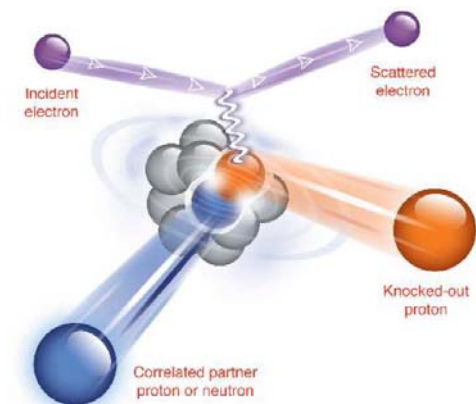
Tensor potential

Background

- Phenomenologically important for
 - Nuclear saturation density and stability of nuclei.
 - Huge influence on the structures of nuclei
 - Mixing of s-wave and d-wave → deuteron
- In OBEP picture, it is obtained from a cancellation between π and ρ .



- Tensor force at short distance is important for **Short Range Correlated (SRC) nucleon pair** and **cold dense nuclear system** such as neutron star
[\[R.Subedi et al., SCIENCE320,1476\(2008\)\]](#)



d-wave BS wave function

(18)

BS wave function for $J^P=1^+$ consists of two orbital components:

s-wave ($l=0$) and **d-wave** ($l=2$)

On the lattice, we prepare T_1^+ state ($\leftrightarrow J^P=1^+$), and decompose it as

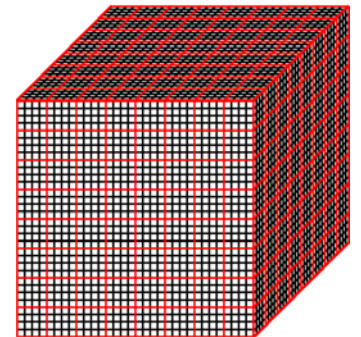
(1) **s-wave** (\leftrightarrow Orbitally A_1^+)

$$\psi_{\alpha\beta}^{(S)}(\vec{r}) = P[\psi](\vec{r}) \equiv \frac{1}{24} \sum_{g \in O} \psi_{\alpha\beta}(g^{-1}\vec{r})$$

(2) **d-wave** (\leftrightarrow Orbitally non- A_1^+)

$$\psi_{\alpha\beta}^{(D)}(\vec{r}) = Q[\psi](\vec{r}) \equiv \psi_{\alpha\beta}(\vec{r}) - \psi_{\alpha\beta}^{(S)}(\vec{r})$$

The cubic group



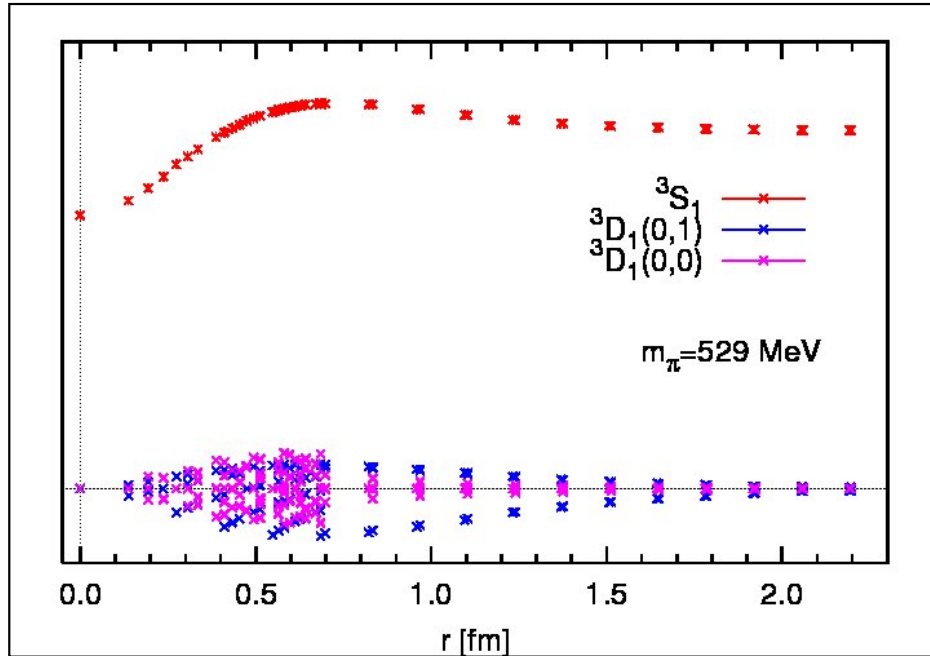
Up to higher order ($l \geq 4$), s-wave and d-wave can be separated.

d-wave BS wave function

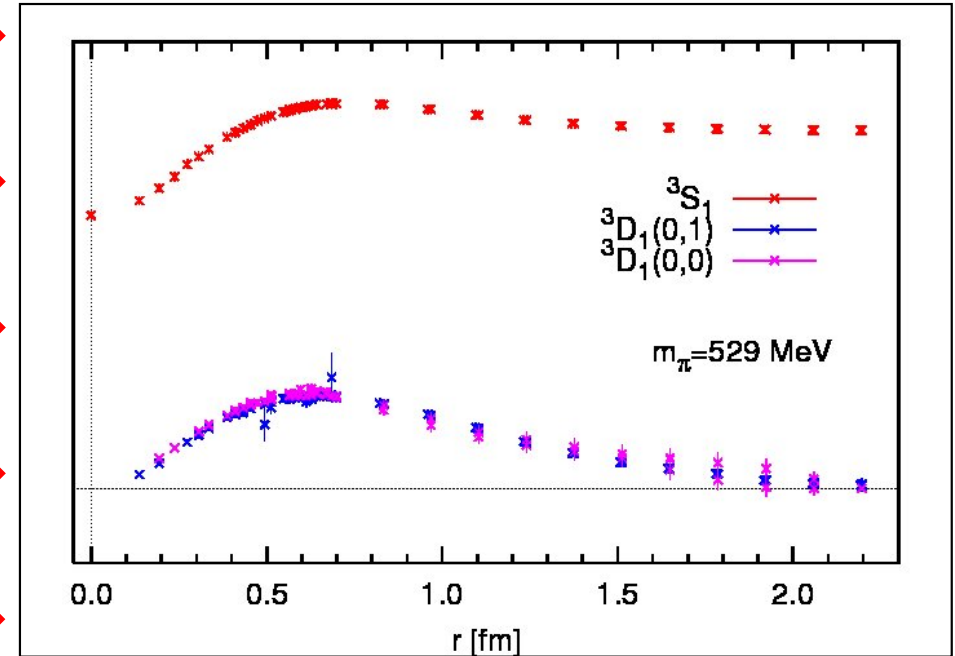
(19)

$$J^P = 1^+, M=0$$

BS wave func. for T_1^+ (total) state



divide it by Y_{1m} and by CG factor



Angular dependence \rightarrow Multi-valued

d-wave \propto "spinor harmonics"

$$\begin{bmatrix} \psi_{\uparrow\uparrow}^{(D)}(\vec{r}) & \psi_{\uparrow\downarrow}^{(D)}(\vec{r}) \\ \psi_{\downarrow\uparrow}^{(D)}(\vec{r}) & \psi_{\downarrow\downarrow}^{(D)}(\vec{r}) \end{bmatrix} \propto \begin{bmatrix} Y_{2,-1}(\hat{r}) & -\frac{2}{\sqrt{6}}Y_{2,0}(\hat{r}) \\ -\frac{2}{\sqrt{6}}Y_{2,0}(\hat{r}) & Y_{2,+1}(\hat{r}) \end{bmatrix}$$

Almost Single-valued

$\rightarrow \psi^{(D)}$ is dominated by d-wave.
($l \geq 4$ contamination is small)

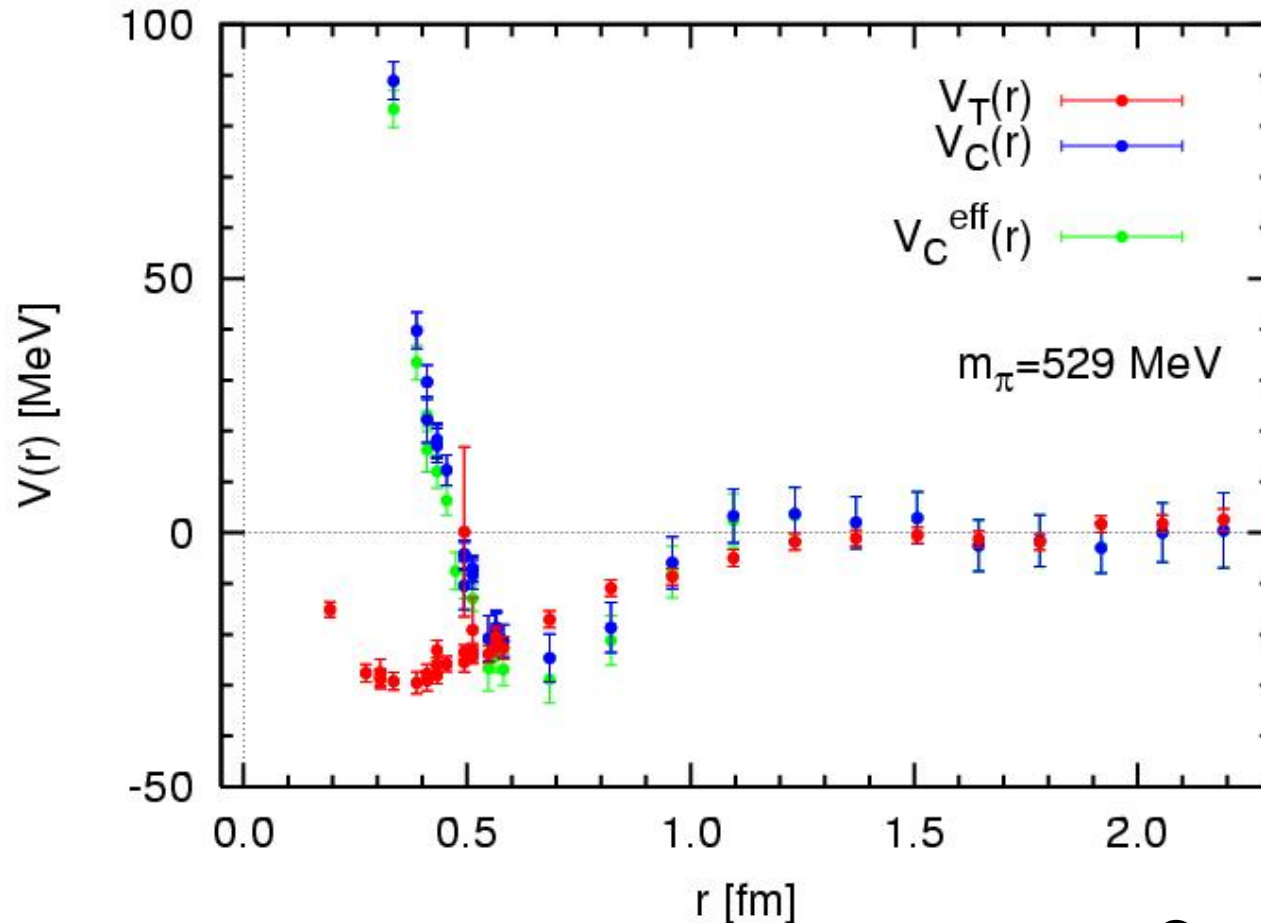
Tensor force (cont'd)

$$\{H_0 + V_C(\vec{r}) + V_T(\vec{r})S_{12}\}\psi(\vec{r}) = E\psi(\vec{r})$$



$$V_C(\vec{r}) \cdot P\psi(\vec{r}) + V_T(\vec{r}) \cdot PS_{12}\psi(\vec{r}) = (E - H_0) \cdot P\psi(\vec{r}) \quad (\text{s-wave})$$

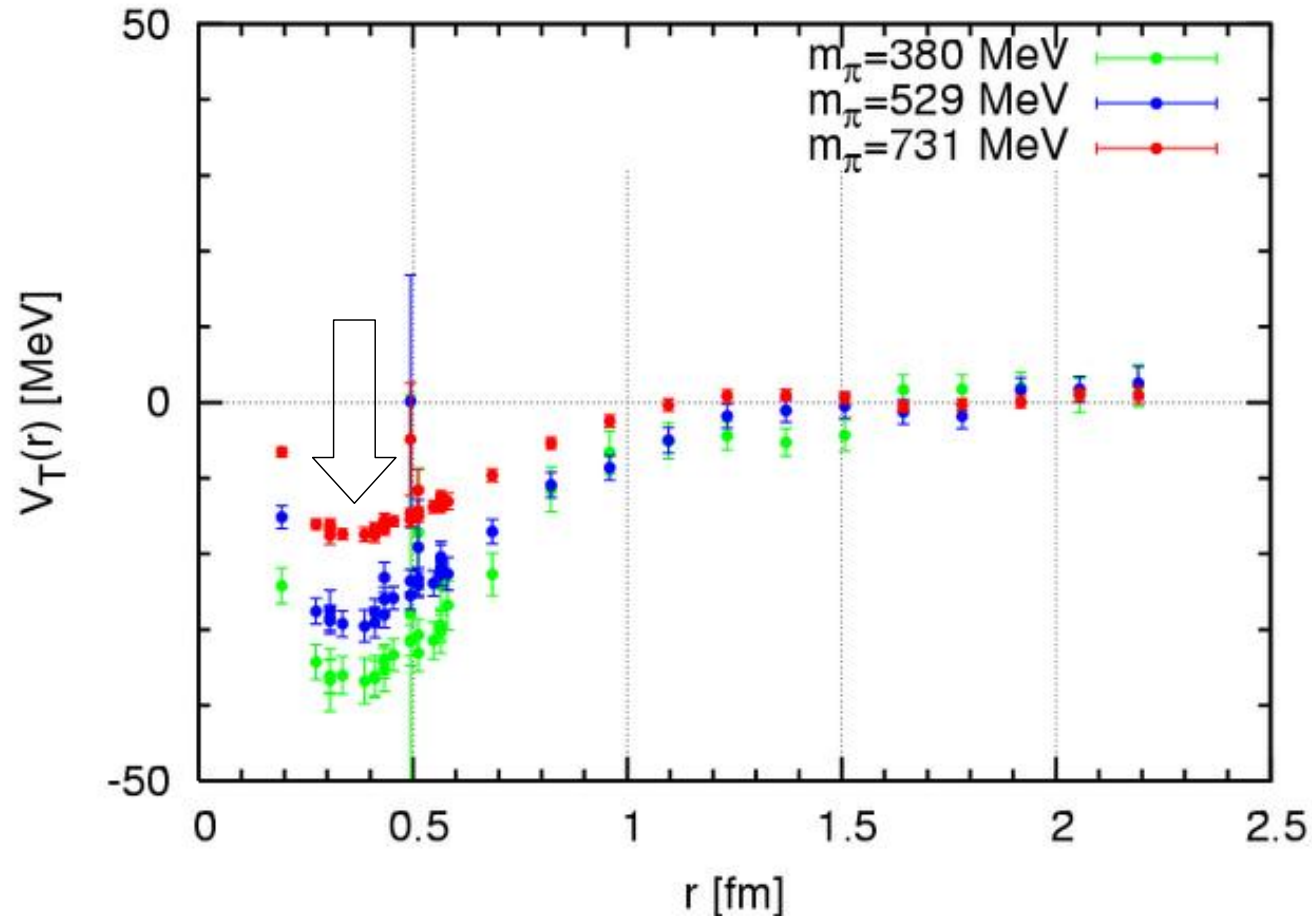
$$V_C(\vec{r}) \cdot Q\psi(\vec{r}) + V_T(\vec{r}) \cdot QS_{12}\psi(\vec{r}) = (E - H_0) \cdot Q\psi(\vec{r}) \quad (\text{d-wave})$$



Qualitative feature is reproduced.

Tensor potential (quark mass dependence)

(21)



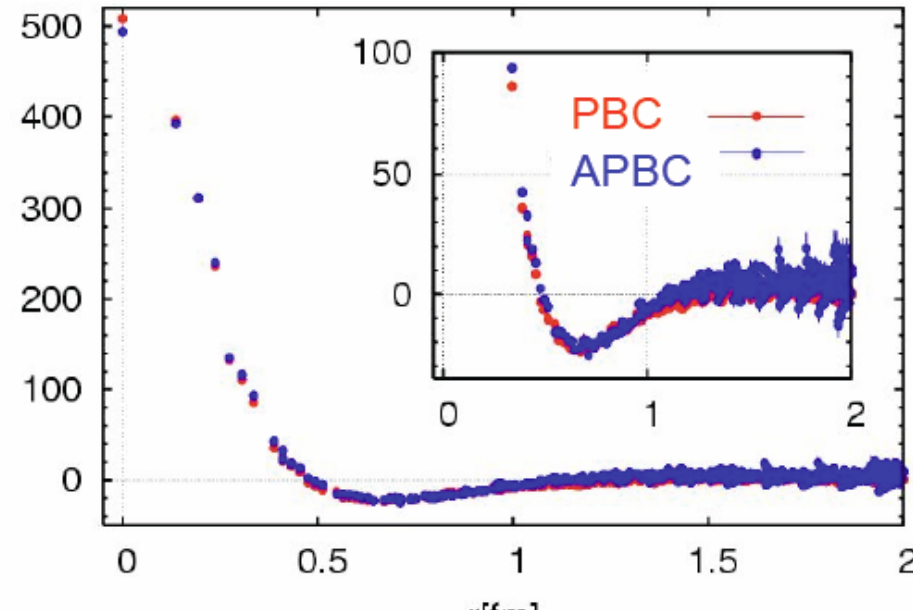
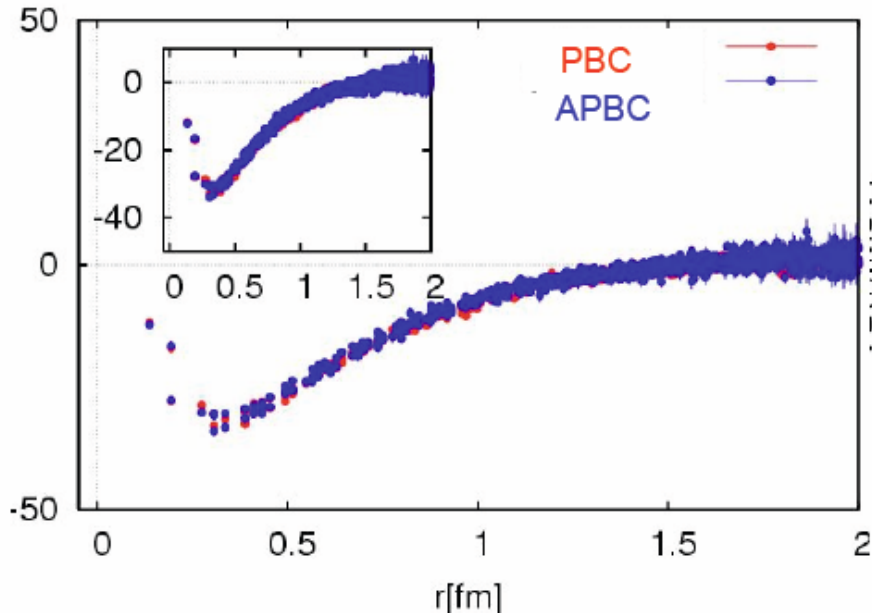
Tensor potential is enhanced in the light quark mass region

Energy dependence of tensor force

Energy dependence is weak for $J^P=1^+$

$t=9$ ${}^3S_1 - {}^3D_1$ $V_T(r)$

3S_1 $V_C(r)$



APBC and PBC are consistent with each other.

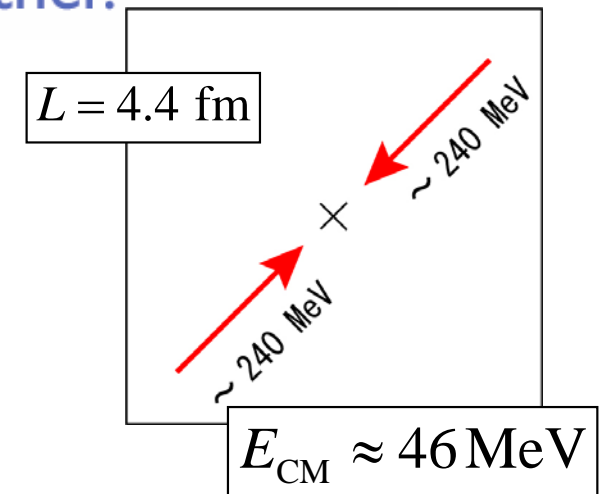
$E \sim 46$ MeV $E \sim 0$ MeV

Small energy dependence implies

→ Derivative expansion works.

These local potentials are safely used

in the energy region $E_{CM} = 0 - 46$ MeV.



2+1 flavor QCD

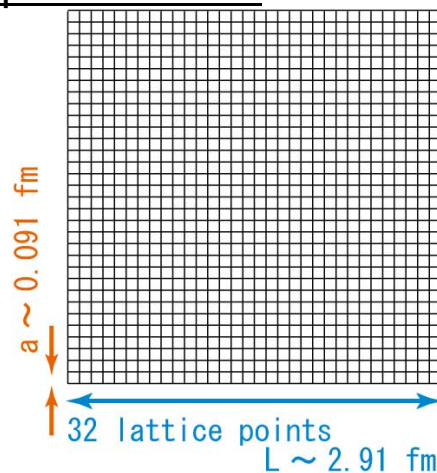
Gauge configurations by PACS-CS Collaboration

2+1 flavor PACS-CS gauge configuration

(24)

PACS-CS coll. is generating 2+1 flavor gauge configurations in significantly light quark mass region on a large spatial volume

- 2+1 flavor full QCD [PACSCS Coll. PRD79(2009)034503].
- Iwasaki gauge action at $\beta=1.90$ on $32^3 \times 64$ lattice
- $O(a)$ improved Wilson quark (clover) action with a non-perturbatively improved coefficient $c_{SW}=1.715$
- $1/a=2.17$ GeV ($a \sim 0.091$ fm). $L=32a \sim 2.91$ fm



PACS-CS



Available through ILDG/JLDG

$K_{ud}=0.13700$ $K_s=0.13640$	$M_{pi}=701$ MeV	$L=2.9$ fm
$K_{ud}=0.13727$ $K_s=0.13640$	$M_{pi}=570$ MeV	$L=2.9$ fm
$K_{ud}=0.13754$ $K_s=0.13640$	$M_{pi}=411$ MeV	$L=2.9$ fm
$K_{ud}=0.13754$ $K_s=0.13660$	$M_{pi}=384$ MeV	$L=2.9$ fm
$K_{ud}=0.13770$ $K_s=0.13640$	$M_{pi}=296$ MeV	$L=2.9$ fm
$K_{ud}=0.13781$ $K_s=0.13640$	$M_{pi}=156$ MeV	$L=2.9$ fm



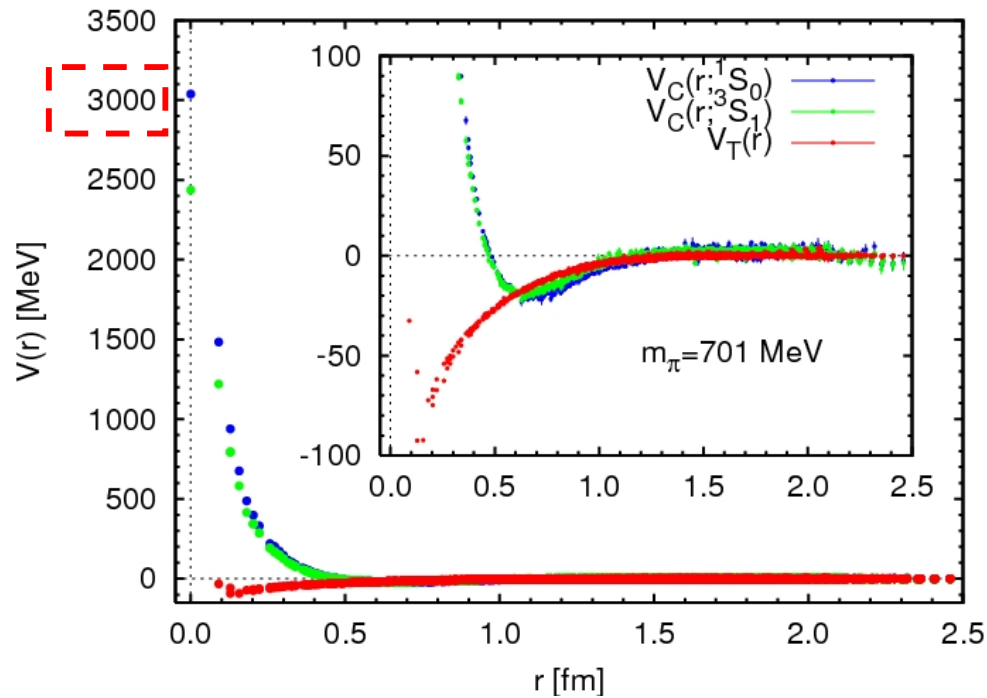
PACS-CS Coll. is currently generating 2+1 flavor gauge config's with **physical m_{pi}** on **$L \sim 6$ fm** lattice.

super computer T2K

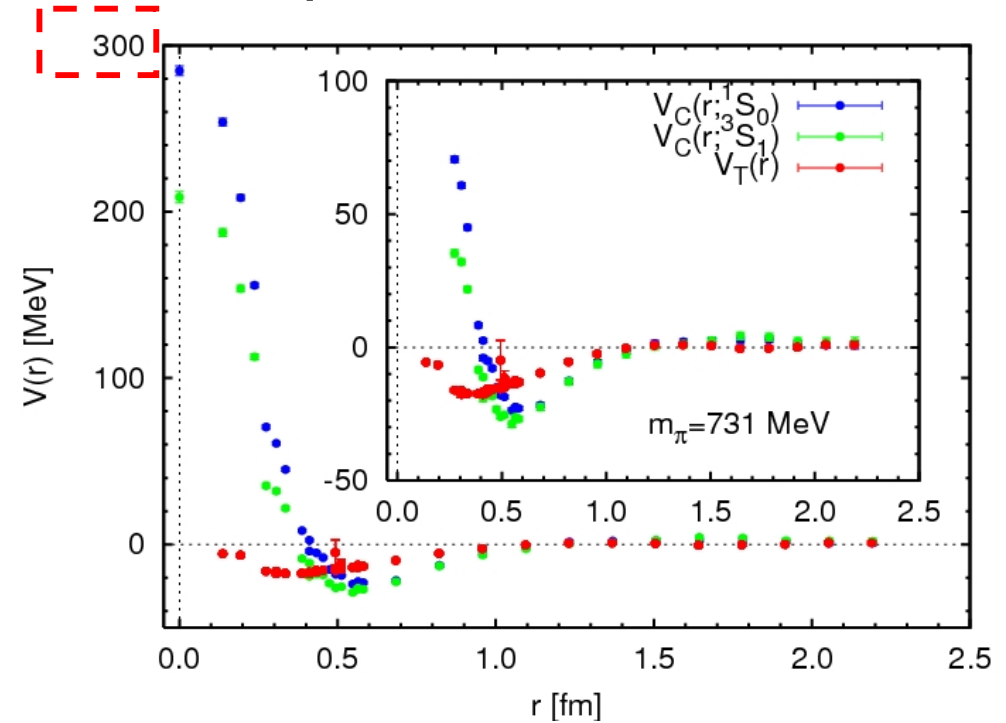


NN potentials

2+1 flavor results



quenched results

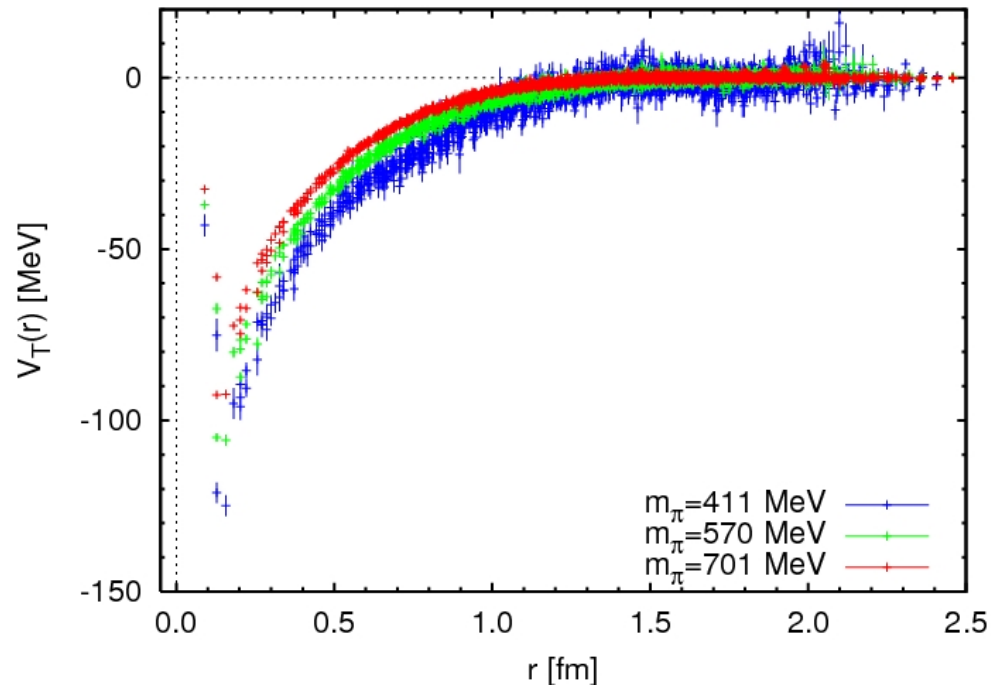
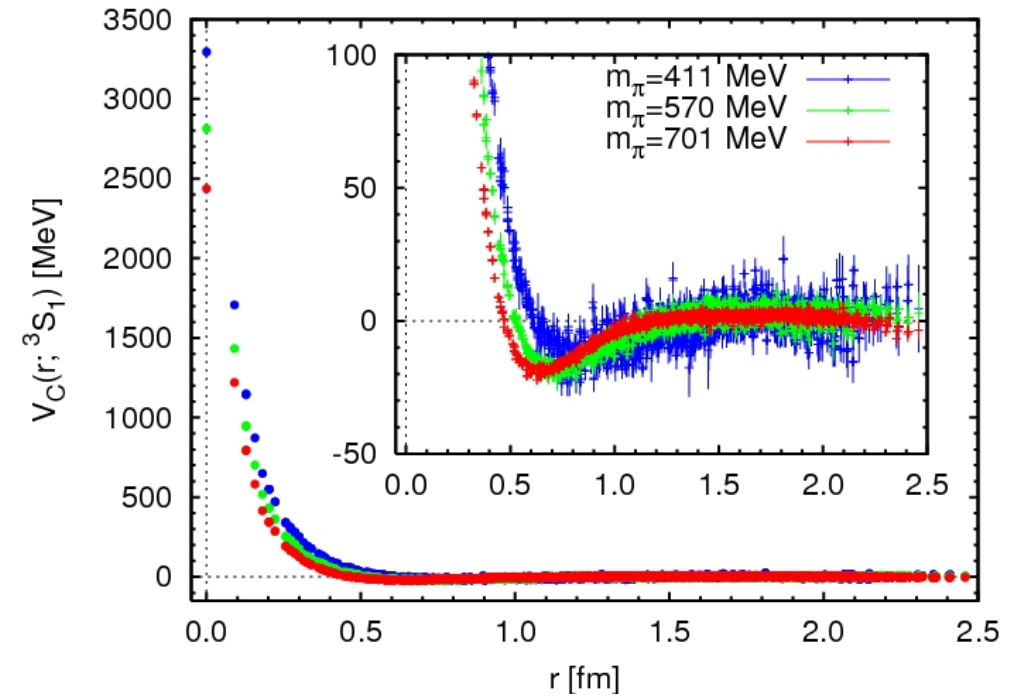
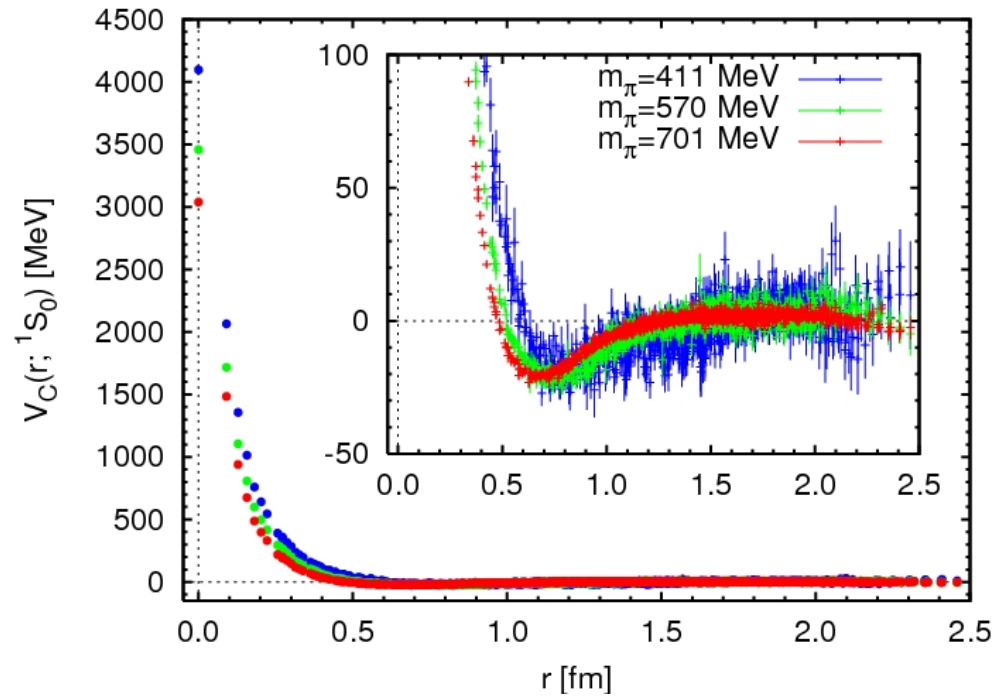


Comparing to the quenched ones,

- (1) Repulsive core and tensor force become significantly stronger.
Reasons are under investigation.
(Discretization artifact is another possibility)
- (2) Attractions at medium distance are similar in magnitude.

NN potentials (quark mass dependence)

(26)

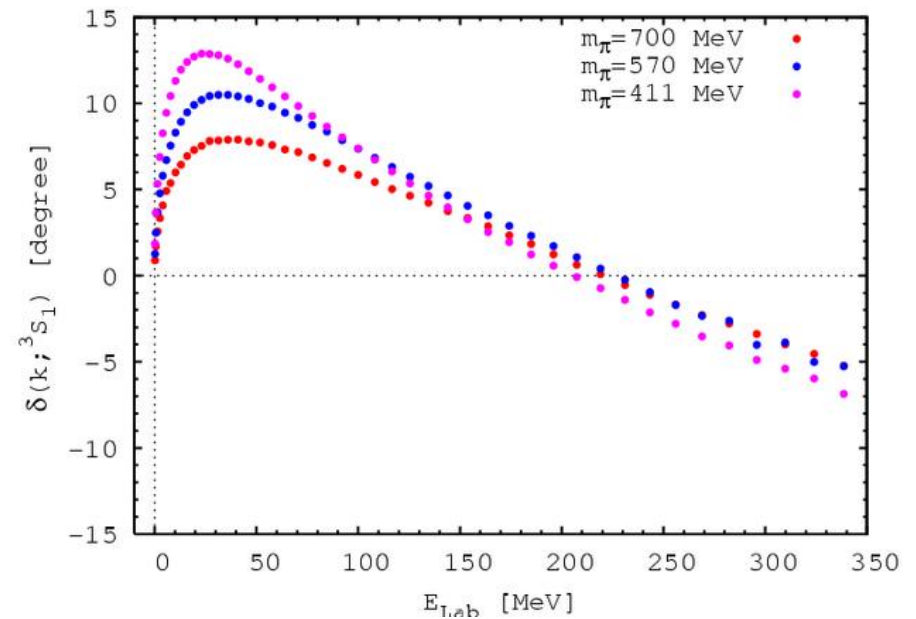
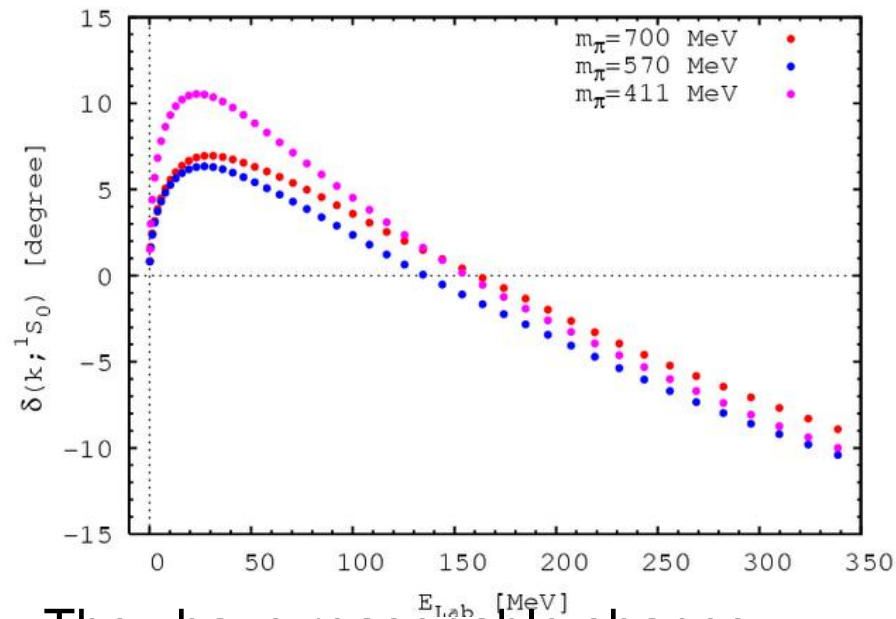
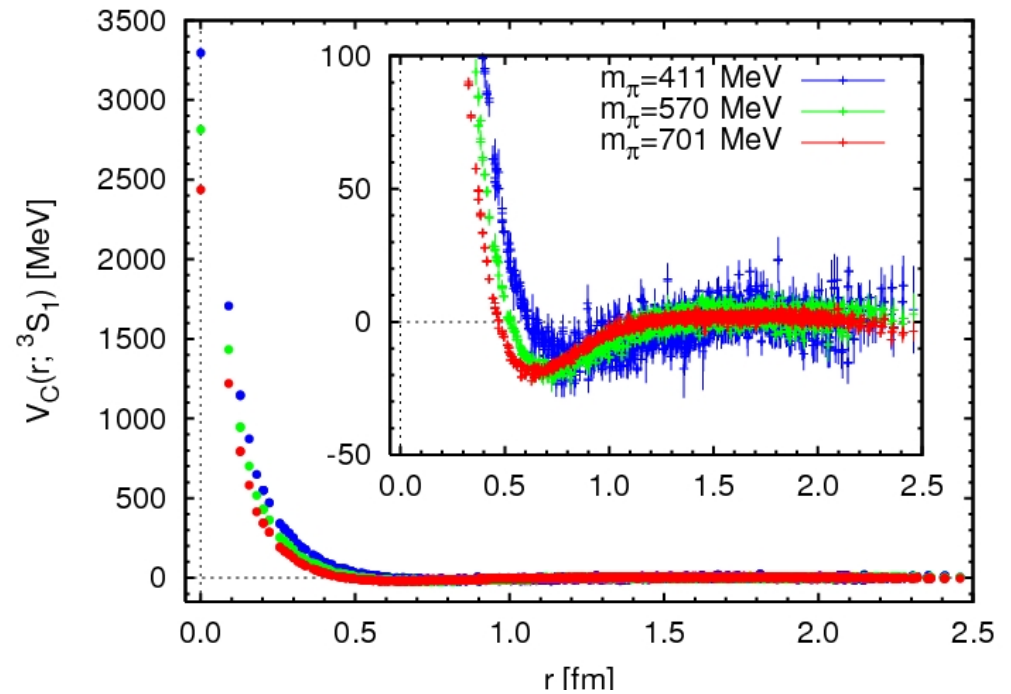
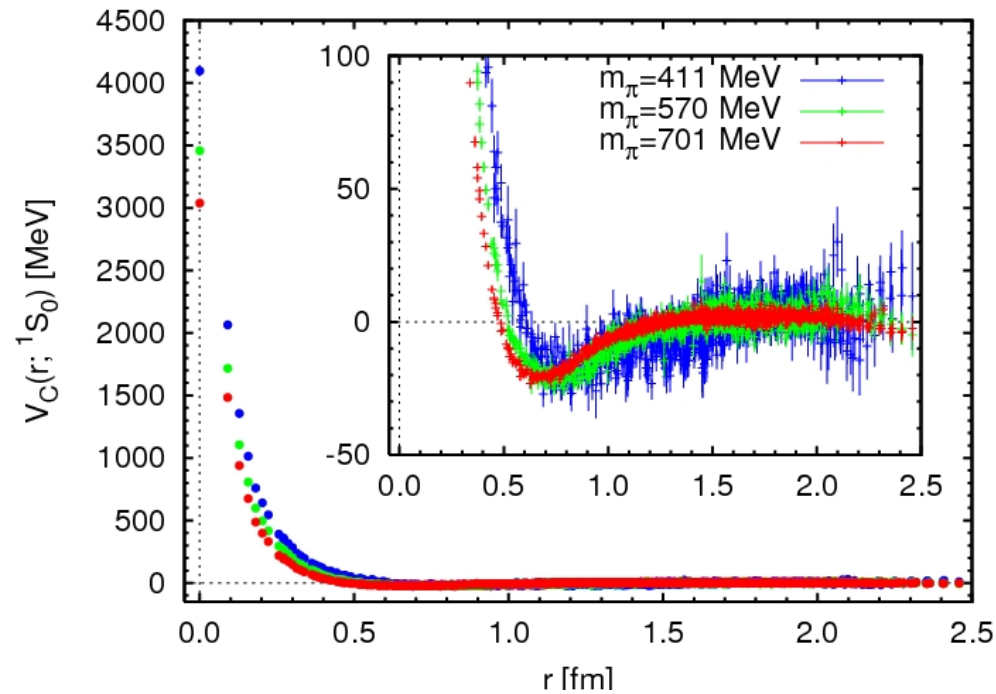


With decreasing quark mass,
interaction range becomes wider.

- Repulsive core grows.
- Attraction becomes stronger
- Tensor force gets stronger

NN (phase shift from potentials)

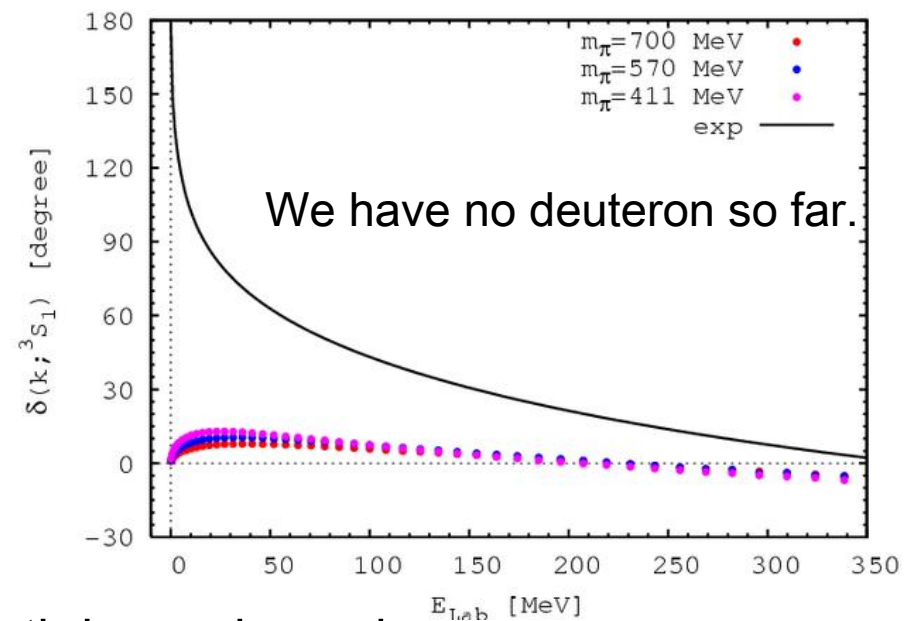
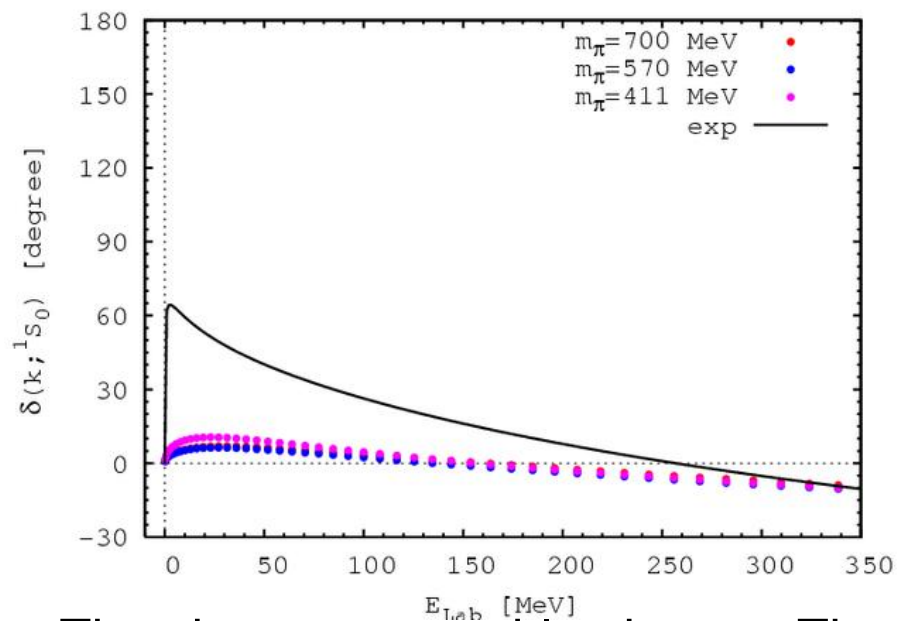
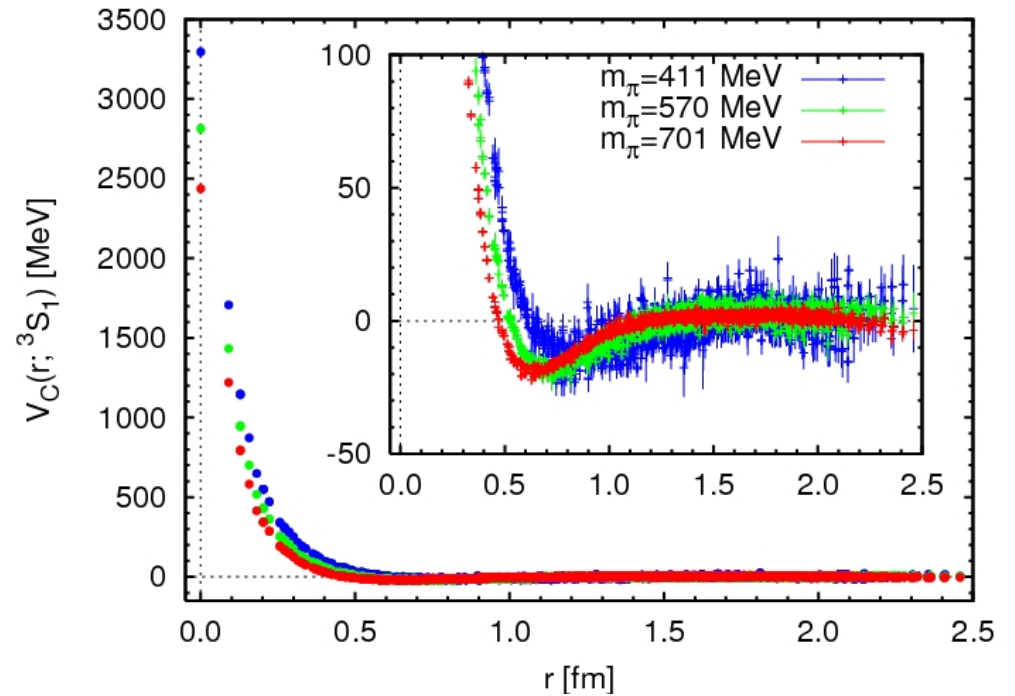
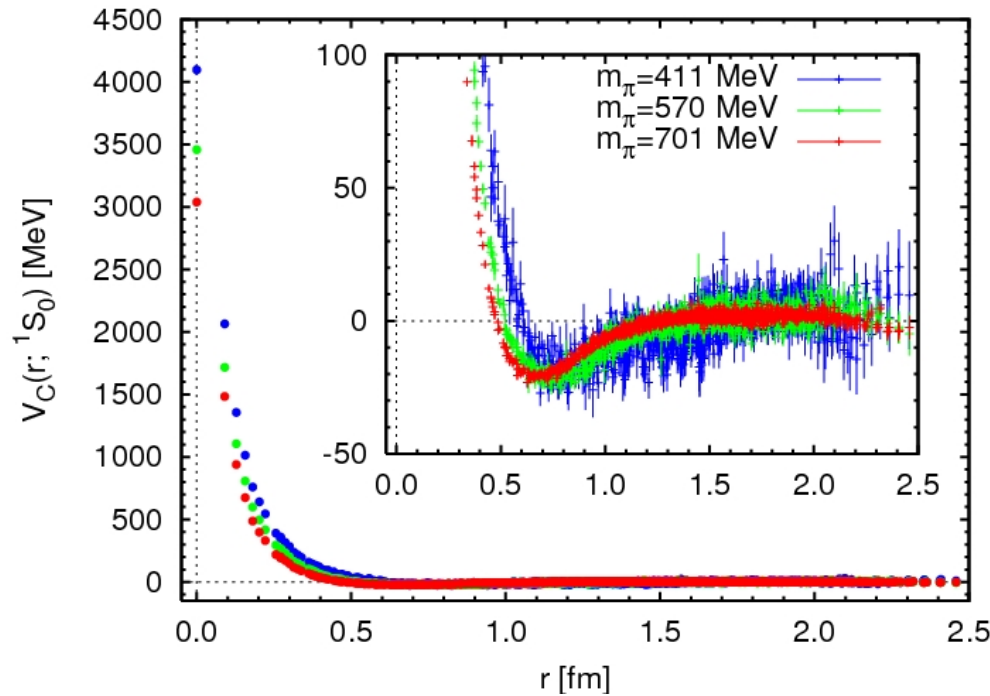
(27)



They have reasonable shapes.

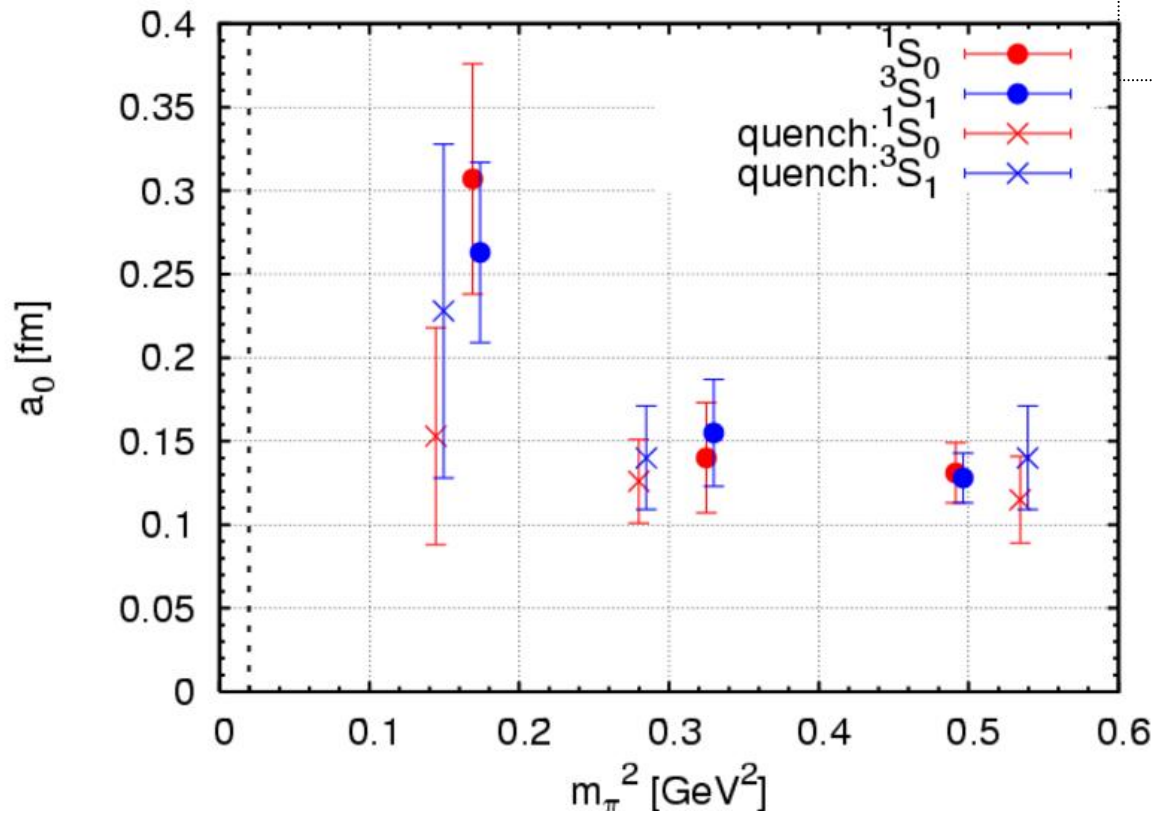
NN (phase shift from potentials)

(28)



They have reasonable shapes. The strength is much weaker.
(Similar behavior is seen in the scattering length.)

NN scattering length



wave function $\rightarrow k^2 \rightarrow$ Luscher's formula

➤ Attractive scattering length

particle physics convention

$a > 0 \leftrightarrow$ attractive

This is in conflict with NPLQCD results:
Repulsive scattering length.

S.R.Beane et al., PRL97,012001(2006).

S.R.Beane et al., arXiv:0912.4243.

Very weak scattering length comparing to the experimental values

$$a_0(^1S_0) \sim 20 \text{ fm}, \quad a_0(^3S_1) \sim -5 \text{ fm}$$

The reason seems to be

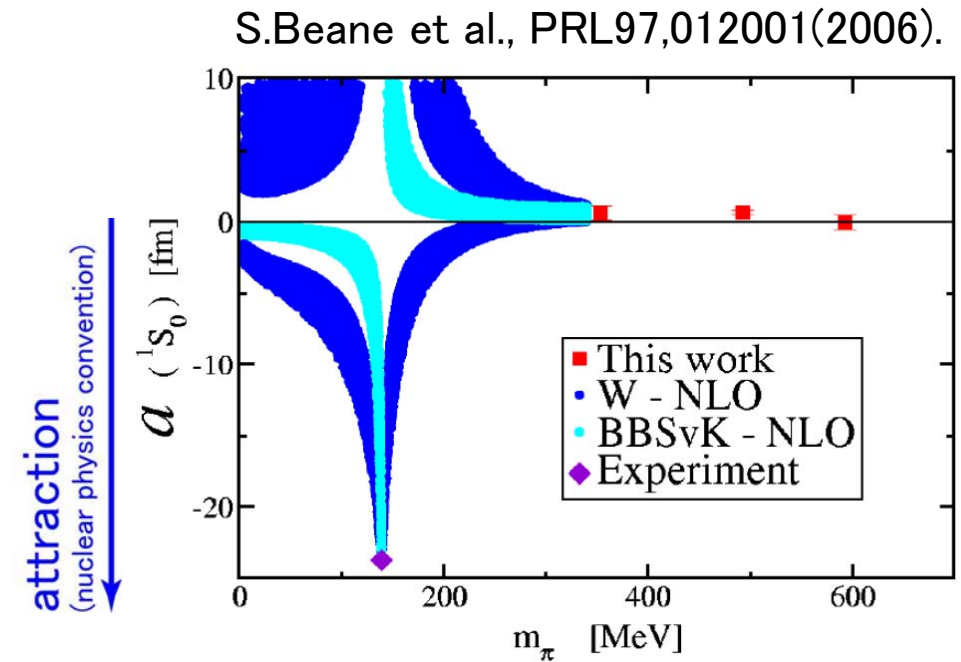
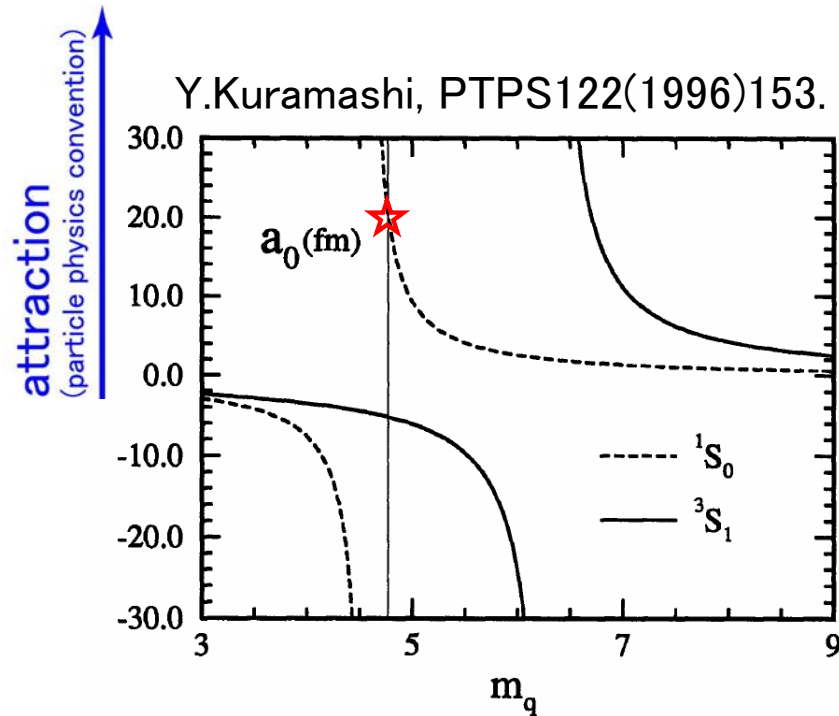
(1) quark mass dependence

(2) slow convergence at long distance region

Reason 1: Quark mass dependence of scattering length

(31)

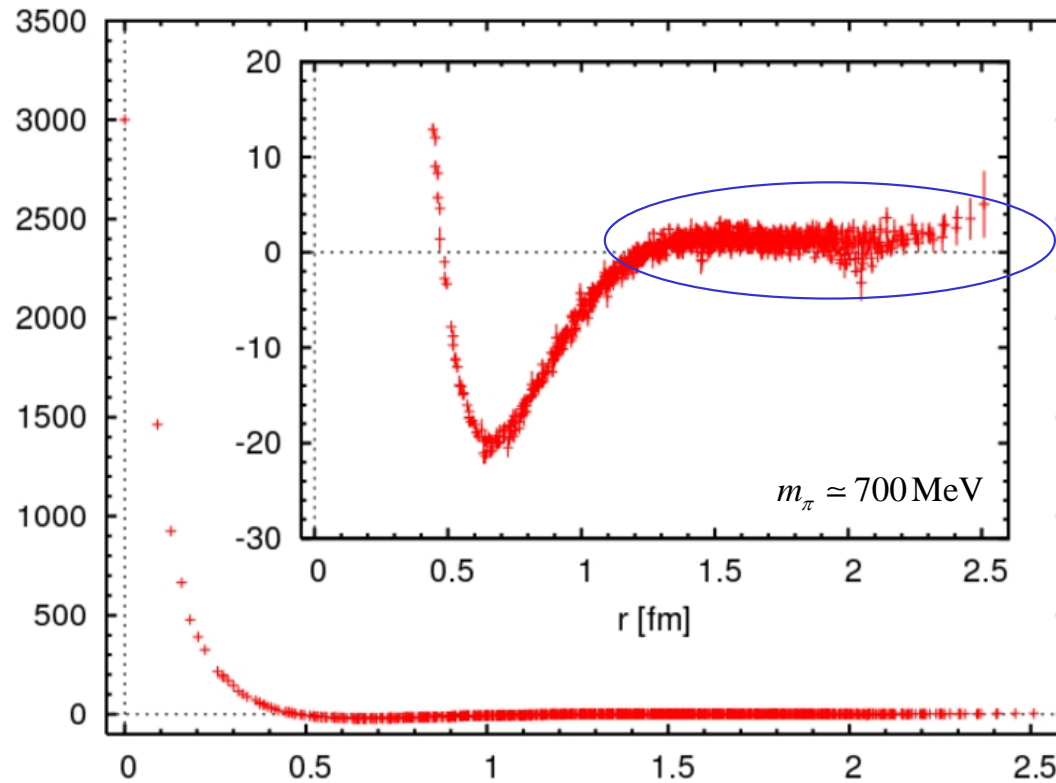
- There are several opinions against quark mass dependence of scattering length.



- It is agreed that the physical quark mass point is in **the unitary region**, where the scattering length shows a rapid increase near a bound state generation.
- ➔ Because our quark mass is heavy and far from the unitary region, the scattering length is small.

Reason 2: Slow convergence at long distance (0)

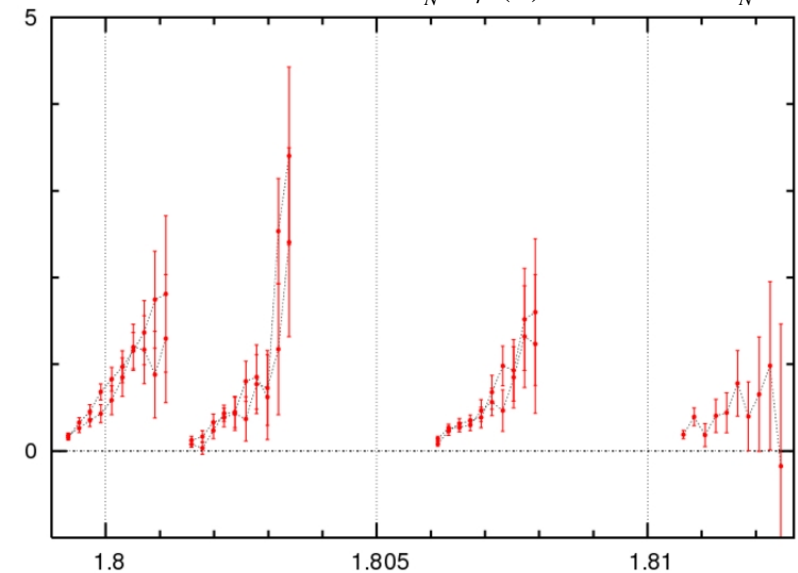
(32)



Convergence of this part seems to be quite slow.

It tends to go up.

$$t \text{ evolution of } \frac{1}{m_N} \frac{\vec{\nabla}^2 \psi(\vec{x})}{\psi(\vec{x})} = V_C(\vec{x}) - \frac{k^2}{m_N}$$



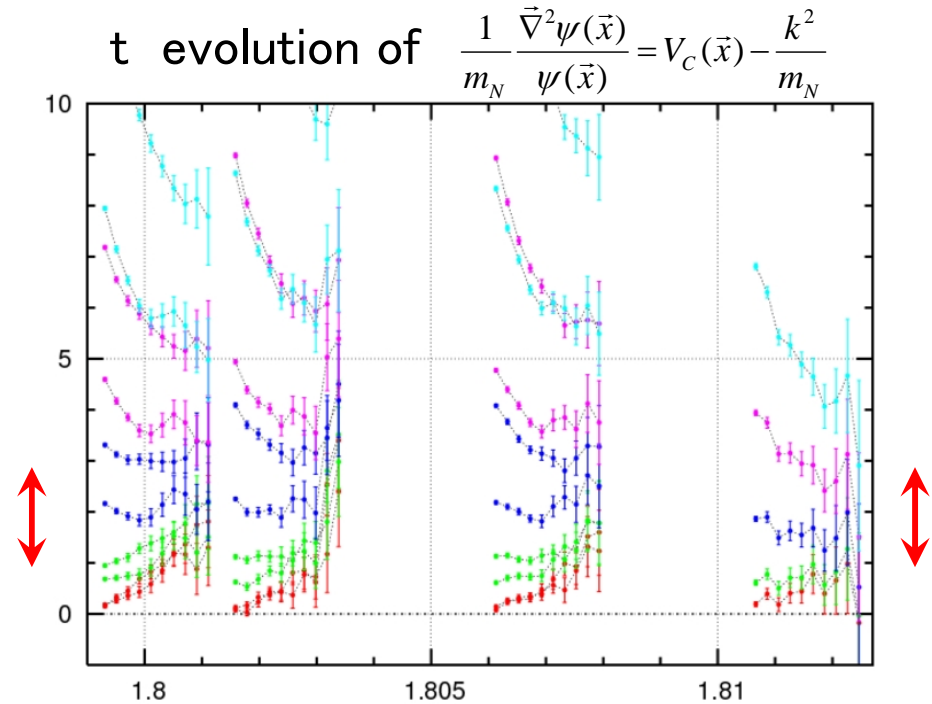
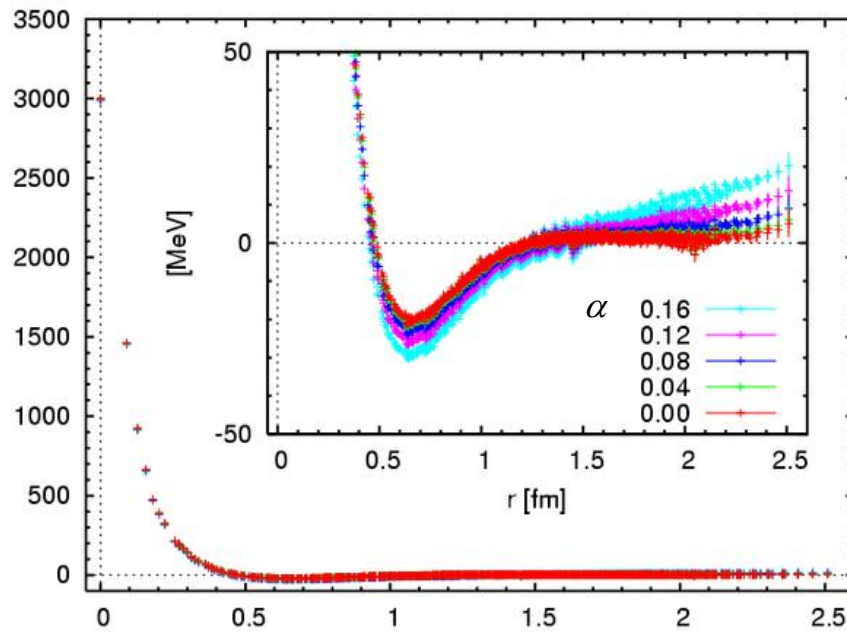
Since the contribution at long distance comes with volume element, even a small deviation may lead to a large uncertainty.

Reason 2: Slow convergence at long distance (1)

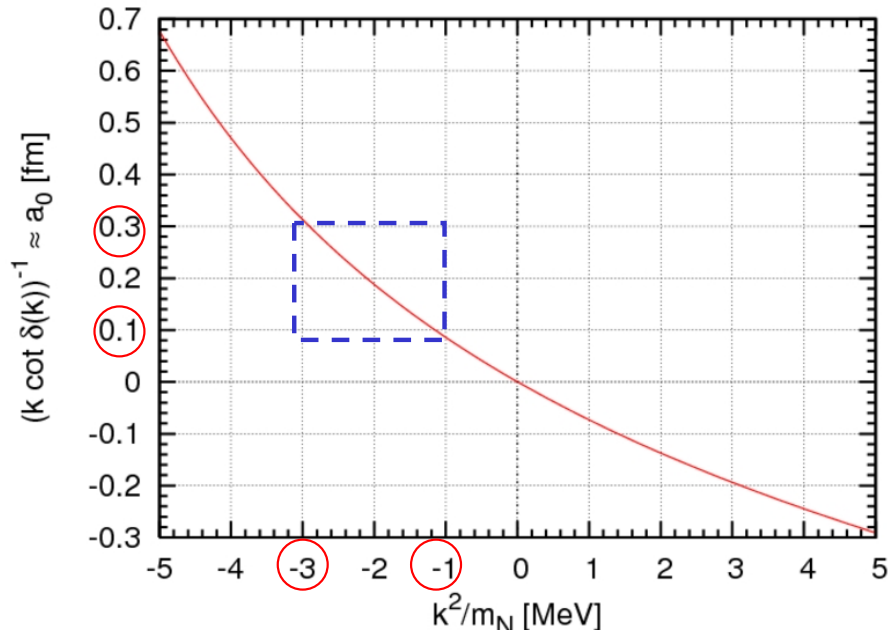
(33)

We use different starting points (source) attempting to boost the convergence.

$$f(x, y, z) = 1 + \alpha (\cos(px) + \cos(py) + \cos(pz)) \text{ with } p \equiv 2\pi / L$$



Luescher's formula indicates



$$\frac{k^2}{m_N} \simeq -1 \text{ to } -3 \text{ MeV} \quad \longrightarrow \quad a_0 \simeq 0.1 - 0.3 \text{ fm}$$

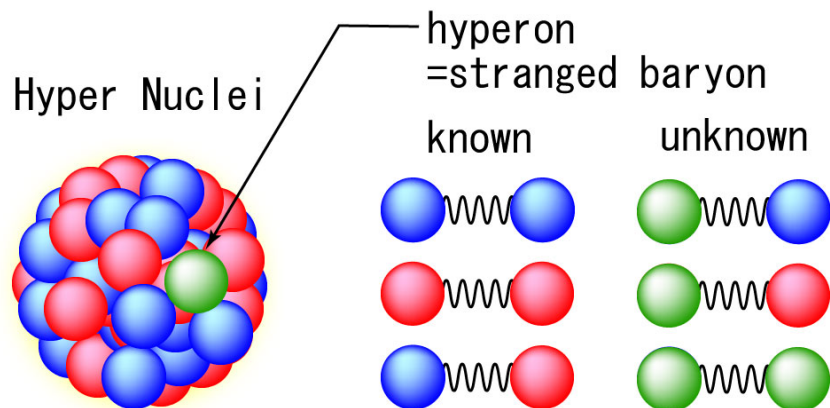
- ◆ This may not be the main reason for the small scattering length.
- ◆ Statistics has to be improved.

Hyperon Potentials

Hyperon potentials

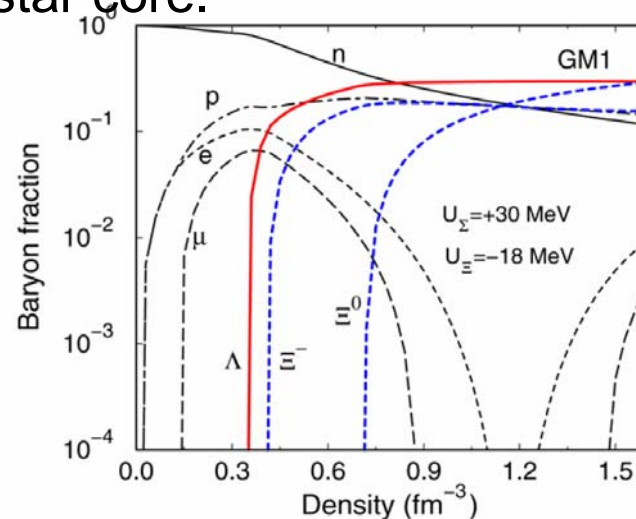
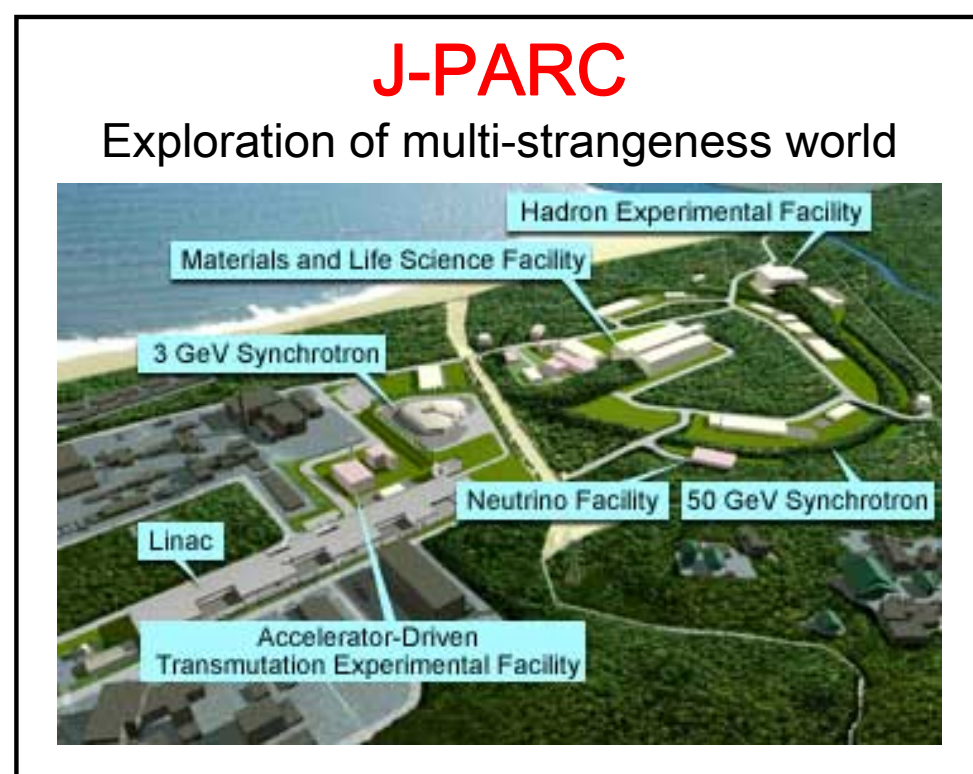
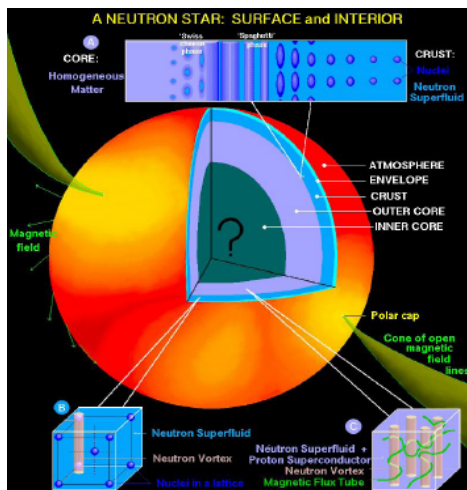
➤ Important for

- structure of hyper nuclei



- equation of state of hyperon matter

→ hyperon matter generation in neutron star core.



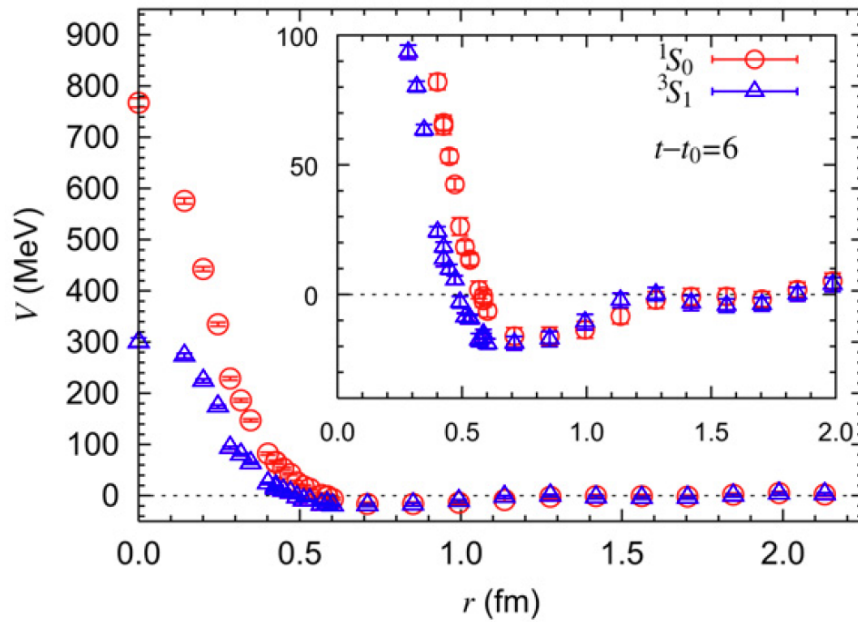
J.Schaffner-Bielich, NPA804('08)309.

➤ Limited number of experimental information

(Direct experiment is difficult due to their short life time)

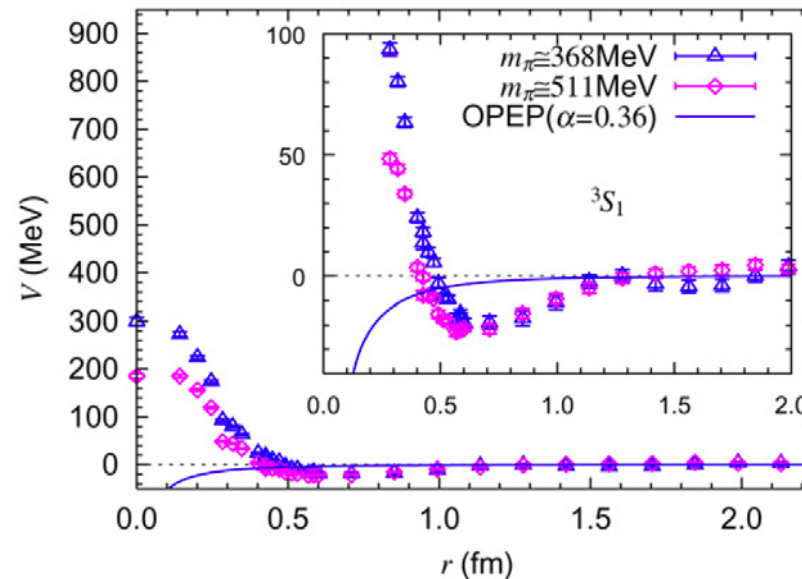
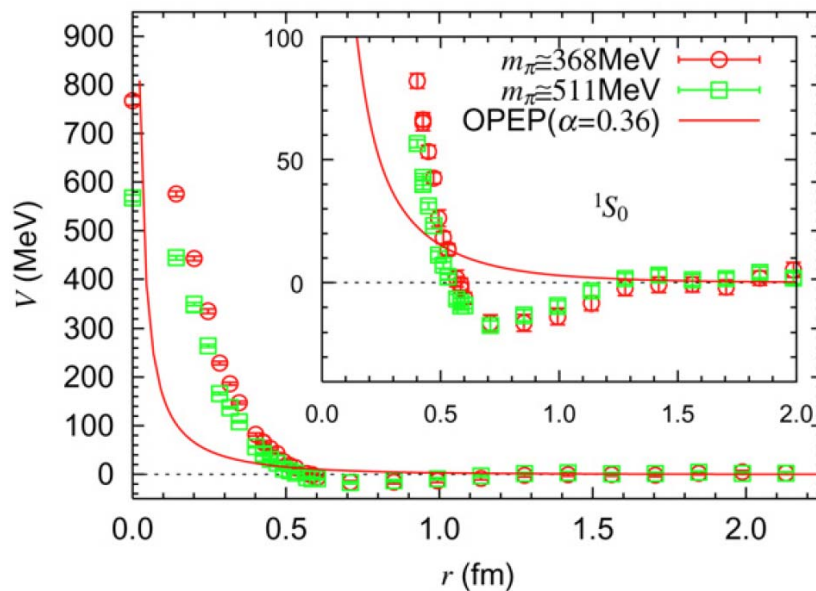
N-Xi potential ($I=1$) by quenched QCD

Nemura, Ishii, Aoki, Hatsuda, (36)
PLB673(2009)136.

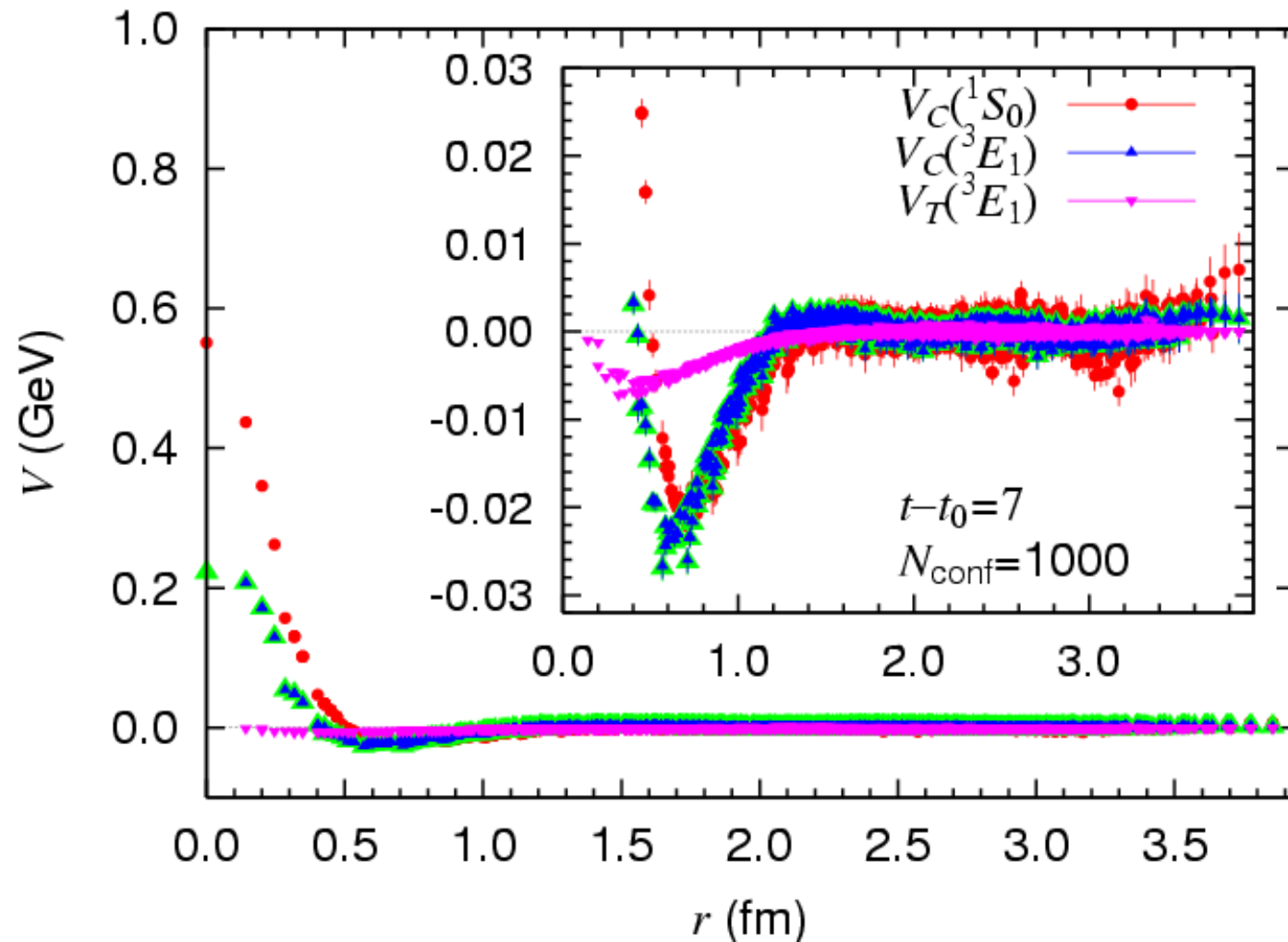


- Repulsive core is surrounded by attraction like NN case.
- Strong spin dependence

quark mass dependence

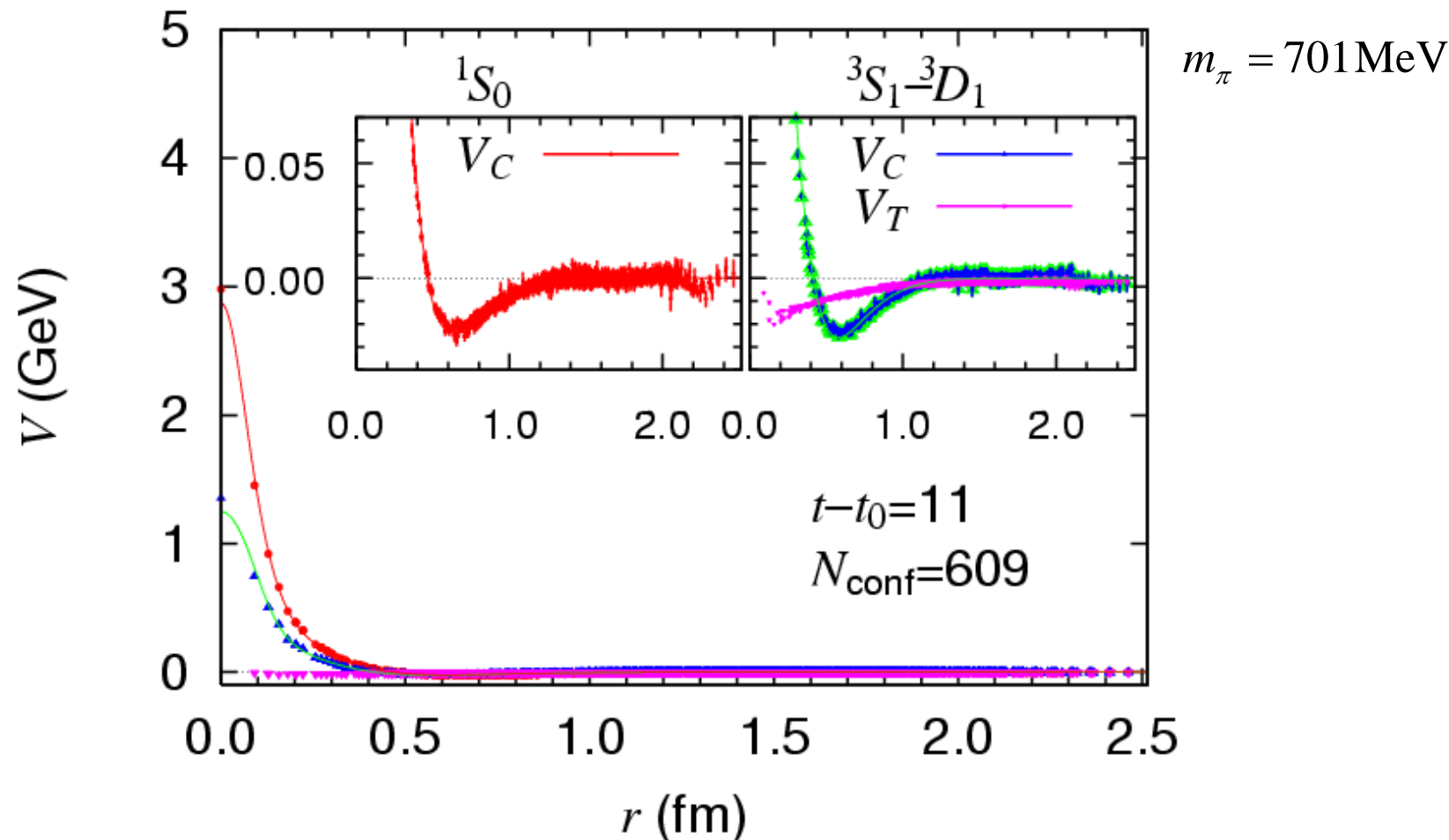


Repulsive core grows with decreasing quark mass.
No significant change in the attraction.



$m_\pi \approx 514 \text{ MeV}$

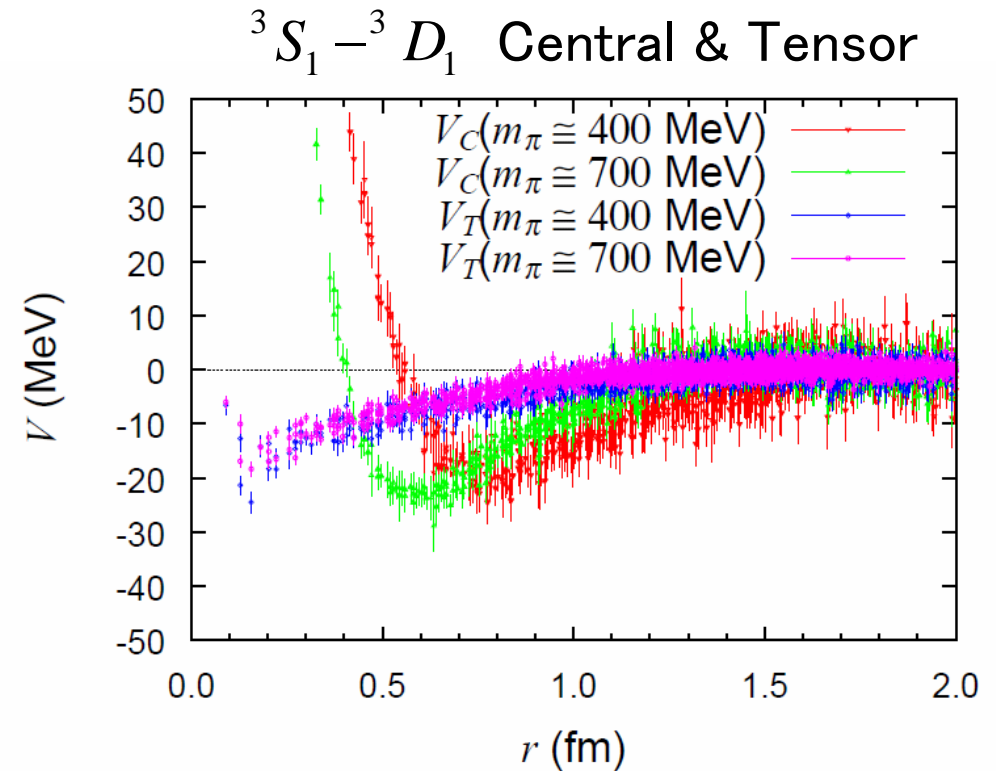
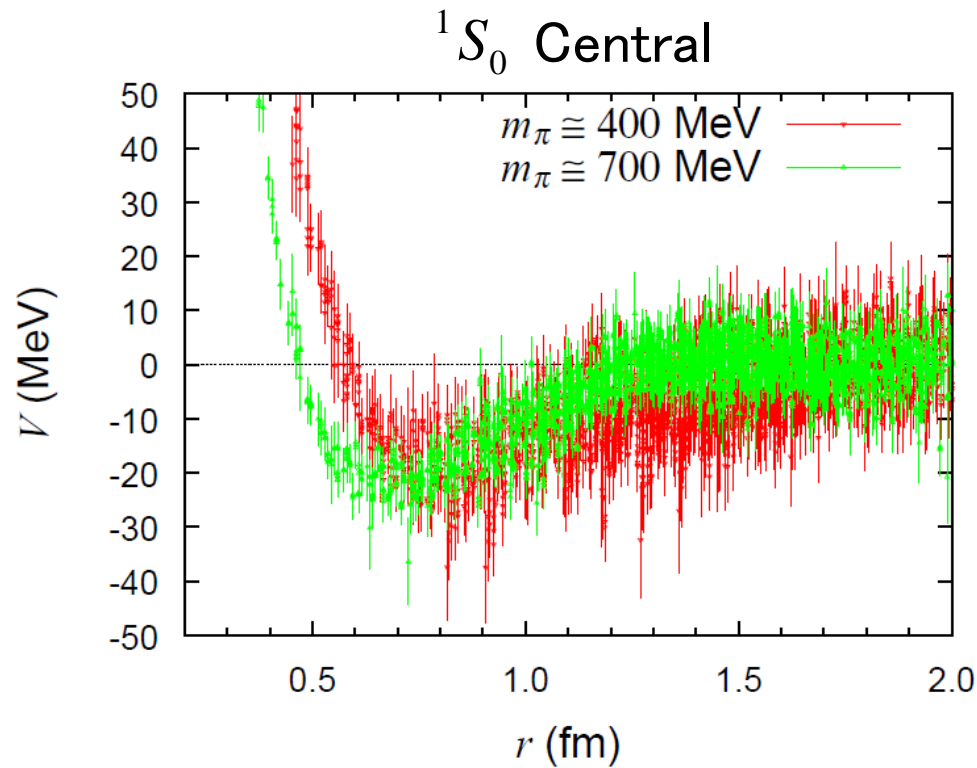
- Repulsive core is surrounded by attractive well.
- Spin dependence of the repulsive core is large.
- Spin dependence of the attraction is small.
- Weak tensor potential



- Repulsive core is surrounded by attractive well.
- Large spin dependence of repulsive core
- Weak tensor force
- Net interaction is attractive.

Quark mass dependence of $N\Lambda$ potential

(39)



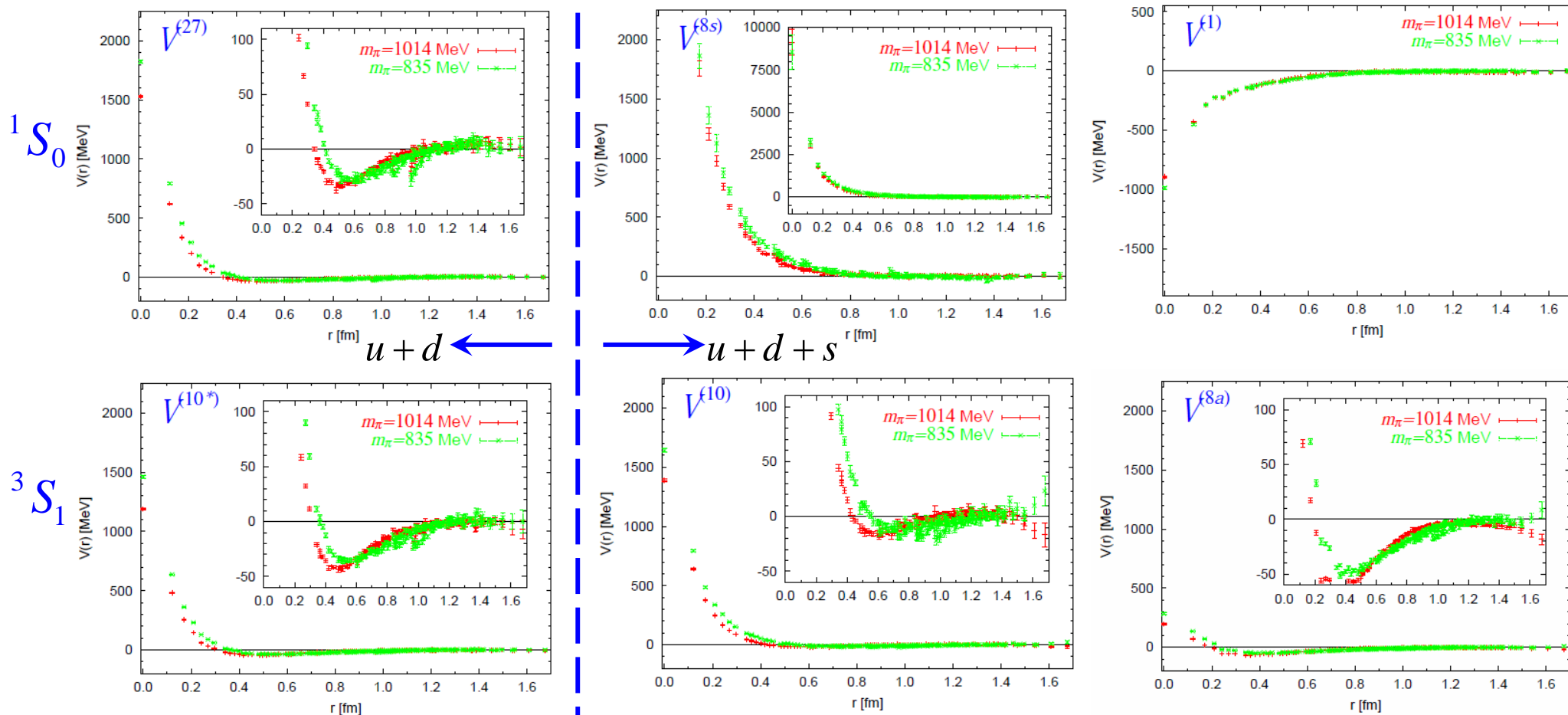
With decreasing u and d quark masses,

- Repulsive core is enhanced.
- Attractive well moves to outer region.
- Small quark mass dependence of tensor potential

Hyperon potential in flavor SU(3) limit

(40)

Aim: A systematic study of short range baryon-baryon interactions



➤ Strong flavor dependence

➤ All distance attraction for flavor 1 representation.

➤ Strong repulsive core for flavor 8_S representation.

➤ Weak repulsive core for flavor 8_A representatin.

➤ This behaviors at short distance are consistent with quark Pauli blocking picture.

For detail, see T.Inoue et al, arXiv:1007.3559 [hep-lat]

Summary

- General strategy (NN potentials from BS wave functions)
 - We introduced the non-local potential, which is faithful to phase shift data by construction.
- Numerical results (based on derivative expansion)
 - Central potential, tensor potential, hyperon potentials ($N\Xi$ [$I=1$] and $N\Lambda$)
 - Derivative expansion of (E-independent) non-local potential works well [$E_{\text{CM}} = 0-46$ MeV]
 - 2+1 flavor QCD results (by PACS-CS gauge config.)
 - NN and $N\Lambda$ (central and tensor potentials) [$L \sim 3$ fm]
 - Phase shift and scattering length are weaker than empirical ones.
 - Improvements in quark mass and convergence at long distance are needed. (Give us time)

Outlook

- Realistic potentials with physical quark mass in a large spatial volume ($L \sim 6$ fm) by using PACS-CS gauge configuration [planned]
- Higher derivative terms (LS force and more), p-wave.
 - More hyperon potentials including coupled channel extension [work in progress]
- Three-baryon potential. [work in progress]
- Origin of the repulsive core [work in progress]
 - Flavor SU(3) limit and its breaking (a systematic study of short range BB interaction)
 - Short distance analysis by Operator Product Expansion
- Applications:
 - Nuclear physics based on lattice QCD
 - Eq. of states of nuclear/hyperon matter for supernovae and neutron stars

END

Backup Slides

Asymptotic form of BS wave function

(44)

[C.-J.D.Lin et al., NPB619,467(2001)]

For simplicity, we consider BS wave function of two pions

$$\psi_{\vec{q}}(\vec{x}) \equiv \langle 0 | N(\vec{x}) N(\vec{0}) | N(\vec{q}) N(-\vec{q}), in \rangle$$

complete set

$$1 = \int \frac{d^3 p}{(2\pi)^3 2E_N(\vec{p})} |N(\vec{p})\rangle \langle N(\vec{p})| + \dots$$

$$= \int \frac{d^3 p}{(2\pi)^3 2E_N(\vec{p})} \langle 0 | N(\vec{x}) | N(\vec{p}) \rangle \langle N(\vec{p}) | N(\vec{0}) | N(\vec{q}) N(-\vec{q}), in \rangle + I(\vec{x})$$

$$Z^{1/2} e^{i\vec{p}\cdot\vec{x}}$$

$$disc. + Z^{1/2} \frac{T(\vec{p}; \vec{q})}{m_N^2 - (2E_N(\vec{q}) - E_N(\vec{p}))^2 + \vec{p}^2 - i\varepsilon}$$

$$= Z \left(e^{i\vec{q}\cdot\vec{x}} + \frac{1}{(2\pi)^3} \int \frac{d^3 p}{2E_N(\vec{p}) 4E_N(\vec{q}) \cdot (E_N(\vec{p}) - E_N(\vec{q}) - i\varepsilon)} T(\vec{p}; \vec{q}) e^{i\vec{p}\cdot\vec{x}} \right)$$

Integral is dominated by the on-shell contribution $E_N(\vec{p}) \approx E_N(\vec{q})$

→ T-matrix becomes the on-shell T-matrix

$$T^{(s\text{-wave})}(s) = \frac{E(\vec{q})}{2|\vec{q}|} (-i) (e^{2i\delta_0(s)} - 1)$$

$$= Z \left(e^{i\vec{q}\cdot\vec{x}} + \frac{1}{2i} (e^{2i\delta_0(s)} - 1) \frac{e^{iqr}}{qr} \right) + \dots$$

The asymptotic form

$$\psi_{\vec{q}}(\vec{x}) = Z e^{i\delta_0(s)} \frac{\sin(qr + \delta_0(s))}{qr} + \dots \quad (\text{s-wave})$$

This is analogous to a non-rela. wave function

Effective Schrodinger equation with E-independent potential

(45)

$$K(\vec{x}; E) \equiv (\vec{\nabla}^2 + k^2) \psi(\vec{x}; E) \quad (\text{localized object: propagating d.o.f. is filtered out})$$

We would like to factorize

$$E \equiv 2\sqrt{m_N^2 + k^2}$$

$$K(\vec{x}; E) = m_N \int d^3 y U(\vec{x}, \vec{y}) \psi(\vec{y}; E)$$

Factorization:

(α is to distinguish states with same E.)

(1) **Assumption:** $\psi(x; E, \alpha)$ for different E and α is linearly independent with each other.

(2) $\psi(x; E, \alpha)$ has a “left inverse” as an integration operator as

$$\int d^3 x \tilde{\psi}(\vec{x}; E', \alpha') \psi(\vec{x}; E, \alpha) = 2\pi \delta(E - E') \delta_{\alpha, \alpha'}$$

(3) $K(x; E, \alpha)$ can be factorized as

$$\begin{aligned} K(\vec{x}; E, \alpha) &= \sum_{\alpha'} \int \frac{dE'}{2\pi} K(\vec{x}; E', \alpha') \times \int d^3 y \tilde{\psi}(\vec{y}; E', \alpha') \psi(\vec{y}; E, \alpha) \\ &= \int d^3 y \left\{ \sum_{\alpha} \int \frac{dE'}{2\pi} K(\vec{x}; E', \alpha') \tilde{\psi}(\vec{y}; E', \alpha') \right\} \psi(\vec{y}; E, \alpha) \end{aligned}$$

$$\equiv m_N U(\vec{x}, \vec{y})$$

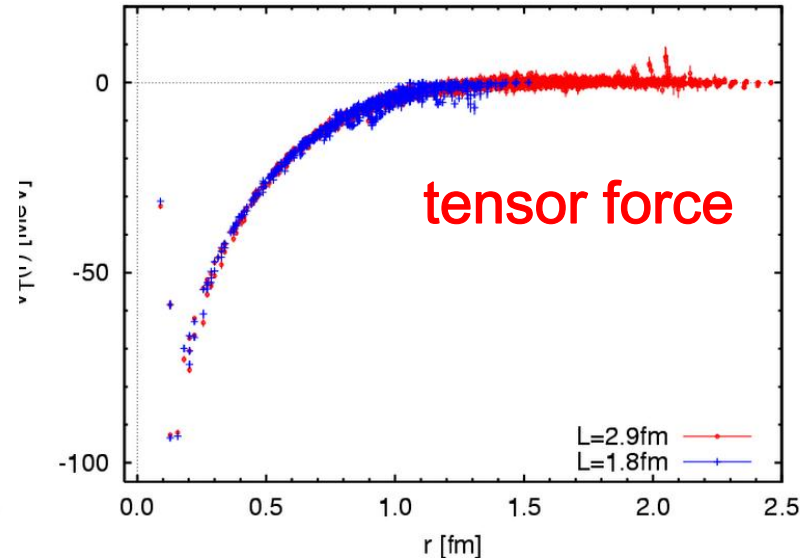
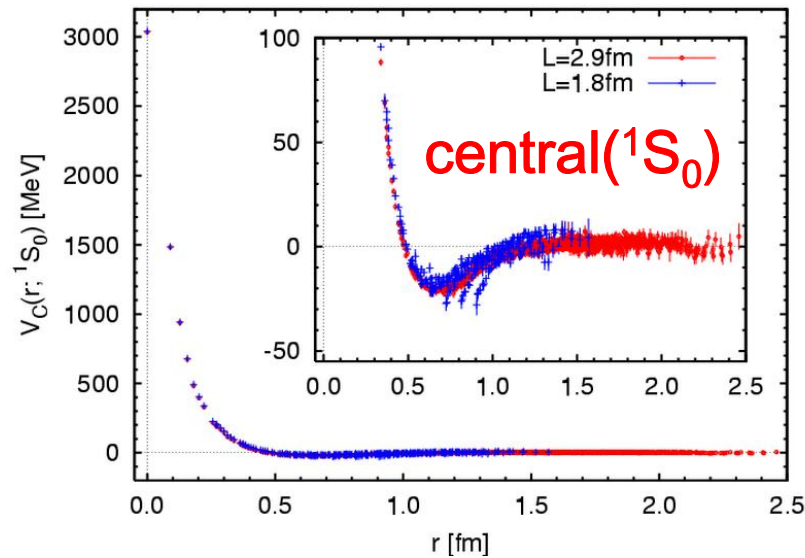
(4) We are left with **an effective Schrodinger equation with an E-independent potential U.**

$$(\vec{\nabla}^2 + k^2) \psi(\vec{x}; E) = m_N \int d^3 y U(\vec{x}, \vec{y}) \psi(\vec{y}; E)$$

(⊗) $U(x,y)$ is obtained by integrating over E. → It does not have E dependence.

Finite size artifact is weak at short distance.

- Finite size artifact on the potential is weak at short distance !
 (Example) $L \sim 3 \text{ fm}$ [RC32x64_B1900Kud01370000Ks01364000C1715]
 $L \sim 1.8 \text{ fm}$ [RC20x40_B1900Kud013700Ks013640C1715]

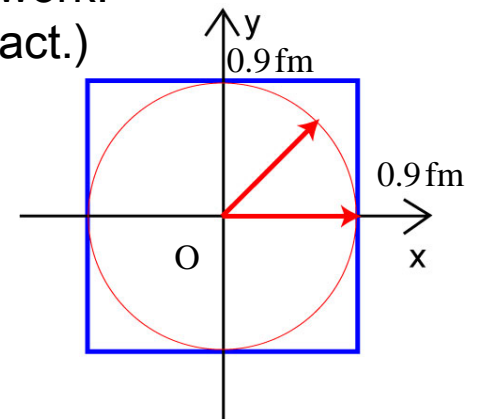


- Central force has to shift by $E=24 \sim 29 \text{ MeV}$.

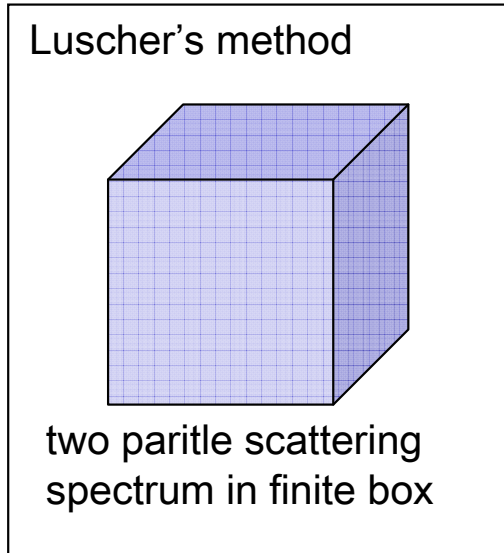
$$V_C(r) = \cancel{E} + \frac{1}{m_N} \frac{\vec{\nabla}^2 \psi(\vec{x})}{\psi(\vec{x})} \quad (\text{for } ^1S_0)$$

However, due to the missing asymptotic region, zero adjustment does not work.
 (Central force has uncertainty in zero adjustment due to the finite size artifact.)

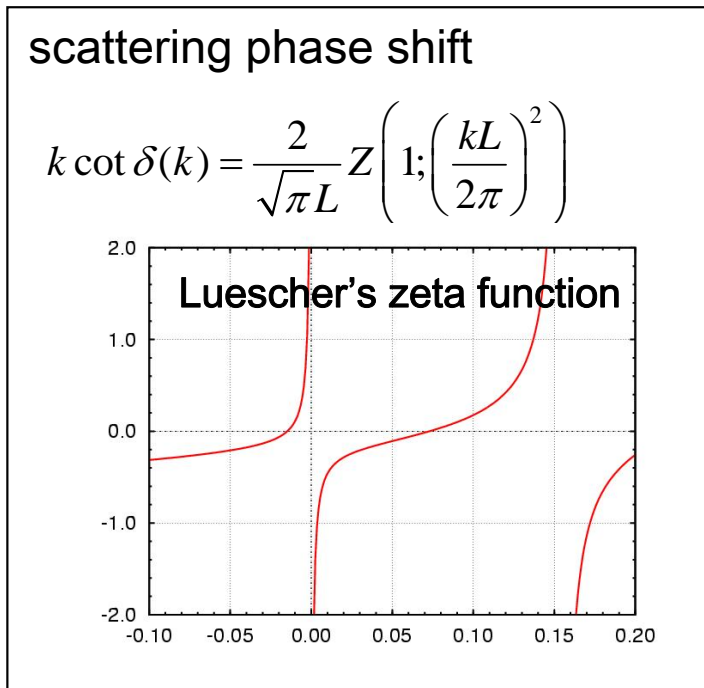
- **Tensor force is free from such uncertainty.**
- **Multi-valuedness of the central force** is due to the finite size artifact.
- Finite size artifacts of short distance part of these potentials are weak !



Background



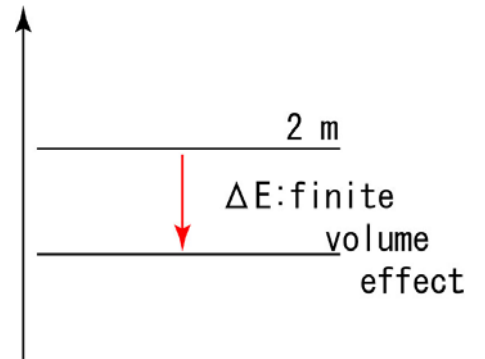
asymptotic momentum $|k|$



- Method, which utilizes temporal correlation (from two particle spectrum)

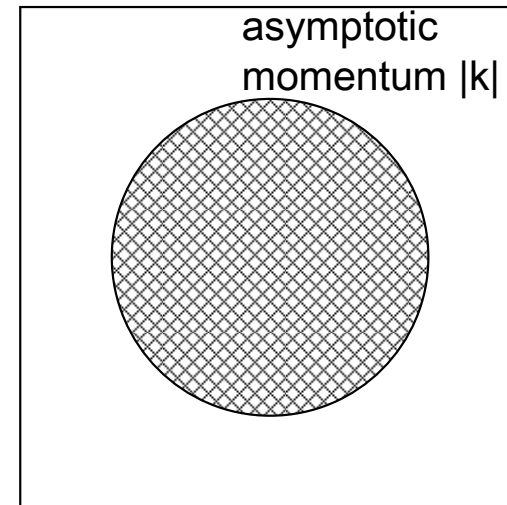
$$R(t) \equiv C_{NN}(t) / (C_N(t))^2 \sim A' \exp(-\Delta E t)$$

$$\Delta E(\vec{k}) \equiv 2 \left(\sqrt{m^2 + \vec{k}^2} - m \right)$$



- Method, which utilizes spatial correlation (from asymptotic behavior of BS wave function)

$$\psi_{\vec{k}}(\vec{r}) \equiv \langle 0 | N(\vec{x}) N(\vec{y}) | N(\vec{k}) N(-\vec{k}), in \rangle$$



Temporal correlation v.s. spatial correlation

(48)

Asymptotic form of BS wave function at long distance $E(\vec{q}) = \sqrt{m^2 + \vec{q}^2}$

$$\psi_{\vec{q}}(\vec{x}) \equiv \langle 0 | N(\vec{x}) N(\vec{0}) | N(\vec{q}) N(-\vec{q}), in \rangle$$

This is related to T-matrix by the reduction formula

$$= \int \frac{d^3 p}{(2\pi)^3 2E(\vec{p})} \langle 0 | N(\vec{x}) | N(\vec{p}) \rangle \cdot \langle N(\vec{p}) | N(\vec{0}) | N(\vec{q}) N(-\vec{q}), in \rangle + I(\vec{x})$$

$$\simeq Z \left(e^{i\vec{q}\cdot\vec{x}} + \frac{1}{(2\pi)^3} \int \frac{d^3 p}{2E(\vec{p}) 4E(\vec{q}) \cdot (E(\vec{q}) - E(\vec{p}) - i\epsilon)} T(\vec{p}, \vec{q}) e^{i\vec{p}\cdot\vec{x}} \right)$$

$$\simeq Z \left(e^{i\vec{q}\cdot\vec{x}} + \frac{1}{2i} \left(e^{2i\delta_0(s)} - 1 \right) \frac{e^{iqr}}{qr} \right) + \dots \text{ (at long distance)}$$

cf) C.-J.D.Lin et al., NPB619,467(2001).
CP-PACS Coll., PRD71,094504(2005).

→ At sufficiently long distance (beyond the range of interaction), BS wave function satisfies the Helmholtz equation:

$$\left(\vec{\nabla}^2 + q^2 \right) \psi_{\vec{q}}(\vec{x}) = 0$$

→

Energy of the state $E(q)$ [temporal correlation]

has to be consistent with

BS wave function at large distance [spatial correlation].

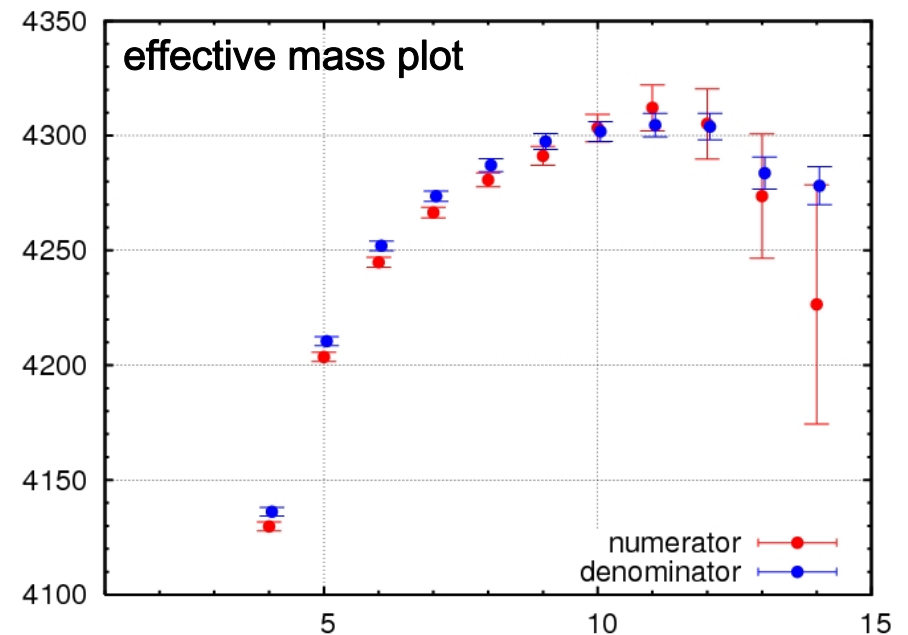
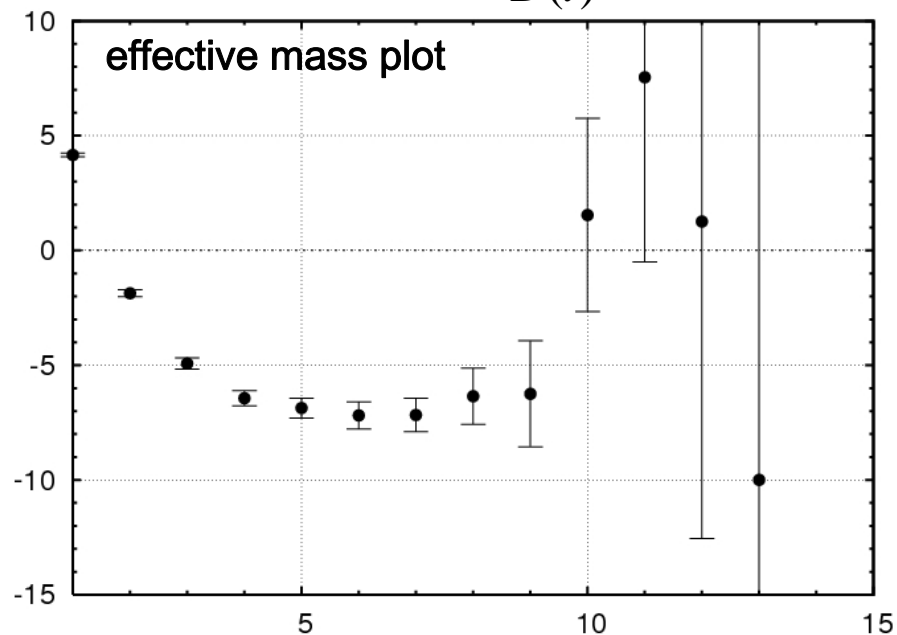
ground state energy

(49)

- BS wave function [wall source]
The information is contained in the long range part, which, however, is not sufficiently converged yet.
- R(t) [wall source]

$$R(t) \equiv \frac{N(t)}{D(t)}$$

$$N(t) \equiv \sum_{\vec{x}} G_{NN}(\vec{x}, t) \quad D(t) \equiv \left(\sum_{\vec{x}} G_N(\vec{x}, t) \right)^2$$



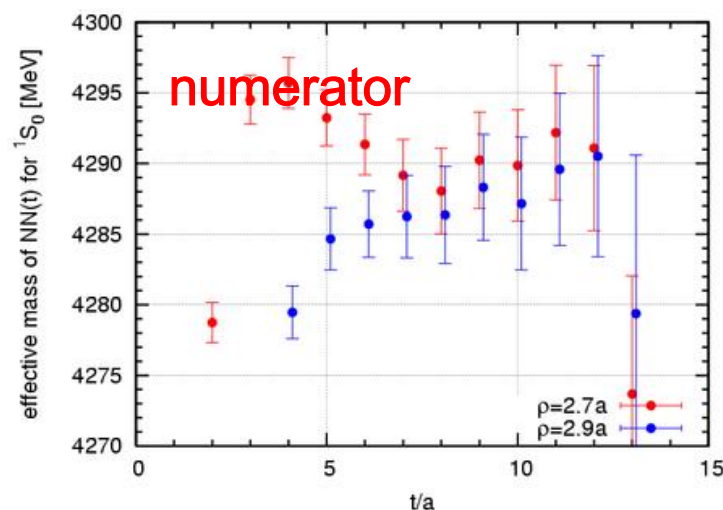
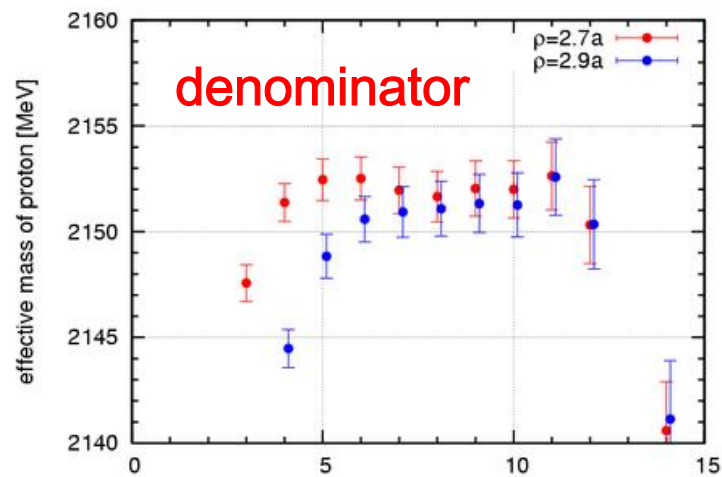
plateaux seem to appear in the region $t \geq 10$ for $N(t)$ and $D(t)$, where $R(t)$ is too noisy to extract any information.

ground state energy(2)

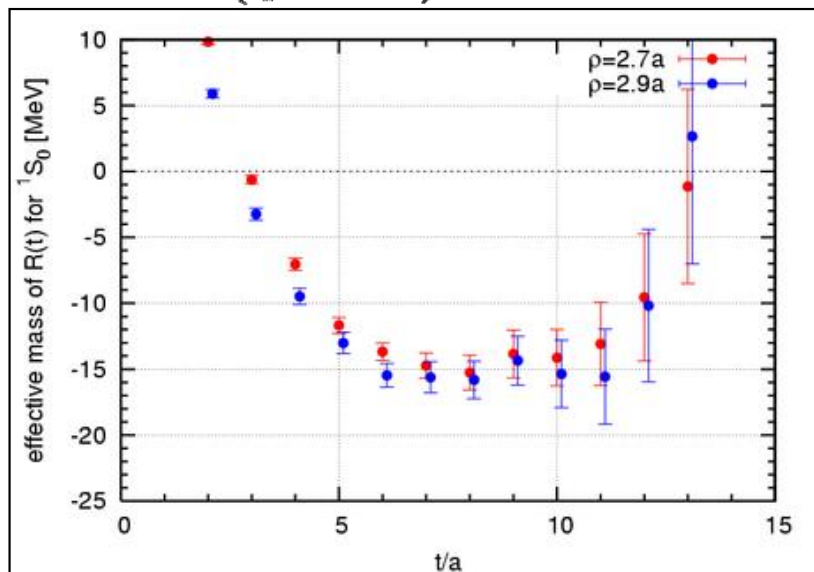
➤ R(t) [smeared source]

It is possible to make the appearance of the plateau at earlier stage by arranging a suitable value of the smearing size.

$$f(\vec{x}) = \sum_{\vec{n} \in Z^3} \exp \left[-\frac{|\vec{x} - L\vec{n}|^2}{\rho^2} \right] \quad (50)$$



$$R(t) \equiv \frac{\sum_{\vec{x}} G_{NN}(\vec{x}, t)^{t/a}}{\left(\sum_{\vec{x}} G_N(\vec{x}, t) \right)^2} \approx A \exp(\Delta E t)$$



➤ common plateau in the region $t \geq 7$.
R(t) in this region $\rightarrow \Delta E \sim -15$ MeV

➤ The identification of the plateaux in the numerator and the denominator may have uncertainty of about 5 MeV.

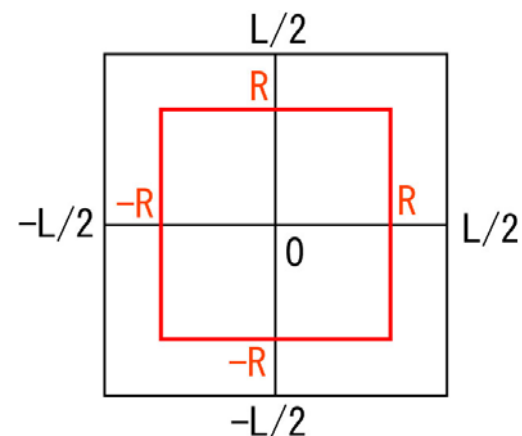
➤ $\Delta E \sim -15$ MeV (± 10 MeV)

ground state energy (3)

(51)

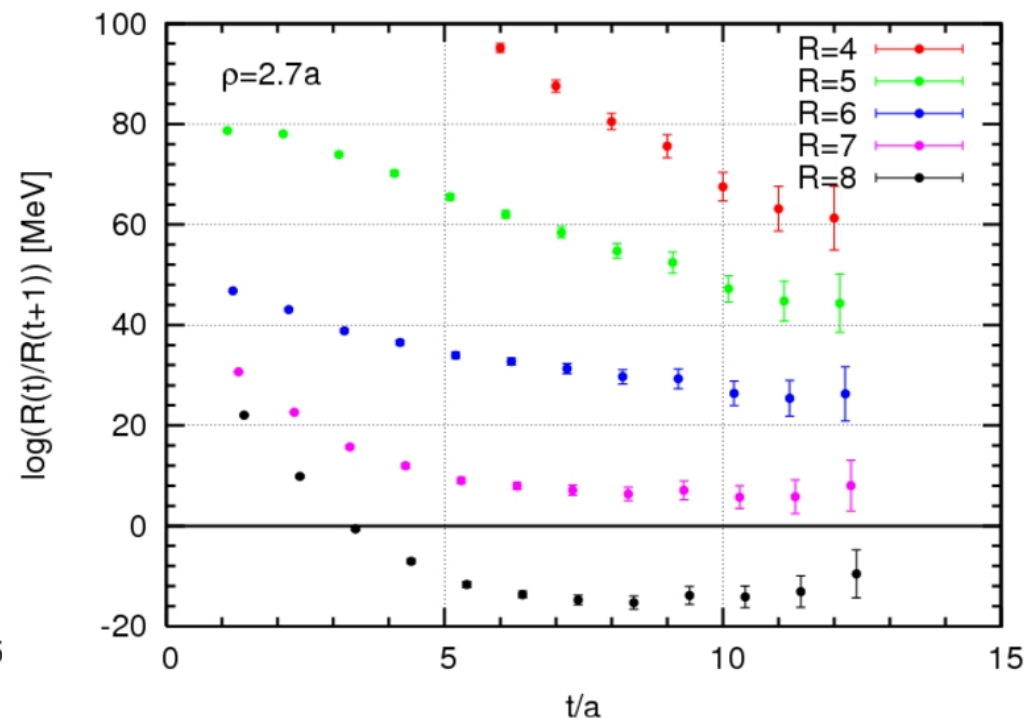
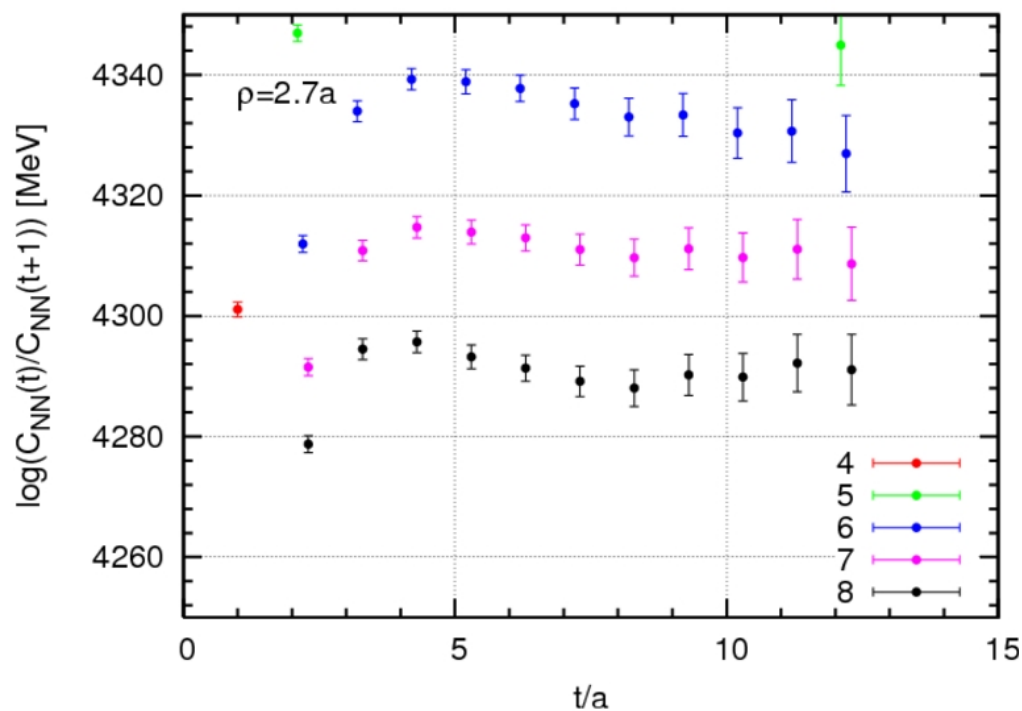
- Naïve identification of the plateau may involve a serious systematic uncertainty.

$$C_{NN}(t; R) \equiv \sum_{-R < x_1, x_2, x_3 \leq R} C_{NN}(\vec{x}; t)$$



$$C_{NN}(t; R)$$

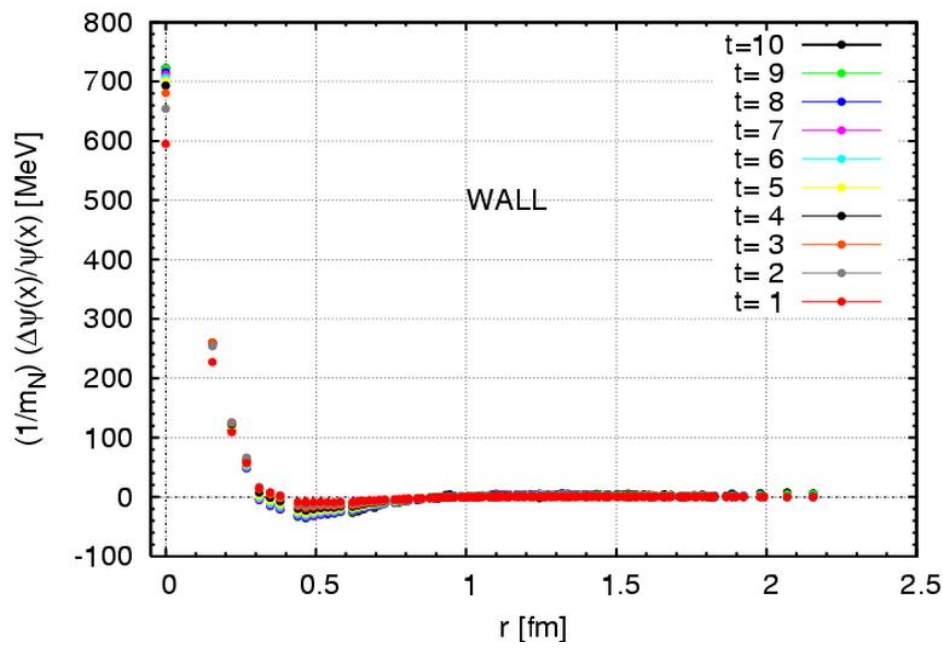
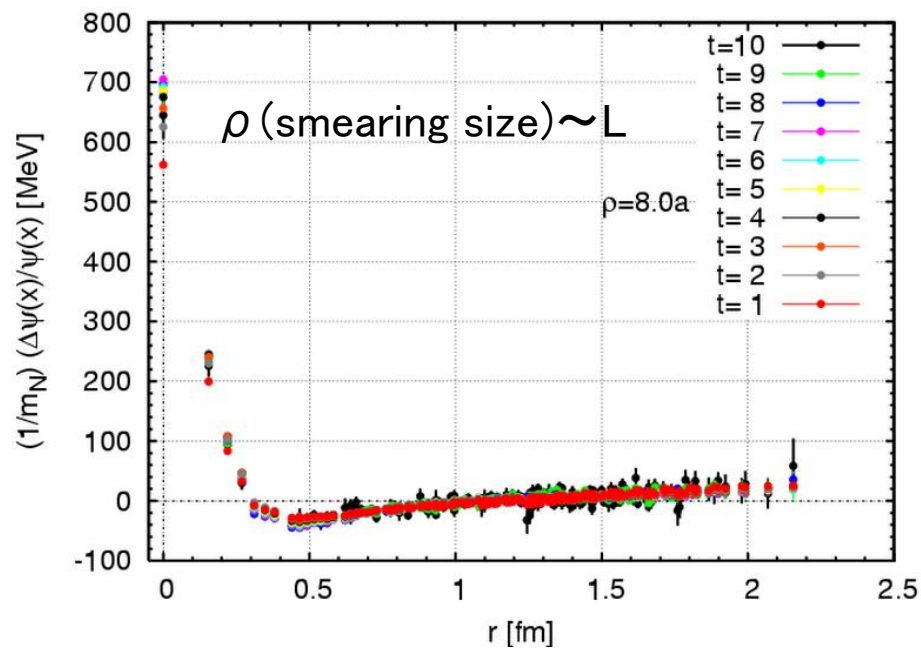
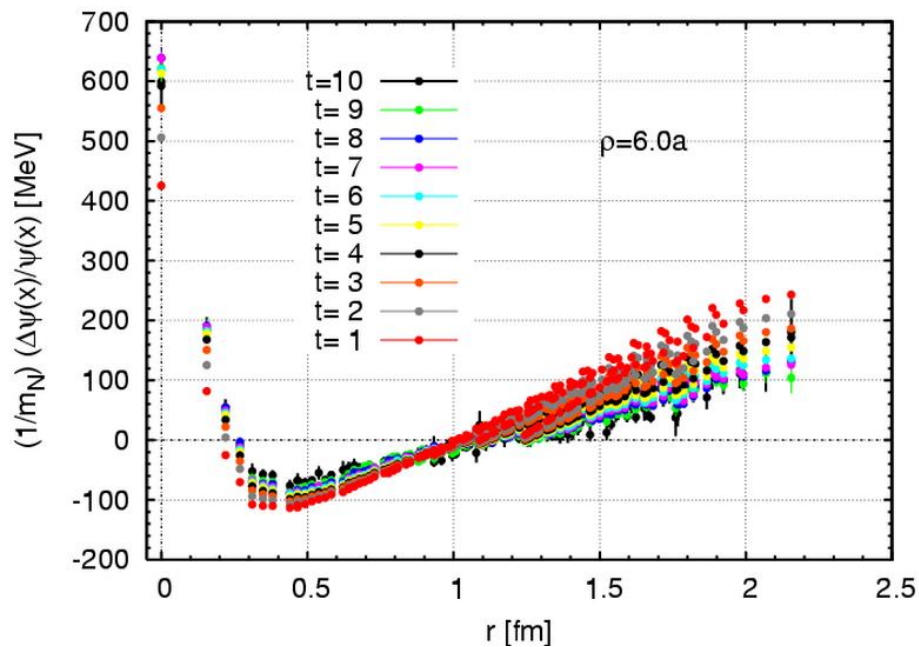
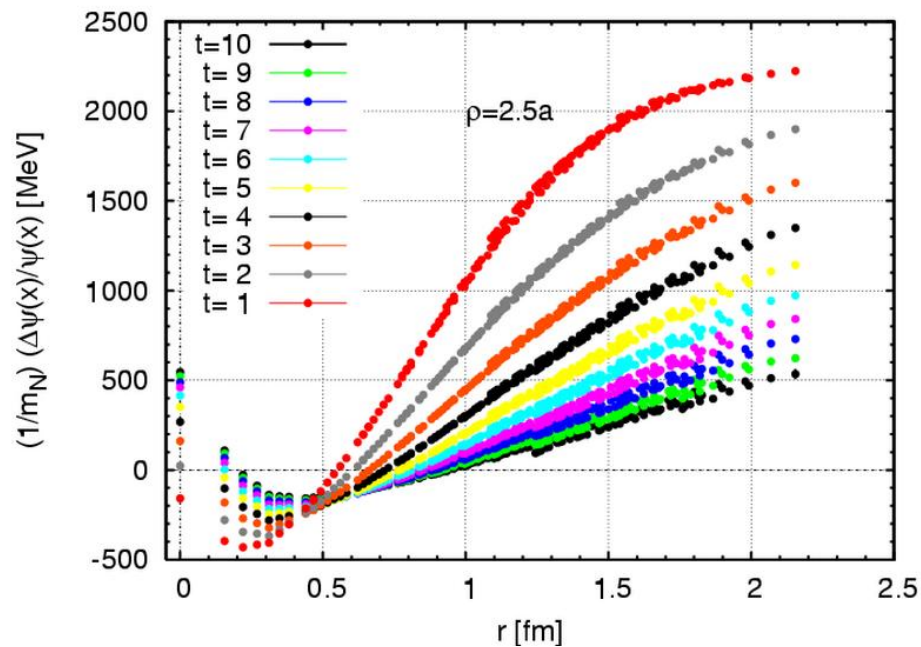
$$R(t; R) \equiv C_{NN}(t; R) / C_N(t)^2$$



- Which plateau is better ? **black data (R=8)** v.s. **purple ones (R=7)** ?
- They are going to converge to a single energy at very large t region. (t/a ~ 100 ?)

Time evolution of $\Delta\psi(x)/\psi(x)$

(52)

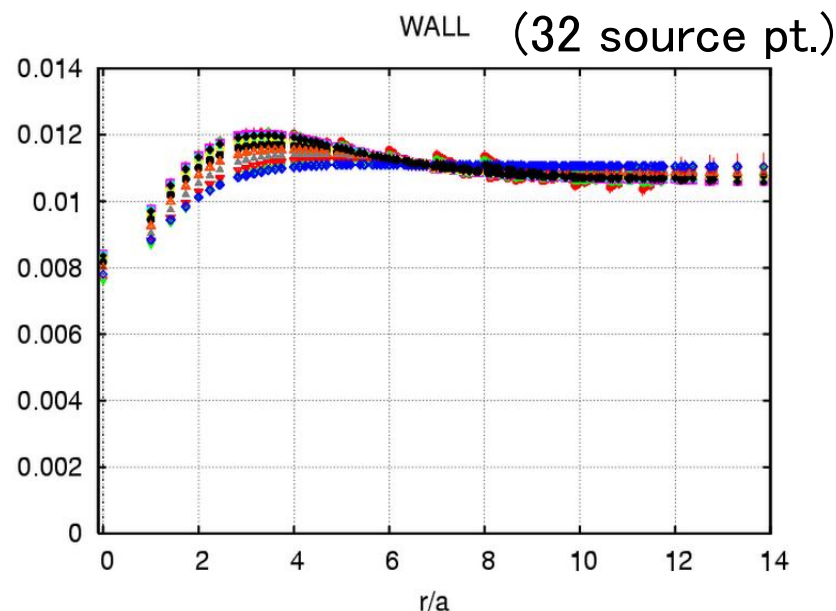
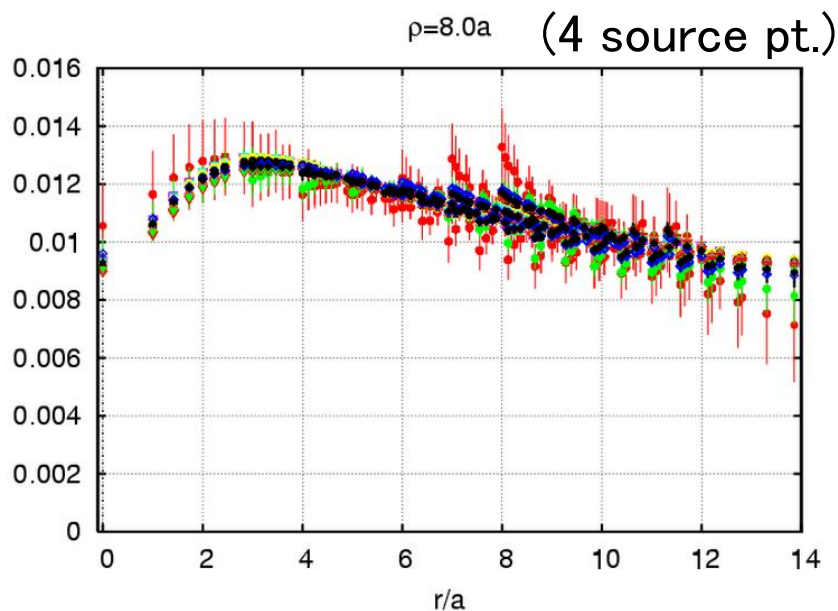
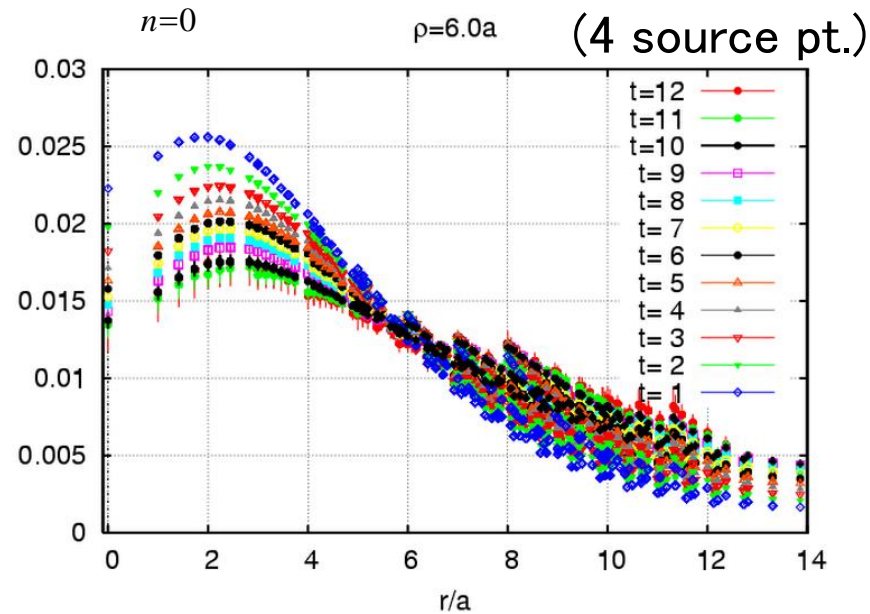
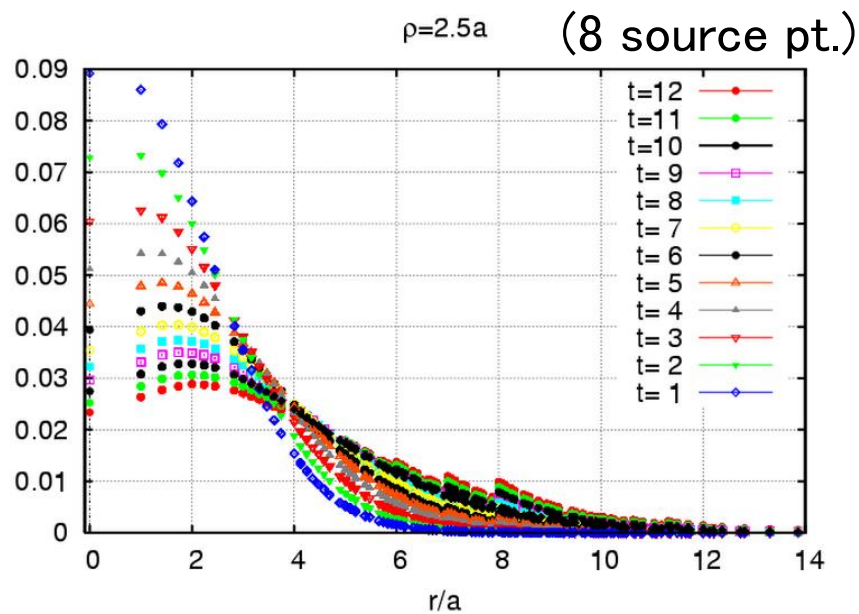


They are going to converge to the wall source result.

Time evolution of 4pt func.

$$C_{NN}(\vec{x}, t) \equiv \langle 0 | T[N(\vec{x}, t)N(\vec{0}, t) \bar{N}(0)\bar{N}(0)] | 0 \rangle \quad (53)$$

$$= \sum_{n=0}^{\infty} \psi_n(\vec{x}) \cdot A_n \exp(-E_n t)$$



These are changing to the shape of the wall source wave function.

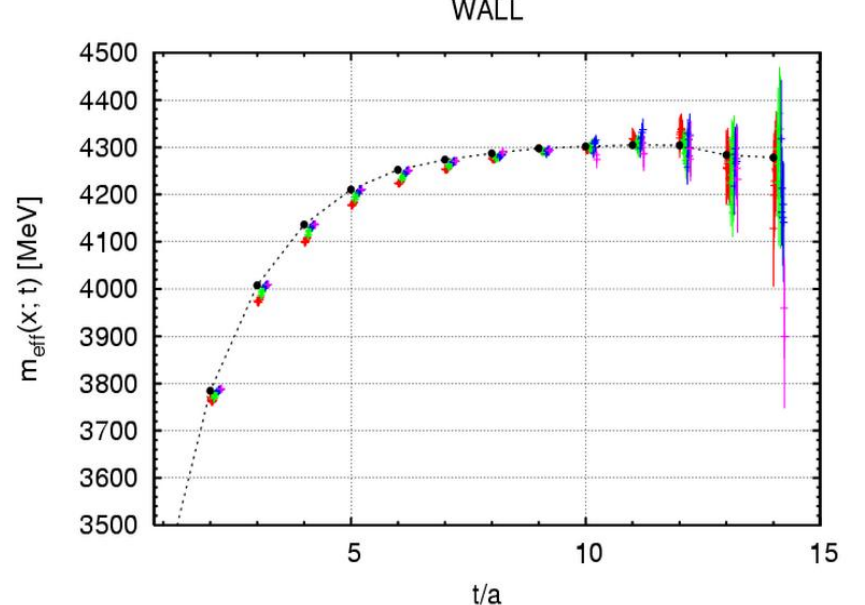
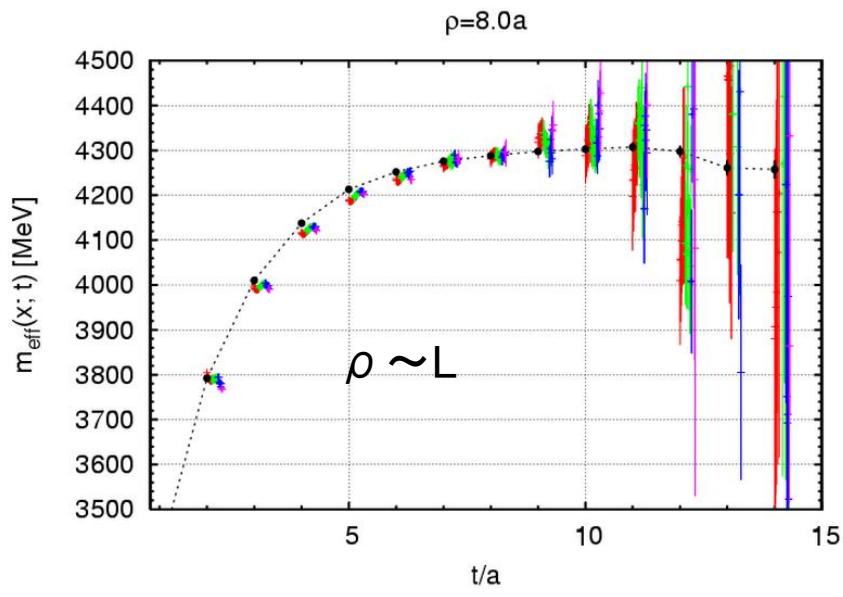
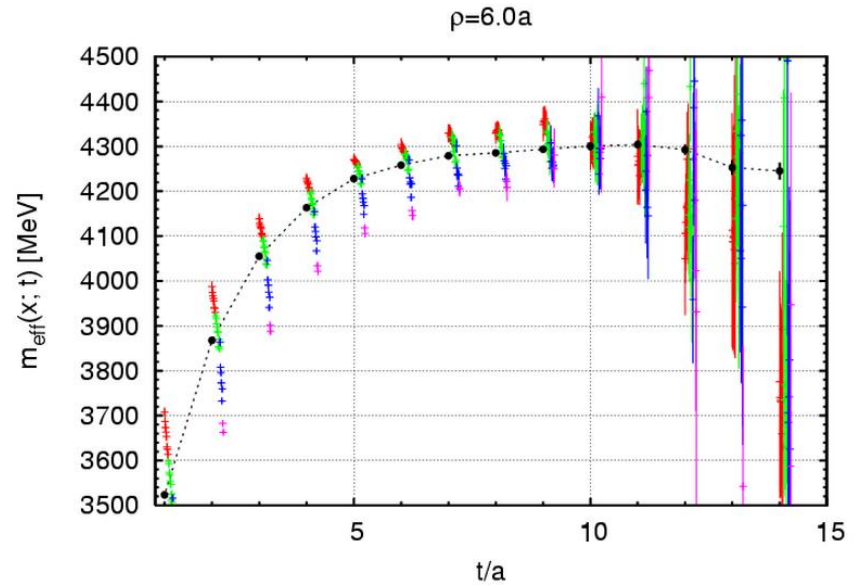
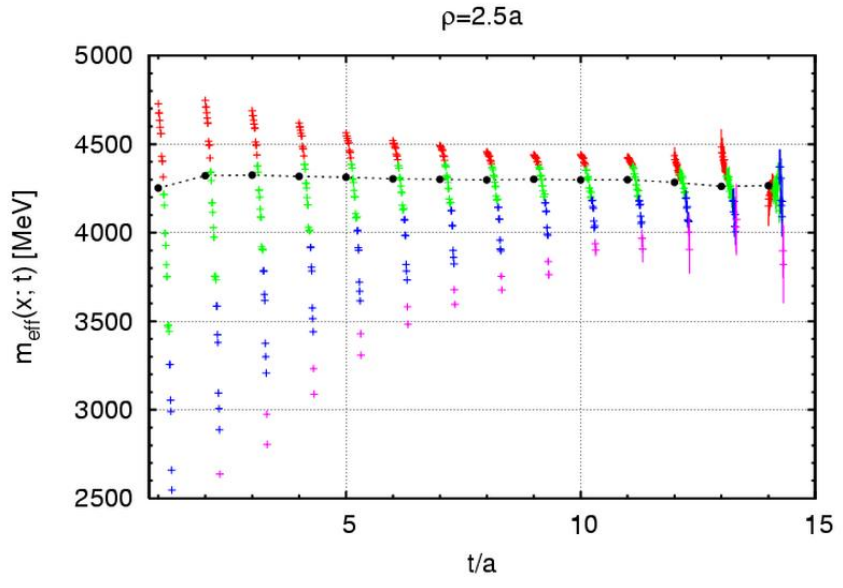
eff 'mass plot of four pt function

(54)

$$C_{NN}(\vec{x}, t) \equiv \langle 0 | T[N(\vec{x}, t)N(\vec{0}, t) \bar{N}(0)\bar{N}(0)] | 0 \rangle$$

$$= \sum_{n=0}^{\infty} \psi_n(\vec{x}) \cdot A_n \exp(-E_n t)$$

$$\log \left[\frac{C_{NN}(\vec{x}, t)}{C_{NN}(\vec{x}, t+1)} \right]$$

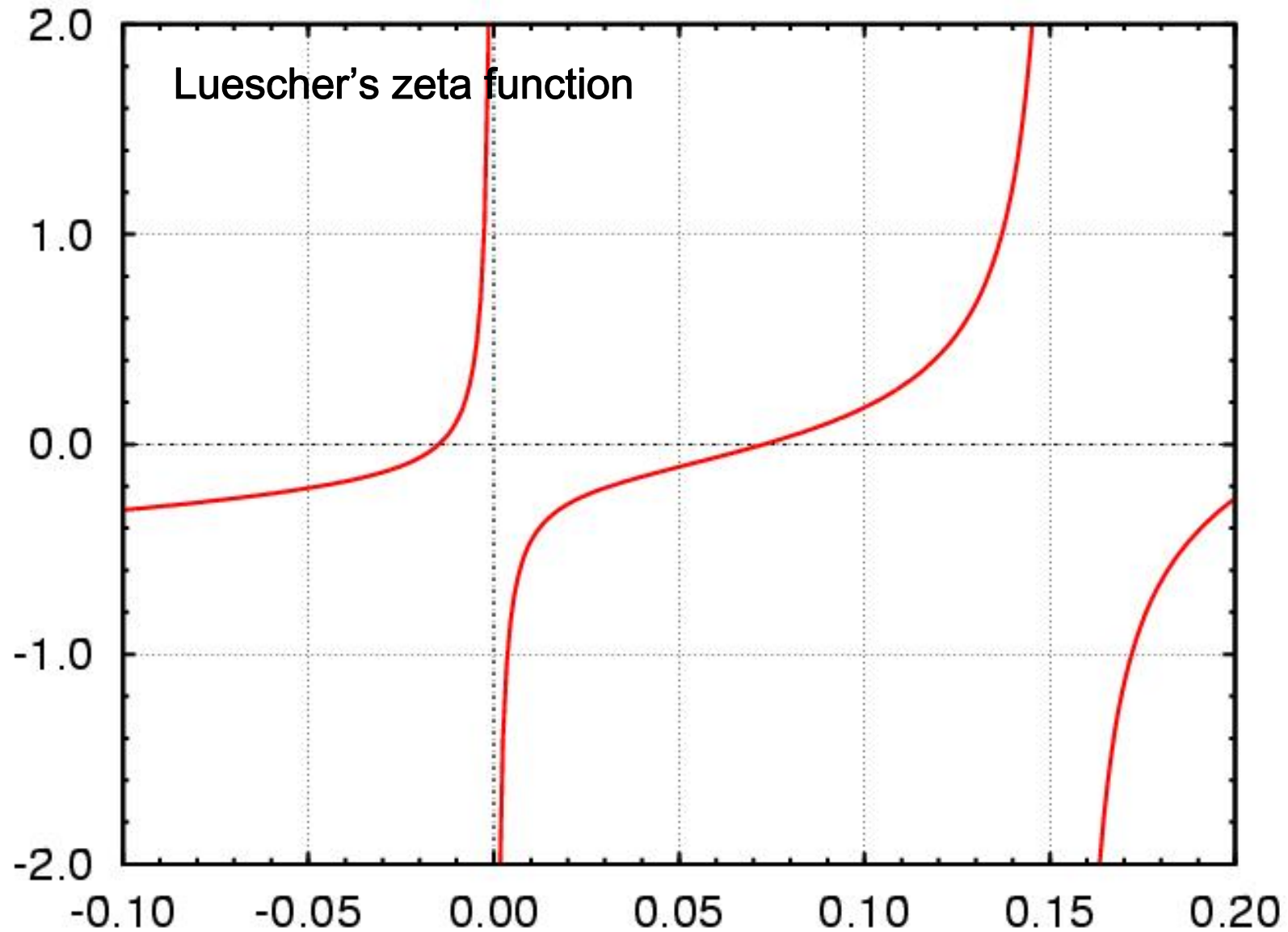


Variation of t-dependence among different spatial points is small for the wall source result.

Luescher's Zeta function

(55)

$$k \cot \delta(k) = \frac{2}{\sqrt{\pi L}} Z \left(1; \left(\frac{kL}{2\pi} \right)^2 \right)$$



General form of NN potential

(56)

★ Imposed constraints:

- Probability (Hermiticity):
- Energy-momentum conservation:
- Galilei invariance:
- Spatial rotation:
- Spatial reflection:
- Time reversal:
- Quantum statistics:
- Isospin invariance:

The most general (off-shell) form of NN potential: [S.Okubo, R.E.Marshak, Ann.Phys.4,166(1958)]

$$V = V^0 + V^\tau \cdot (\vec{\tau}_1 \cdot \vec{\tau}_2)$$

$$V^i = V_0^i + V_\sigma^i \cdot (\vec{\sigma}_1 \cdot \vec{\sigma}_2) + V_{LS}^i \cdot (\vec{L} \cdot \vec{S}) + \{V_T^i, S_{12}\} + \frac{1}{2} \{V_{\sigma p}^i, (\vec{\sigma}_1 \cdot \vec{p})(\vec{\sigma}_2 \cdot \vec{p})\} + \frac{1}{2} \{V_Q^i, Q_{12}\}$$

$$Q_{12} \equiv \frac{1}{2} [(\vec{\sigma}_1 \cdot \vec{L})(\vec{\sigma}_2 \cdot \vec{L}) + (\vec{\sigma}_2 \cdot \vec{L})(\vec{\sigma}_1 \cdot \vec{L})]$$

where $V_j^i = V_j^i(\vec{r}^2, \vec{p}^2, \vec{L}^2)$, $\vec{p} \equiv i\vec{\nabla}$

★ the terms up to $O(p)$ → the conventional form of the potential

$$V = V_0(r) + V_\sigma(r) (\vec{\sigma}_1 \cdot \vec{\sigma}_2) + V_{LS}(r) \vec{L} \cdot \vec{S} + V_T(r) S_{12} + O(\vec{\nabla}^2).$$

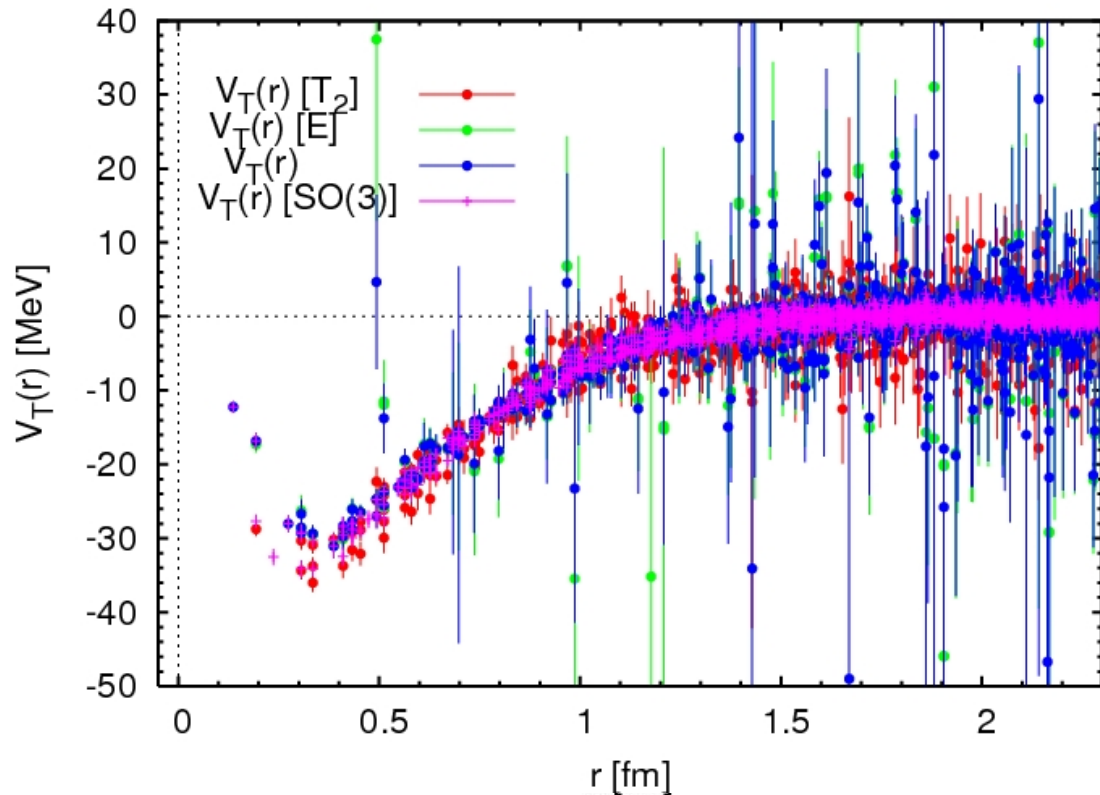
 $V_C(r)$

Tensor potential (E v.s. T_2 representation)

(57)

d-wave \leftrightarrow E-rep + T_2 -rep

We may play with this "1 to 2" correspondence.



No significant change
except for sizes of statistical errors

1. The simplest choice

Regard E-rep as d-wave

Unobtainable pt.: $(\pm n, \pm n, \pm n)$
(pt. where Y_{lm} vanishes)

2. Cubic group friendly choice

$$V_T(\vec{r}) \Rightarrow V_T^{(E)}(\vec{r}) \quad \& \quad V_T^{(T_2)}(\vec{r})$$

Maximum # of unobtainable pt.
 $(\pm n, \pm n, \pm n)$, z-axis, xy-plane

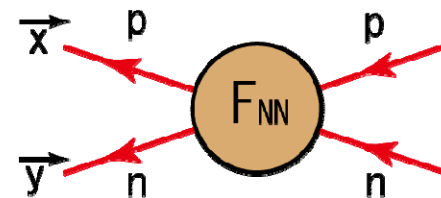
3. Angle-dependent combination of E and T_2 -rep. to achieve Minimum # of unobtainable pt. (0,0,0)

[SO(3) sym must be good.]

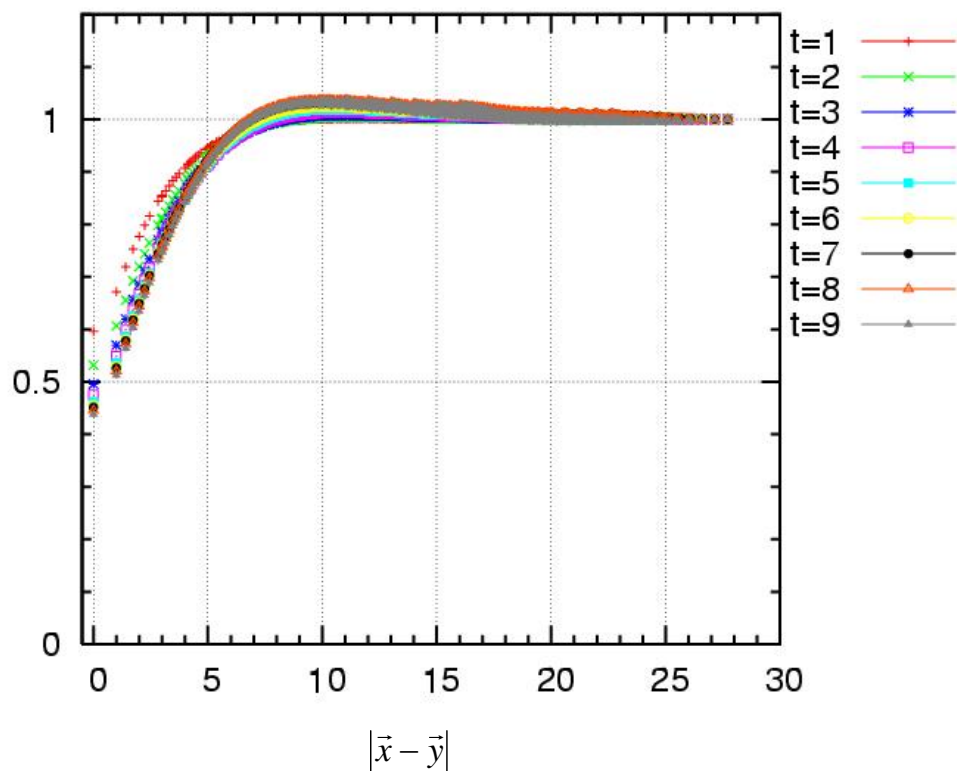
Four point nucleon correlator to BS wave function

(58)

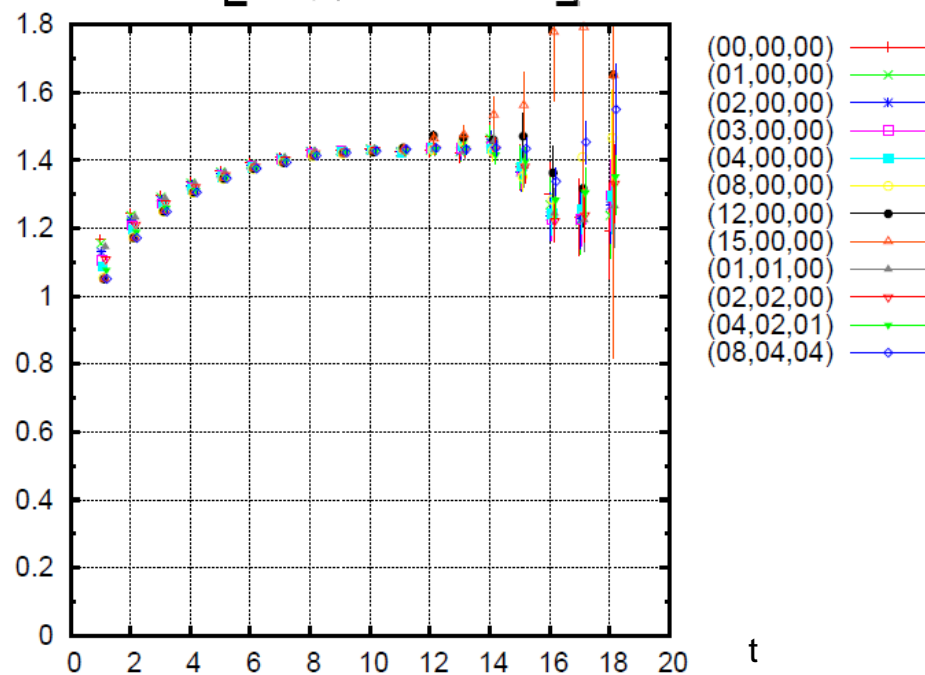
$$\begin{aligned}
 C_{NN}(\vec{x} - \vec{y}, t) &\equiv \langle 0 | T [p(\vec{x}, t+0) n(\vec{y}, t) \bar{p}(0) \bar{n}(0)] | 0 \rangle \\
 &= \sum_m \langle 0 | p(\vec{x}) n(\vec{y}) | m \rangle e^{-E_m t} \langle m | \bar{p}(\vec{0}) \bar{n}(\vec{0}) | 0 \rangle \\
 &= A_0 \psi_{E_0}(\vec{x} - \vec{y}) \exp(-E_0 t) + \dots
 \end{aligned}$$



$C_{NN}(\vec{x}; t)$



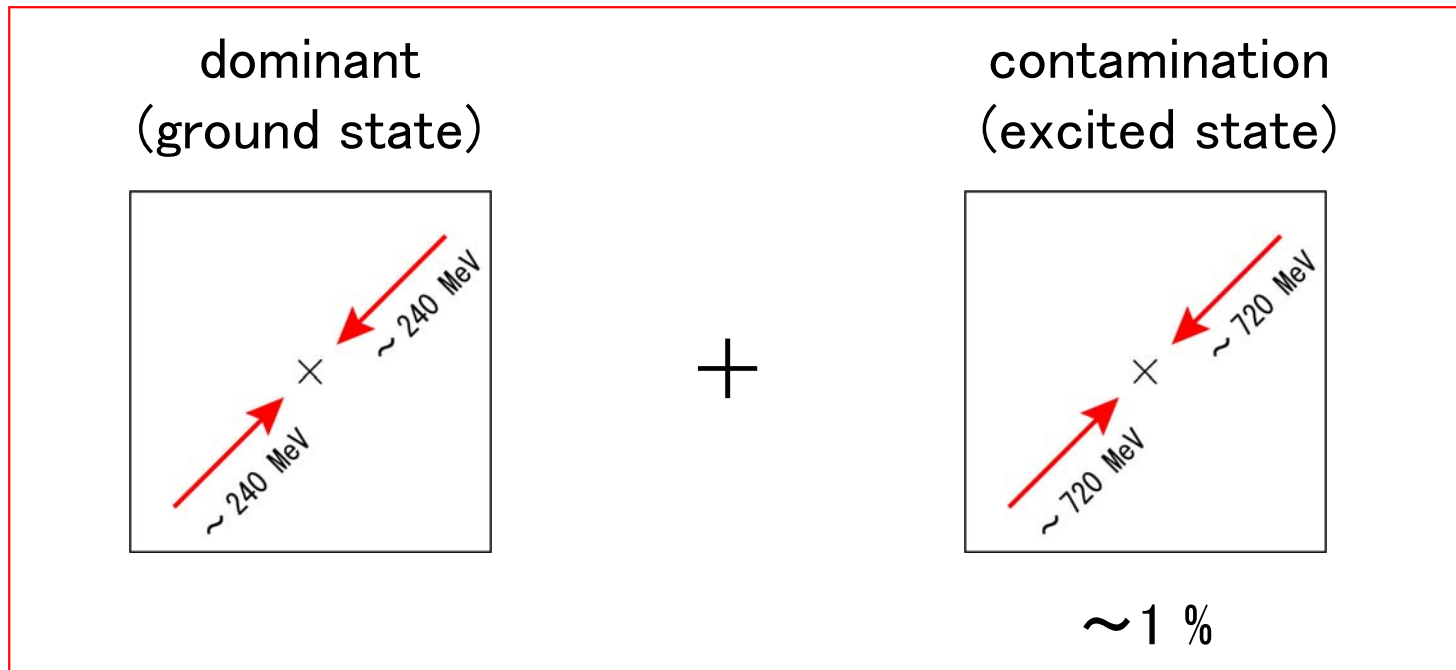
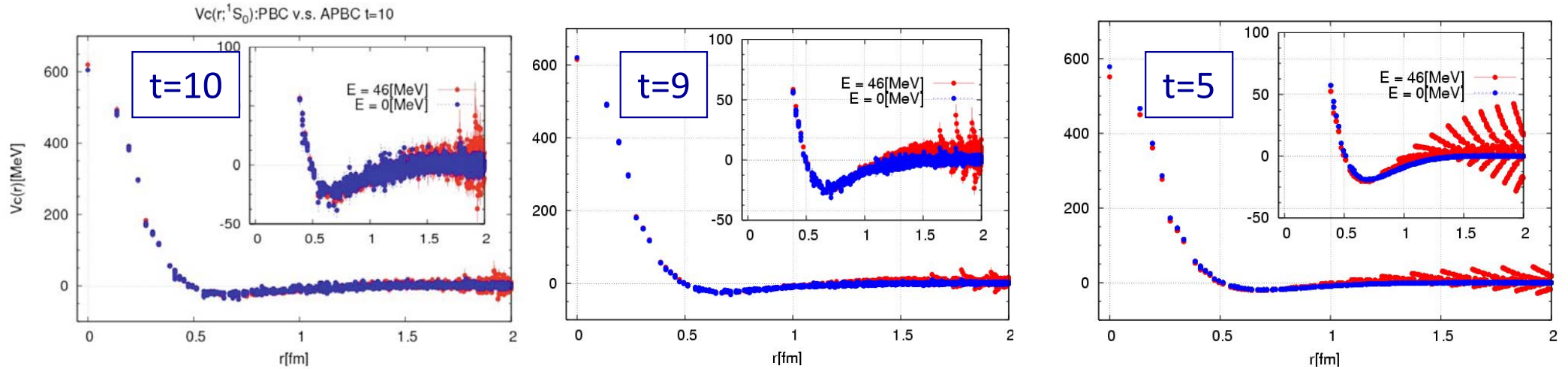
$\log \left[\frac{C_{NN}(\vec{x}, t)}{C_{NN}(\vec{x}, t+1)} \right]$



Ground state saturation around $t \sim 8$ (?).

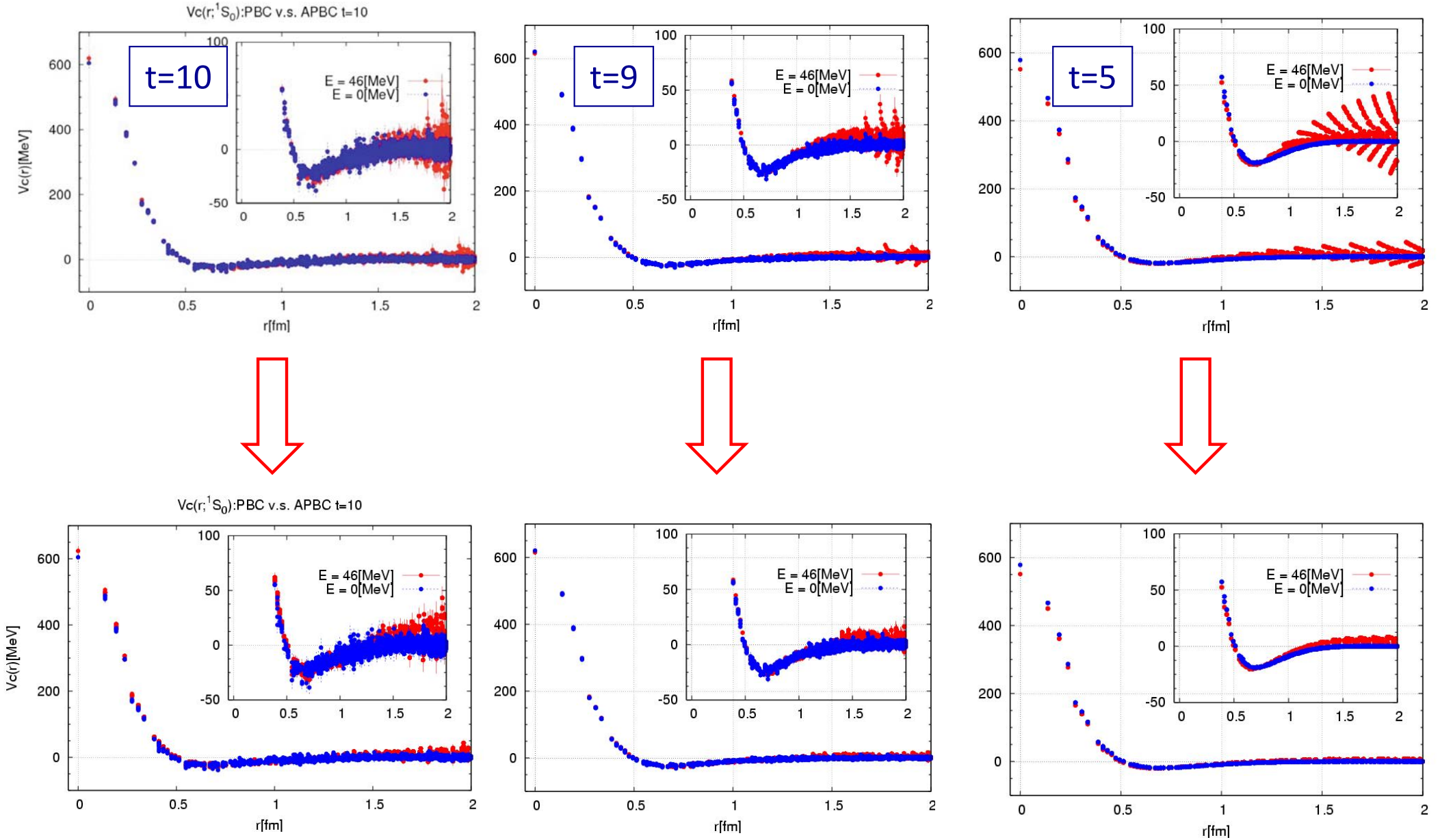
Exploding behavior at $r > 1.5$ fm is due to contamination from excited state

(59)



There are spatial regions where this excited state contamination is reduced. If we restrict ourselves to this region, the results become improved.

Exploding behavior at $r > 1.5$ fm is due to contamination from excited state (60)



work in progress by K.Murano

Tensor force (cont'd)

(61)

- Derivative expansion up to local terms

$$V(\vec{x}, \vec{\nabla}) = V_C(r) + V_T(r) \cdot S_{12} + V_{LS}(r) \cdot \vec{L} \cdot \vec{S} + \{V_D(r) \cdot \vec{\nabla}^2\} + \dots$$

- Schroedinger eq for $J^P=1^+(I=0)$

$$\{H_0 + V_C(\vec{r}) + V_T(\vec{r})S_{12}\}\psi(\vec{r}) = E\psi(\vec{r})$$



$$V_C(\vec{r}) \cdot P\psi(\vec{r}) + V_T(\vec{r}) \cdot PS_{12}\psi(\vec{r}) = (E - H_0) \cdot P\psi(\vec{r}) \quad (\text{s-wave})$$

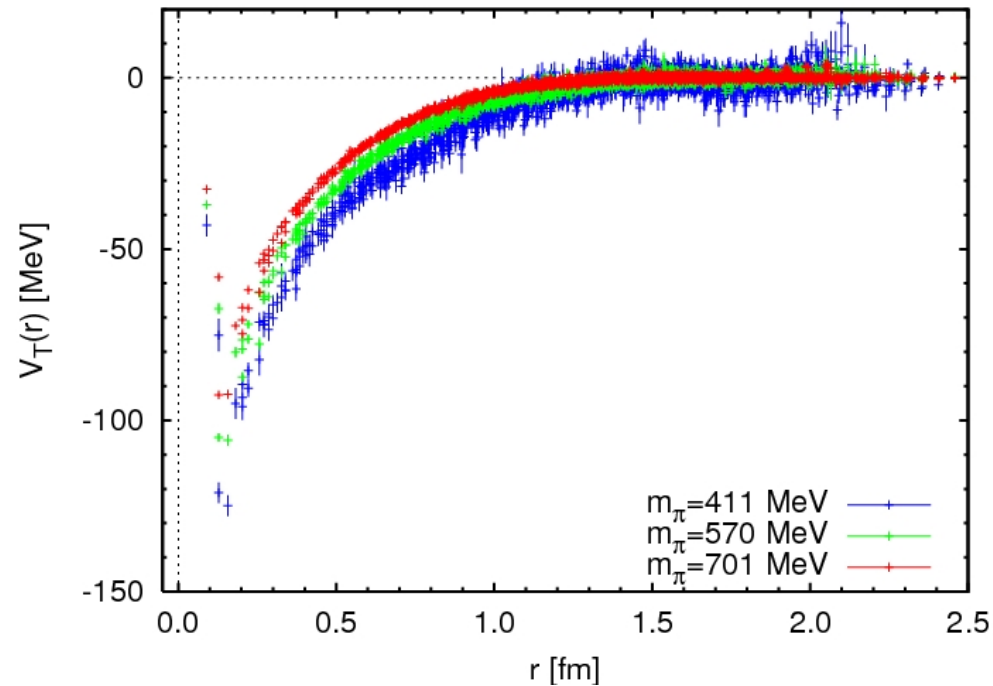
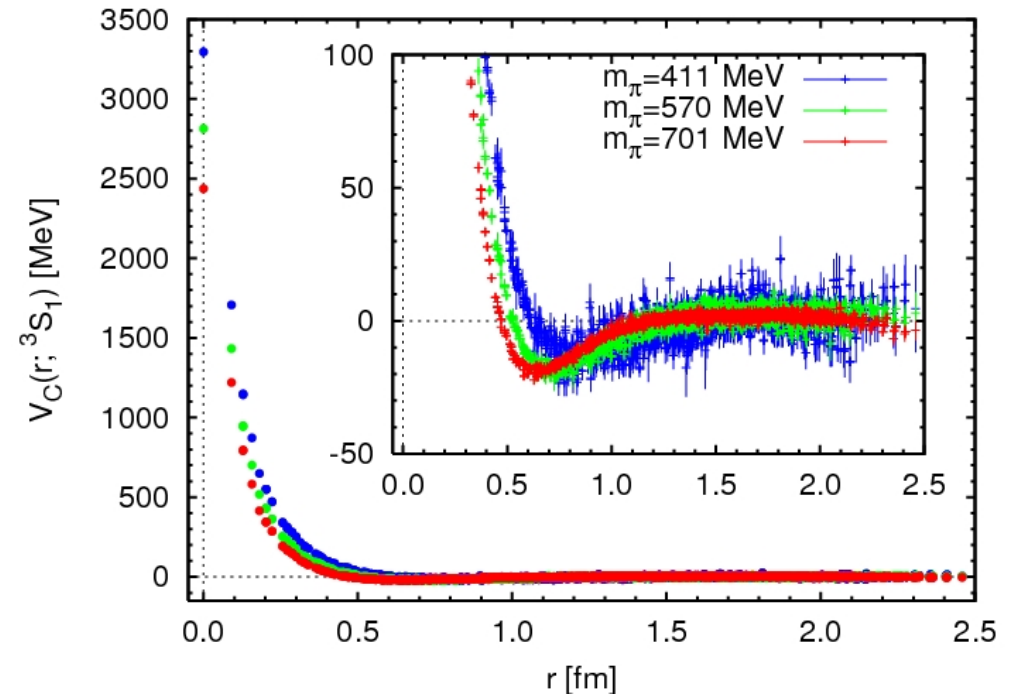
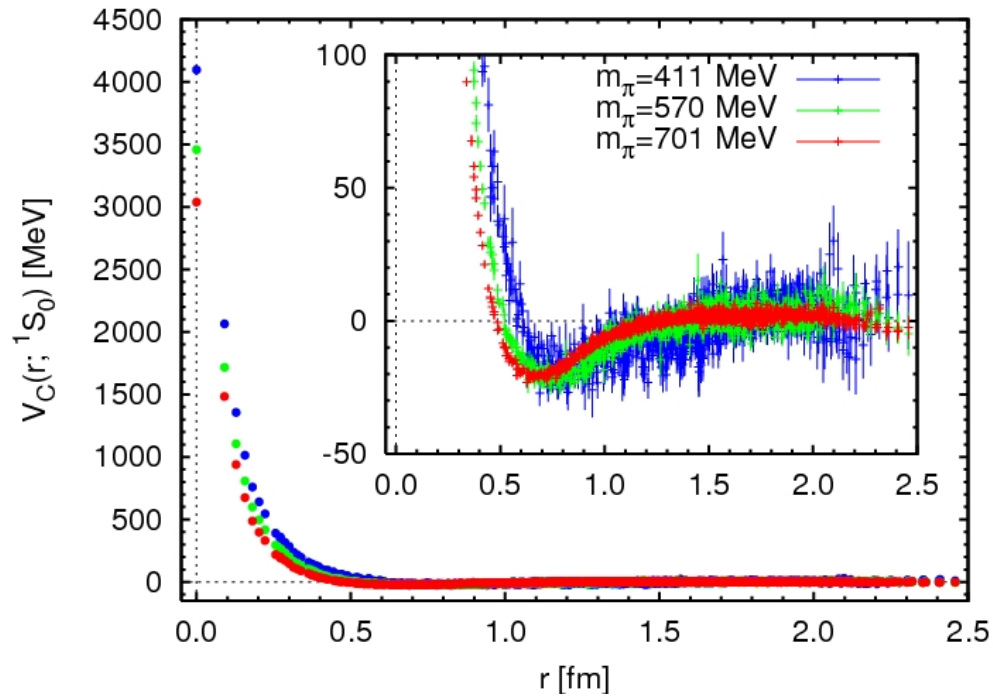
$$V_C(\vec{r}) \cdot Q\psi(\vec{r}) + V_T(\vec{r}) \cdot QS_{12}\psi(\vec{r}) = (E - H_0) \cdot Q\psi(\vec{r}) \quad (\text{d-wave})$$

- Solve them for $V_C(r)$ and $V_T(r)$ point by point

$$\begin{bmatrix} P\psi(\vec{r}) & PS_{12}\psi(\vec{r}) \\ Q\psi(\vec{r}) & QS_{12}\psi(\vec{r}) \end{bmatrix} \cdot \begin{bmatrix} V_C(\vec{r}) \\ V_T(\vec{r}) \end{bmatrix} = (E - H_0) \begin{bmatrix} P\psi(\vec{r}) \\ Q\psi(\vec{r}) \end{bmatrix}$$

NN potentials (quark mass dependence)

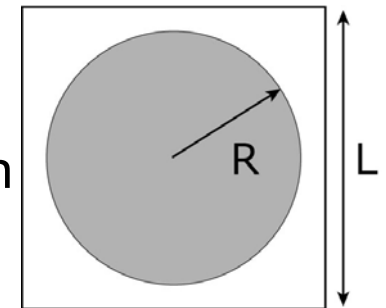
(62)



With decreasing quark mass,
interaction range becomes wider.

- Repulsive core grows.
- Attraction becomes stronger
- Tensor force gets stronger

Limit of Luescher's condition
is reached
by $m_\pi = 411$ MeV
in $L \sim 2.9$ fm lattice.



Luscher's condition
 $R < L/2$